

**DESIGN AND OPTIMIZATION OF HIGH-PERFORMANCE
SURFACE PLASMON RESONANCE BASED PHOTONIC CRYSTAL
FIBER BIOSENSOR FOR ENHANCED DETECTION AND DIVERSE
APPLICATIONS**

by

Md. Faiyaz Abrar Fahim (190021137)

Redwan-Ul-Bari (190021119)

Mizanur Rahman (190021109)

A Thesis Submitted to the Academic Faculty in Partial Fulfillment of the Requirements
for the Degree of

BACHELOR OF SCIENCE IN ELECTRICAL AND ELECTRONIC ENGINEERING



Department of Electrical and Electronic Engineering
Islamic University of Technology (IUT)
Gazipur, Bangladesh

June 2024

**DESIGN AND OPTIMIZATION OF
HIGH-PERFORMANCE SURFACE
PLASMON RESONANCE BASED
PHOTONIC CRYSTAL FIBER
BIOSENSOR FOR ENHANCED
DETECTION AND DIVERSE
APPLICATIONS**

Approved by:



Prof. Dr. Mohammad Rakibul Islam

Supervisor & Head

Department of Electrical and Electronic Engineering

Islamic University of Technology (IUT)

Boardbazar, Gazipur-1704

Date:

28-06-24

Declaration of Authorship

We, Md. Faiyaz Abrar Fahim (190021137), Redwan-Ul-Bari (190021119) & Mizanur Rahman (190021109) declare that the thesis paper titled "DESIGN AND OPTIMIZATION OF HIGH-PERFORMANCE SURFACE PLASMON RESONANCE BASED PHOTONIC CRYSTAL FIBER BIOSENSOR FOR ENHANCED DETECTION AND DIVERSE APPLICATIONS" is the accumulation of research carried out under the supervision of Dr. Mohammad Rakibul Islam, Professor & Head, Department of Electrical and Electronic Engineering (EEE), Islamic University of Technology (IUT).

We Confirm that:

- This work was conducted in partial fulfilment of the requirements for the Degree of Bachelor of Science (BSc.) in Electrical and Electronic Engineering (EEE) at this university.
- There has been no prior submission of any part of this thesis for any other qualification or degree.
- All consulted sources and quoted works have been carefully acknowledged and cited. Aside from these references, this thesis is entirely our own work.

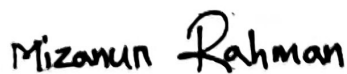
Signatures of Students:



Md. Faiyaz Abrar Fahim
Student ID: 190021137



Redwan-Ul-Bari
Student ID: 190021119



Mizanur Rahman
Student ID: 190021109

Acknowledgements

We begin this work by expressing our heartfelt gratitude to Almighty Allah (SWT.), whose boundless mercy has endowed us with the wisdom, skills, and capability to complete this engineering project. It is by His blessings that we outlasted all the challenges that came our way to this milestone. This work is a testimony that aspirations can be turned into achievement through perseverance, hard work, and faith.

Firstly, we express our profound thanks to our mentor, Prof. Dr. Mohammad Rakibul Islam. His unwavering guidance and immense patience have been crucial in navigating the challenges of this research. His deep knowledge of the subject, combined with great patience and belief in us, has dramatically helped improve our academic experience and work ethic. A truly big thank you for this invaluable contribution on his part.

Our heartfelt thanks go to our family members, whose constant support, affection, and prayers have been our foundation throughout this journey. They have been the primary source of support and motivation for all of us. We would like to thank our dear and loving parents who have made innumerable sacrifices, motivated us, and believed in our potential first and foremost for us to advance in achieving our aspirations.

Last but not least, we thank our friends who joined us on this journey through thick and thin, criticism, morale-boosting, and companionable efforts. Their encouragement and kindness made it possible for us to be enthusiastic and to keep our morale high. Otherwise, this labor of love would not have been possible. We also express our heartfelt gratitude to all those who have touched our academic lives once again.

Abstract

Over the years, various designs for traditional photonic crystal fibers (PCFs) and surface plasmon resonance photonic crystal fibers (SPR-PCFs) have been proposed, each demonstrating different structures, sensitivities, and confinement losses. Building on a comprehensive review of previous studies, we present a photonic crystal fiber biosensor based on surface plasmon resonance (SPR) with outstanding performance characteristics, designed using COMSOL Multiphysics 6.1. In this study, we developed a sensor incorporating air holes of varying diameters, strategically positioned to optimize performance. By meticulously fine-tuning all fiber parameters, we achieved a maximum amplitude sensitivity (AS) of 965.976 RIU^{-1} and a wavelength sensitivity (WS) of $134,000 \text{ nm/RIU}$, with a maximum sensor resolution of $4 \times 10^{-4} \text{ RIU}$ for the x-polarization. For the y-polarization, we attained a maximum amplitude sensitivity (AS) of 1167.53 RIU^{-1} and a wavelength sensitivity (WS) of $125,000 \text{ nm/RIU}$, with a maximum sensor resolution of $5 \times 10^{-4} \text{ RIU}$. Additionally, the sensor achieved a maximum figure of merit (FOM) of 832.422 for the x-polarization and 1246.986 for the y-polarization. The maximum birefringence observed was 1.980×10^{-3} . The overall analyte sensing range is from refractive indices 1.35 to 1.42 , and the sensor has a fabrication tolerance limit of $\pm 5\%$. With its enhanced performance in terms of sensitivity, we believe that this SPR-based PCF biosensor can potentially contribute to the detection of unknown analytes and play a significant role in medical diagnostics.

Contents

Declaration of Authorship	iii
Acknowledgements	iv
Abstract	v
1 Introduction	1
1.1 Background Study	1
1.2 Problem Statement	3
1.3 Research Objective	4
1.4 Motivation	5
1.5 Thesis Framework	7
2 Comprehensive Review of Literature and Theoretical Framework	9
2.1 Literature Review	9
2.2 Photonic Crystal Fiber	10
2.2.1 Brief Overview	10
2.2.2 Guiding Mechanisms	11
2.2.3 Classification of PCF	11
2.2.4 High Index Guiding Fibers	12
2.2.5 The Bandgap Effect	12
2.2.6 Hollow-Core and Solid-Core Fibers	13
2.3 Surface Plasmon Resonance	13
2.3.1 Brief Overview	13
2.3.2 Basic Working Principle	14
2.3.3 Surface Plasmon Wave	15
2.3.4 Evanescent field	15
2.4 Utility of SPR PCFs	15
2.5 Different SPR Based PCF Sensor Design	16
2.5.1 Introduction	16
2.5.2 Internal Sensing-based Sensor	16
2.5.3 External Sensing-based Sensor	17

2.5.4	Prism-based Sensor	17
2.5.5	D-shaped Sensor	17
2.5.6	Plasmonic Material Silver-based Sensor	18
2.5.7	Bimetallic Silver-Graphene-based Sensor	18
2.5.8	Bimetallic Silver-Gold-based Sensor	18
2.5.9	Bimetallic Silver-TiN-based Sensor	19
2.5.10	Plasmonic Material Gold-based Sensor	19
2.5.11	Bimetallic Gold- TiO_2 -based Sensor	19
2.5.12	ITO-based Sensor	20
3	Mathematical Modelling	21
3.1	Computational study of Performance Parameters	21
3.2	Conventional PCF sensors' characteristics	21
3.2.1	Confinement loss (CL)	21
3.2.2	Effective Material Loss (EML)	22
3.2.3	Relative Sensitivity	22
3.2.4	Effective cross-sectional area (A_{eff})	23
3.2.5	Effective refractive index (n_{eff})	23
3.2.6	Numerical Aperture	23
3.2.7	Dispersion	23
3.3	SPR-PCF based sensors' characteristics	24
3.3.1	Amplitude Sensitivity	24
3.3.2	Wavelength Sensitivity	24
3.3.3	Full Width at Half Maximum	24
3.3.4	Figure of Merit (FOM)	25
3.3.5	Temperature Sensitivity	25
3.3.6	Magnetic Field (MF) Sensitivity	25
3.3.7	Resolution	26
3.3.8	Novel dual peak shift sensitivity for structures having two consecutive resonance peaks	26
3.4	SPR-PCF based polarization filters' characteristics	27
3.4.1	Cross-talk (CT)	27
3.4.2	Output Power (Pout)	27
3.4.3	Extinction Ratio (ER)	27
3.4.4	Confinement Loss Ratio (CLR)	28
3.5	Computational study of the materials used	28
3.5.1	Zeonex	28
3.5.2	Air	28

3.5.3	Fused Silica (SiO_2)	28
3.5.4	Gold	29
3.5.5	AZO	30
3.5.6	Titanium dioxide (TiO_2)	31
3.5.7	Ethanol	31
4	Proffered Design for Highly Sensitive SPR-PCF Sensor	32
4.1	Introduction:	32
4.2	Geometrical Structure of Model and Distribution of Field	33
4.3	Experimental Setup:	36
4.4	Design Optimization	37
4.4.1	Gold Layer Optimization:	37
4.4.2	TiO_2 Layer Optimization:	39
4.4.3	Air Hole Optimization:	40
4.4.4	Analysis of sensor performance at optimized parameters:	42
4.5	Final Results & Comparative Analysis:	48
5	Sensor Fabrication	50
5.1	Fabrication Process for the Proposed SPR-PCF Sensor	50
5.2	Design and Preform Preparation	50
5.2.1	Structural Design:	50
5.2.2	Preform Fabrication:	50
5.3	Drawing and Structuring	51
5.3.1	Drawing Process:	51
5.3.2	Assembly:	51
5.4	Coating with Gold and TiO_2	52
5.4.1	Chemical Vapor Deposition (CVD):	52
5.4.2	Photolithography:	52
5.5	Final Assembly and Testing	52
5.5.1	Sensor Assembly:	52
5.5.2	Performance Testing:	52
5.5.3	Fabrication Tolerance:	53
6	Conclusion And Future Work	56
6.1	Conclusion	56
6.2	Future Work and Scopes of Improvement	57
7	Demonstration of Outcome Based Education	59
7.1	Introduction	59

7.2	Course Outcomes (COs) Addressed	60
7.3	Aspects of Program Outcomes Addressed	67
7.4	Knowledge Profiles (K3-K8) Addressed	70
7.5	Use of Engineering Problems	74
7.6	Socio-Cultural, Environmental, And Ethical Impact	75
7.6.1	Cultural Diversity and Sensitivity	75
7.6.2	Environmental Sustainability	75
7.6.3	Ethical Standards	75
7.6.4	Community Engagement	76
7.6.5	Impact Evaluation	76
7.6.6	Compliance and Ethical Framework	76
7.6.7	Continuous Monitoring and Enhancement	76
7.7	Attributes of Ranges of Complex Engineering Problem Solving (P1 – P7) Addressed	77
7.8	Attributes of Ranges of Complex Engineering Activities (A1-A5) Addressed	82
	Bibliography	86

List of Figures

2.1	SPR based PCF - Optical Transducer [37]	10
2.2	Change in Transmittance Due to Difference in Light Guidance [42]	12
2.3	Different Types of Cores (a) Solid Core, (b) Hollow Core, (c) Doped Core [43]	13
2.4	Surface Plasmon Resonance Based Shift in Transmittance[42]	14
2.5	Different SPR sensors (a) Internal [26], (b) External [48]	17
2.6	Different SPR sensors (a) Prism Based [49], (b) D-Shaped [50]	18
2.7	Different SPR sensors (a) Silver Based [51], (b) Silver Graphene Based [27]	19
2.8	Different SPR sensors (a) Gold Based [52], (b) Gold TiO_2 Based [53]	20
2.9	ITO Based SPR Sensor [54]	20
4.1	Proffered Sensor 2D cross-sectional view	33
4.2	Field Distribution of (a) code mode (x-pol), (b) code mode (y-pol) and (c) SPP mode (x-pol), (d) SPP mode (y-pol)	34
4.3	Dispersion property of the core and SPP mode and loss graph for RI 1.35 [x-pol]	35
4.4	Dispersion property of the core and SPP mode and loss graph for RI 1.35 [y-pol]	35
4.5	Experimental Setup	36
4.6	Confinement loss curves at analyte RI of 1.35 (solid lines) and 1.36 (dashed lines) for $t_g = 25$ nm, 30 nm, 35 nm	38
4.7	Amplitude Sensitivity curves for $t_g = 25$ nm, 30 nm, 35 nm at analyte RI of 1.35	38
4.8	Confinement loss curves at analyte RI of 1.35 (solid lines) and 1.36 (dashed lines) for $t_t = 15$ nm, 20 nm, 25 nm	39
4.9	Amplitude Sensitivity curves for $t_t = 15$ nm, 20 nm, 25 nm at analyte RI of 1.35	39
4.10	Confinement loss curves at analyte RI of 1.35 (solid lines) and 1.36 (dashed lines) for $d_1 = 0.85 \mu\text{m}$, $0.9 \mu\text{m}$, and $0.95 \mu\text{m}$	40
4.11	Amplitude Sensitivity curves for for $d_1 = 0.85 \mu\text{m}$, $0.9 \mu\text{m}$, and $0.95 \mu\text{m}$ at analyte RI of 1.35	41

4.12	Confinement loss curves at analyte RI of 1.35 (solid lines) and 1.36 (dashed lines) for $d_2 = 0.4 \mu\text{m}$, $0.5 \mu\text{m}$, and $0.6 \mu\text{m}$	41
4.13	Amplitude Sensitivity curves for for $d_2 = 0.4 \mu\text{m}$, $0.5 \mu\text{m}$, and $0.6 \mu\text{m}$ at analyte RI of 1.35	42
4.14	Confinement Loss curves for x-pol (RI 1.35-1.40)	43
4.15	Confinement Loss curves for x-pol (RI 1.41-1.42)	43
4.16	Amplitude Sensitivity Curves for X-pol	44
4.17	Confinement Loss curves for y-pol (RI 1.35-1.40)	44
4.18	Confinement Loss curves for y-pol (RI 1.31-1.42)	45
4.19	Amplitude Sensitivity Curves for Y-pol	45
4.20	Polynomial fitting curve for the relationship between RI and RW in the x-polarized mode.	46
4.21	Plotting of RW and sensor length with varying analyte RI	46
4.22	Plotting birefringence and the real part of the effective refractive index as a function of wavelength	47
5.1	Stacking, Drawing and Masking	51
5.2	Fabrication of the proffered sensor	53
5.3	CL spectrum at analyte RI 1.35 with a variation of $\pm 5\%$ in (a) parameter d_1 and (b) parameter d_2	54
5.4	CL spectrum at analyte RI 1.35 with a variation of $\pm 5\%$ in parameter t_g	54

List of Tables

4.1	Sensor performance for analyte RI 1.35–1.42	48
4.2	Comparative Analysis of Sensor Performance	49
5.1	Fabrication tolerance analysis by variation of d_1	55
5.2	Fabrication tolerance analysis by variation of d_2	55
5.3	Fabrication tolerance analysis by variation of t_g	55
7.1	COs Addressed	60
7.2	Justification of the COs and their corresponding POs	66
7.3	Program Outcomes Addressed	69
7.4	Knowledge Profiles	70
7.5	Justification of Knowledge Profiles	73
7.6	P1-P7 addressed	77
7.7	Justification of the Attributes of Ranges of Complex Engineering Problem Solving (P1 – P7)	81
7.8	A1-A5 addressed	82
7.9	Justification of the Attributes of Ranges of Complex Engineering Activities (A1–A5)	85

List of Abbreviations

SP	Surface Plasmon
SPR	Surface Plasmon Resonance
SPW	Surface Plasmon Wave
SPP	Surface Plasmon Polariton
RIU	Refractive Index Unit
RI	Refractive Index
RW	Resonance Wavelength
NIR	Near-infrared Region
TIR	Total Internal Reflection
TE	Transverse Electric
TM	Transverse Magnetic
FEM	Finite Element Method
PML	Perfectly Matched Layer
PCF	Photonic Crystal Fiber
PBG	Photonic Band Gap
THz	Terahertz
AS	Amplitude Sensitivity
AI	Amplitude Interrogation
WS	Wavelength Sensitivity
WI	Wavelength Interrogation
LSPR	Localized Surface Plasmon Resonance
EML	Effective Material Loss
CL	Confinement Loss
CLR	Confinement Loss Ratio
ER	Extinction Ratio
NA	Numerical Aperture
FOM	Figure of Merit
FWHM	Full Width at Half Maximum
EMF	Electromagnetic Field
CT	Crosstalk

Chapter 1

Introduction

1.1 Background Study

Over the past few decades, optical fibers have revolutionized telecommunications, becoming the core medium for high-speed data transmission over long distances[1]. Traditional solid-core optical fibers, developed in the mid-20th century, provided significant improvements in bandwidth and transmission efficiency compared to electrical cables[2]. However, these fibers faced challenges, including high leakage loss and limited refractive index contrast. To address these limitations, photonic crystal fibers (PCFs) were introduced[3]. First conceptualized by Yeh et al. in 1978, PCFs incorporate a periodic arrangement of air holes along the fiber length, which enhances their guiding properties and allows for a high degree of design flexibility. This innovative structure enables PCFs to overcome the drawbacks of conventional optical fibers, offering lower loss and higher controllability of light propagation[4].

Photonic crystal fibers are a unique category of optical fibers that utilize a periodic microstructure to confine and guide light[5]. Unlike traditional fibers that rely solely on total internal reflection, PCFs can guide light through a combination of mechanisms, including modified total internal reflection and photonic bandgap effects[3]. The design of PCFs can be tailored by varying the size, shape, and arrangement of the air holes, which allows for precise control over their optical properties[6]. This versatility makes PCFs suitable for a wide range of applications, from telecommunications and medical diagnostics to environmental monitoring and chemical sensing. The ability to engineer PCFs for specific functions has led to significant advancements in optical fiber technology.

Surface plasmon resonance (SPR) is an optical phenomenon that occurs when light interacts with free electrons on a metal surface, inducing collective oscillations known as surface plasmons[7][8]. This resonance condition is highly sensitive to changes in the refractive index of the surrounding medium, making SPR an effective method for detecting biochemical analytes. SPR-based sensors leverage this sensitivity to provide real-time, label-free detection with high specificity[9]. The integration of SPR with optical fibers, particularly PCFs, has opened new avenues for the development of highly

sensitive sensors capable of detecting minute changes in the refractive index[10]. These SPR-PCF sensors are increasingly used in various fields, including biomedical diagnostics, environmental monitoring, and food safety[11].

Combining SPR technology with photonic crystal fibers has led to the creation of advanced sensors with enhanced performance characteristics[8][7]. SPR-PCF sensors capitalize on the unique guiding properties of PCFs and the high sensitivity of SPR to develop devices that can detect subtle changes in the refractive index of analytes[12]. This integration allows for the development of sensors with high sensitivity and specificity, capable of operating in challenging environments. The versatility of PCFs in terms of structural design and material composition further enhances the performance of SPR-based sensors. Researchers have explored various PCF designs and plasmonic materials to optimize sensor performance, resulting in significant advancements in the field.

Despite their advantages, SPR-PCF sensors face several challenges that need to be addressed to maximize their potential[13]. One major challenge is achieving a balance between high sensitivity and low confinement loss[14]. Many SPR-PCF sensors either exhibit high sensitivity with significant loss or low sensitivity with minimal loss, necessitating further optimization. Fabrication complexity is another issue, as the intricate design and manufacturing processes of SPR-PCF sensors, especially those involving internal or external metal coatings, can be costly and technically demanding. Additionally, practical implementation challenges such as alignment, integration with existing systems, and ensuring consistent performance in real-world conditions must be overcome.

Recent research efforts have focused on addressing these challenges by exploring innovative PCF structures and optimizing the use of plasmonic materials[1]. For instance, hexagonal core PCF sensors have been developed for specific applications like milk sensing in the dairy industry. By fine-tuning geometric parameters such as core diameter and porosity, researchers have achieved sensors with high sensitivity and low loss[15]. Another example is the quadrature cluster SPR-PCF sensor, designed for multidimensional applications by optimizing structural parameters like bimetallic layer thickness and air hole diameter[16]. Bent-core LSPR-PCF sensors offer wideband double peak sensing capabilities, utilizing double peaks to introduce novel sensing parameters such as double peak shift sensitivity[17]. Additionally, D-shaped PCF-based polarization filters have been designed for S and U band applications, featuring high crosstalk and minimal insertion loss, making them ideal for optical communication systems[18].

The potential applications of SPR-PCF sensors are vast and diverse. In healthcare, these sensors can be used for early disease detection and monitoring, providing real-time

data on biochemical interactions[7]. Environmental monitoring is another key application area, where SPR-PCF sensors can detect pollutants and hazardous substances with high accuracy. In the food industry, these sensors ensure quality control by detecting contaminants and ensuring the safety of food products. Furthermore, in telecommunications, SPR-PCF sensors enhance the performance of optical networks by providing precise control over light propagation, thereby improving signal quality and reducing losses.

The integration of surface plasmon resonance technology with photonic crystal fibers represents a significant advancement in the field of optical sensing[7]. By addressing the challenges in sensor design and optimizing their performance, researchers are paving the way for the widespread adoption of SPR-PCF sensors in various applications. Continued exploration of novel PCF structures and plasmonic materials promises to further enhance the sensitivity, accuracy, and practical applicability of these sensors. This ongoing research and development will contribute to advancements in healthcare, environmental safety, food quality, and telecommunications, demonstrating the transformative potential of SPR-PCF technology.

1.2 Problem Statement

Despite advancements in photonic crystal fiber (PCF) technology and surface plasmon resonance (SPR) sensing, several challenges impede their optimal performance and practical application. High confinement loss, where light escapes from the core into the cladding, reduces sensitivity and accuracy[19]. Balancing high sensitivity with low confinement loss remains complex, as improving one often worsens the other.

The fabrication of SPR-PCF sensors is technically challenging and costly[20]. These sensors require precise control over geometric parameters and the application of plasmonic materials. Internal and external metal coatings add complexity, making the production process expensive and limiting scalability. For instance, D-shaped PCFs need careful polishing, further complicating fabrication.

Practical implementation in real-world applications also presents hurdles. Ensuring consistent performance across various conditions and integrating these sensors into existing systems is challenging[21]. Issues like alignment, durability, and reliability must be addressed. Additionally, the high sensitivity to environmental changes, while beneficial for detection, can lead to false positives or fluctuating readings, necessitating robust calibration techniques[22].

The main challenges include:

- **High confinement loss:** Reduces sensitivity and accuracy.

- **Fabrication complexities:** Requires precise control over design and materials, increasing costs.
- **Implementation issues:** Ensuring consistent performance and integration into systems.
- **Environmental sensitivity:** Can cause false positives, needing robust calibration.

Current SPR-PCF sensor designs are often complex, difficult to fabricate, and challenging to model and optimize. This complexity increases variability in sensor performance, making uniformity across batches difficult. Novel designs that simplify fabrication while maintaining high performance are needed.

In summary, while SPR-PCF sensors show great promise for applications in biomedical diagnostics, environmental monitoring, and more, significant challenges remain. Addressing high confinement loss, fabrication complexities, practical implementation issues, and the need for simplified designs is essential for maximizing the potential of SPR-PCF sensors and enabling their broader adoption.

1.3 Research Objective

The primary objective of this research is to advance the development of photonic crystal fiber (PCF) sensors integrated with surface plasmon resonance (SPR) technology. By addressing the existing challenges in sensor performance and fabrication, this research aims to design, optimize, and validate novel SPR-PCF sensors that demonstrate enhanced sensitivity, accuracy, and practical applicability. The specific goals of this research include:

- **Investigate Existing SPR-PCF Sensor Designs:** Conduct a comprehensive review of current SPR-PCF sensor designs to identify their strengths and weaknesses. This includes analyzing performance metrics such as sensitivity, confinement loss, fabrication complexity, and practical implementation issues.
- **Optimize Geometric Parameters:** Explore various PCF structures and configurations to optimize geometric parameters, such as core diameter, air hole size, and arrangement. The goal is to achieve high sensitivity with minimal confinement loss.
- **Innovate Plasmonic Material Application:** Experiment with different plasmonic materials and coating techniques to enhance the interaction between the plasmonic layer and the analyte. This includes evaluating both internal and external metal coatings for their impact on sensor performance.

- **Develop Simplified Fabrication Techniques:** Design novel PCF sensor structures that simplify the fabrication process while maintaining or improving performance. This involves creating designs that are easier to produce and scale up, reducing costs and technical barriers.
- **Improve Practical Implementation:** Address practical challenges related to the real-world application of SPR-PCF sensors. This includes developing robust calibration techniques to mitigate environmental sensitivity and ensuring consistent performance across varying conditions.
- **Evaluate Performance Through Simulation and Experimentation:** Utilize computational simulations and experimental validation to assess the performance of proposed sensor designs. This includes measuring parameters such as sensitivity, resolution, confinement loss, and response time.
- **Compare with Existing Technologies:** Benchmark the performance of newly developed SPR-PCF sensors against existing sensors and technologies. This comparison will help demonstrate the advantages and potential applications of the new designs.
- **Explore Multidimensional Applications:** Investigate the potential of SPR-PCF sensors for multidimensional sensing applications, including biomedical diagnostics, environmental monitoring, and telecommunications. This involves tailoring sensor designs for specific use cases and evaluating their effectiveness in detecting various analytes.

By achieving these objectives, this research aims to contribute significantly to the field of optical sensing, paving the way for the development of highly efficient, reliable, and versatile SPR-PCF sensors. The ultimate goal is to facilitate the broader adoption of these sensors in various scientific, industrial, and medical applications, enhancing their practical utility and impact.

1.4 Motivation

The integration of photonic crystal fiber (PCF) technology with surface plasmon resonance (SPR) offers a transformative approach to optical sensing, driven by several compelling motivations. This research seeks to advance SPR-PCF sensors to address existing limitations, enhance various applications, and contribute significantly to both academic and industrial fields.

Current optical fiber technologies and sensing methods face significant challenges such as high confinement loss, fabrication complexities, and practical implementation

issues[23]. These limitations hinder the performance and broader adoption of sensors in critical applications. By developing SPR-PCF sensors, this research aims to overcome these barriers, enhancing sensitivity, accuracy, and practicality. Addressing these limitations is crucial for improving existing technologies and providing more efficient and reliable sensing solutions.

In the biomedical field, the early and accurate detection of diseases is crucial for effective treatment and patient outcomes. SPR-PCF sensors can detect biomolecular interactions with high sensitivity and specificity, enabling real-time, label-free diagnostics[9]. This capability can revolutionize healthcare by facilitating early detection of conditions such as cancer, infectious diseases, and other medical disorders. The potential to improve healthcare diagnostics through more efficient and less invasive methods is a strong motivator for this research.

Environmental monitoring is essential for detecting pollutants, hazardous substances, and environmental changes. SPR-PCF sensors can play a critical role in monitoring air and water quality, detecting toxic chemicals, and ensuring environmental safety[24]. Real-time, accurate data on environmental conditions can enable early detection of contamination events, allowing for prompt action to mitigate health risks and environmental damage. Developing advanced sensors to contribute to a safer and cleaner environment is a significant motivator for this research.

Ensuring the safety and quality of food products is another important application for SPR-PCF sensors[24]. These sensors can detect contaminants, pathogens, and chemical residues in food, ensuring compliance with safety standards and protecting public health. Enhancing food safety through reliable and sensitive detection methods drives the exploration of SPR-PCF sensors in this domain. Improved monitoring of food quality can help prevent foodborne illnesses and ensure consumer safety.

The telecommunications industry relies on advanced optical fibers for high-speed, long-distance data transmission with minimal loss. SPR-PCF sensors can enhance optical networks by providing precise control over light propagation, improving signal quality, and reducing losses[25]. Developing sensors that support high-speed, high-capacity communication systems is motivated by the growing demand for reliable telecommunications infrastructure. Integrating SPR technology with PCFs aims to contribute to the advancement of next-generation communication networks.

Academically, developing SPR-PCF sensors represents a significant contribution to optical sensing and fiber optics[9]. The research findings can provide valuable insights into designing, optimizing, and applying advanced sensors, fostering further innovation. Industrially, the potential applications in healthcare, environmental monitoring, food safety, and telecommunications highlight the broad impact of these sensors. Bridging the gap between academic research and practical industrial applications drives this research.

The future prospects of SPR-PCF sensors are vast and promising. Continued advancements in sensor design and fabrication can lead to even more sensitive, accurate, and versatile sensors. Integrating these sensors into portable and wearable devices opens new avenues for real-time monitoring and diagnostics[24]. Exploring and realizing these future possibilities fuels the dedication to advancing SPR-PCF sensor technology.

And so, this research is motivated by the potential to address current limitations, enhance various applications, and contribute to both academic and industrial progress. Developing advanced SPR-PCF sensors aims to create transformative solutions with a meaningful and lasting impact across multiple fields.

1.5 Thesis Framework

The thesis book consists of six distinct chapters. A brief synopsis of each chapter is given below:

- **Chapter-1 Introduction:** The introduction provides the background and context for the study, highlighting the significance of photonic crystal fibers (PCFs) and surface plasmon resonance (SPR) technologies. It identifies key challenges in current SPR-PCF sensors, such as high confinement loss and fabrication complexities. The research objectives focus on designing and optimizing novel SPR-PCF sensors to enhance performance. The chapter also discusses the motivation behind the research, emphasizing its potential impact in fields like healthcare, environmental monitoring, and telecommunications.
- **Chapter-2 Comprehensive Review of Literature and Theoretical Framework:** This chapter provides an extensive review of the literature and theoretical foundations relevant to the study of Surface Plasmon Resonance (SPR) and Photonic Crystal Fiber (PCF) sensors. It begins with a critical analysis of existing research, identifying key gaps and opportunities for further investigation. The chapter elaborates on the fundamental principles of PCFs and SPR, detailing their operational mechanisms and structural designs. It further examines the advantages and limitations of SPR-based PCF sensors, exploring various sensor designs, including both internal and external sensing configurations, and the application of different plasmonic materials.
- **Chapter-3 Mathematical Modelling:** The mathematical modeling chapter presents the theoretical frameworks used to analyze sensor performance. It covers key performance metrics like confinement loss, sensitivity, and effective refractive index, and explores characteristics specific to SPR-PCF sensors. These models provide the basis for the sensor design and optimization efforts that follow.

- **Chapter-4 Proffered Design for Highly Sensitive SPR-PCF Sensor:** This chapter presents the design of a novel SPR-PCF sensor, detailing its structure and field distribution. It explains the experimental setup used for validation and describes the optimization process for key components like the gold and TiO_2 layers. The final section presents the optimized sensor's performance, offering a comparative analysis against existing designs.
- **Chapter-5 Sensor Fabrication:** The sensor fabrication chapter outlines the practical steps taken to build the proposed SPR-PCF sensor. It covers the design and preform preparation, drawing and structuring, and the coating process using techniques like Chemical Vapor Deposition (CVD). The chapter concludes with the final assembly and performance testing of the sensor.
- **Chapter-6 Conclusion And Future Work:** Drawing the conclusion of our work while presenting our visions for the future. We explain how we can continue forward with the research and how we can find ways to improve the existing model design and results.
- **Chapter-7 Demonstration of Outcome-Based Education:** This chapter connects the research to educational outcomes, demonstrating how it addresses specific Course Outcomes (COs) and Program Outcomes (POs). It discusses the socio-cultural, environmental, and ethical impacts of the research, emphasizing its broader significance beyond technical contributions.
- **Bibliography:** Finally we have listed all references cited throughout the thesis, ensuring proper credit is given to sources and providing a resource for further reading.

Chapter 2

Comprehensive Review of Literature and Theoretical Framework

2.1 Literature Review

Due to the flexible structure design, infinite single-mode transmission, anomalous dispersion, high birefringence, large mode field area, nonlinear effect and many other excellent characteristics, photonic crystal fiber (PCF) has incomparable advantages over traditional fiber in many fields[26].

In 2020, Tianshu Li et al.[27] proposed an H-type sensor with silver-graphene layers externally deposited with a detection range is 1.33–1.41 and operating in the wavelength range of 600–1050 nm. Md. Biplob et al.[28] designed a SPR-PCF sensor with a quasi D-type dual core structure. It operates in the 1080–1560 nm wavelength range with an RI detection range of 1.42–1.46. A novel PCF-SPR sensor with three layers of regular hexagonal air holes proposed by Zipeng Guo et al.[29] obtained a wide RI detection range of 1.35–1.46 at 1200–1450 nm. In 2022, Satyendra Jain et al.[30] studied a PCF sensor with an outer surface coated with gold film, and the detection range of the RI is from 1.35 to 1.40 at a wavelength range of 500–1350 nm. In the same year, Ahmed A. Saleh Falah et al.[31] reported a D-shaped PCF sensor with an open microchannel. Its RI detection range is 1.330–1.435, and the operating wavelength is 550–1300 nm.

From the above literature, we can see that the detection range of existing reported PCF-SPR RI sensors is generally narrow. Recently, a dual-core PCF-based sensor with max AS of 6829 RIU^{-1} was proposed by Mahfuz et al.[32] which also has a high FOM. However, it exhibited zero birefringence, low WS (28000 nm/RIU), and comparatively narrow sensing range. Islam et al.[33] introduced a birefringent sensor with considerable AS. Nevertheless, the birefringence and the WS values were not up to the mark.

A recent anisotropic PCF design proposed by A.K Shakya et al.[34] shows a maximum WS of 20,000 nm/RIU and a maximum AS of 3167 RIU^{-1} . In 2020, M.R Islam et al.[35] proposed a sensor based on localized surface plasmon resonance (LSPR) with

simultaneous use of gold and aluminium doped zinc oxide (AZO) as plasmonic materials. This sensor exhibits maximum amplitude sensitivity of 8485.2 RIU^{-1} along with maximum wavelength sensitivity of 46300 nm/RIU in the direction of y-polarization whenever AZO is used as the middle plasmonic material.

Moving forward in 2022, M.R Islam et al.[36] proposed a bi-cluster and double array-based biosensor with maximum amplitude sensitivity of 3807 RIU^{-1} and maximum wavelength sensitivity of $80,500 \text{ nm/RIU}$. On the same year M.R Islam et al.[20] came up with a highly sensitive quadrature cluster-based surface plasmon resonance photonic crystal fiber (QC-SPR-PCF) sensor for detecting unspecified analytes within the RI span of 1.32 to 1.43. This fiber shows the highest amplitude sensitivity of 5274 RIU^{-1} with ultra-high wavelength sensitivity of $75,000 \text{ nm/RIU}$ at optimum conditions.

2.2 Photonic Crystal Fiber

2.2.1 Brief Overview

Optical fibers are at the heart of today's telecommunications. In any communication, they form the primary transmission medium. The transmittal of data over long distances at much higher bandwidths is done using these optical fibers rather than electrical cables. The total loss of these fiber channels is 0.2 dB/km for 1550 nm . The bandwidth of a single optical fiber link would be about 50 THz . However, due to some of the drawbacks of traditional optical fibers, like low refractive index differences and significant leakage loss, photonic crystal fibers (PCF) came into play to address the above problems. The concept of a PCF was first discussed in 1978 by Yeh et al. He proposed surrounding a fiber core with Bragg grating, which is near one-dimensional photonic crystal.

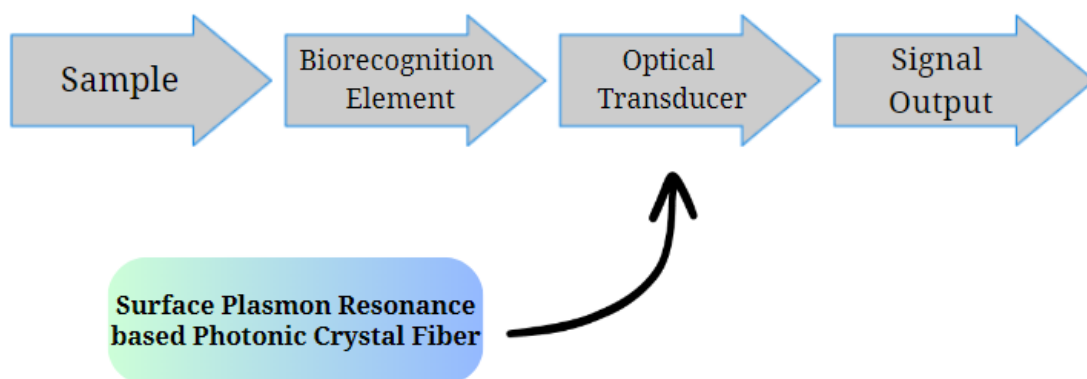


FIGURE 2.1: SPR based PCF - Optical Transducer [37]

Photonic Crystal Fiber or PCF is a type of particular class of optical fiber in which a cladding and air holes enclose the fiber core. The PCFs are fibers with adjustable

geometry and outstanding wave-guiding properties. PCFs have a periodic order of low refractive index material (core) surrounded by a cladding with higher RI. The background material used usually is pure silica, and the low-index results from air capillaries inserted along the entire length of the fiber[38]. Birefringence is an important characteristic for sustaining polarization in porous fiber sensing applications[39]. The guiding properties of the fiber are also affected by changing the shapes of air holes severely. The geometry of the core and cladding areas also play an essential part in the operation of the fiber. With increasing attention to porous core fibers, highly efficient guiding mechanisms in a wide range of applications have been designed, having either even or uneven structures for square, elliptical, hexagonal, decagonal, octagonal, and kagome. These porous core fibers receive more attention due to their meager effective material loss (EML), high birefringence, and higher core power fraction. Thus, one may say that simply by tuning the geometry, a myriad of designs of PCFs become possible.

2.2.2 Guiding Mechanisms

A typical optical fiber allows light to travel inside it through total internal reflection because the refractive index of the core is higher than the cladding, allowing light to be confined within the core. In the case of a photonic crystal fiber (PCF), two different guiding mechanisms for light can be seen, depending on the structure. In solid core PCFs, the total internal reflection may be the same as for conventional fibers because the light is confined to the core. In this case, silica solid can be used to make the core material higher than the cladding's refractive index. The core is surrounded by a network of air capillaries that lower the refractive index of the cladding[40]. These fibers, also known as index-guiding PCFs, guide light in the process of modified TIR.

On the other hand, in hollow-core fibers, the photonic band gap mechanism is exploited. In this guiding mechanism, the core has air holes, which lower the refractive index of the core than the cladding[41]. Thus, light travels due to the existence of a bandgap. We know that the photonic crystal permits only the photons having a bandgap higher than that of the cladding region. The others travel through the core since all these photons are evanescent in the cladding region.

2.2.3 Classification of PCF

PCFs can be broadly classified based on their guiding mechanisms and structural designs. The primary classifications include high index guiding fibers and photonic bandgap fibers. High index guiding fibers, also known as index-guiding PCFs, rely on total internal reflection (TIR) for light propagation, similar to conventional fibers. In contrast,

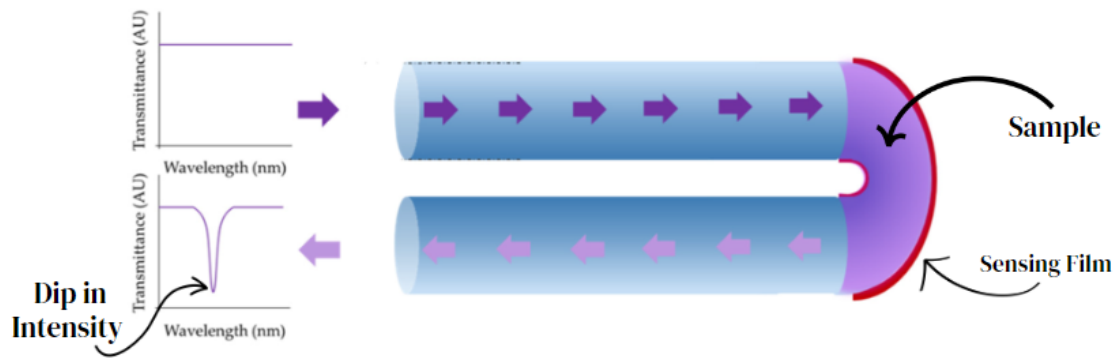


FIGURE 2.2: Change in Transmittance Due to Difference in Light Guidance [42]

photonic bandgap fibers guide light through photonic bandgap effects, where light propagation is prohibited in certain wavelength ranges due to the periodic structure of the fiber.

2.2.4 High Index Guiding Fibers

High index guiding fibers are designed with a solid core surrounded by air holes, creating a higher refractive index in the core compared to the cladding. This design leverages the principle of total internal reflection to confine light within the core. These fibers are advantageous for applications requiring single-mode operation, as they can maintain a single propagation mode over a broad wavelength range. Additionally, high index guiding fibers exhibit low loss and dispersion characteristics, making them suitable for high-speed communication systems.

2.2.5 The Bandgap Effect

The photonic bandgap effect in PCFs arises from the periodic arrangement of air holes in the fiber, which creates a bandgap that prohibits light propagation within certain wavelength ranges. This effect is analogous to electronic bandgaps in semiconductors, where electron movement is restricted within specific energy bands. In PCFs, the photonic bandgap can be engineered by adjusting the size, shape, and arrangement of the air holes. This tunability allows for the development of fibers with tailored transmission properties, enabling applications in wavelength filtering, dispersion management, and sensing.

2.2.6 Hollow-Core and Solid-Core Fibers

PCFs can also be categorized based on the core structure into hollow-core and solid-core fibers. Hollow-core PCFs have a core region consisting of a large air hole, surrounded by a periodic cladding structure. These fibers guide light primarily through the air core, resulting in lower scattering and absorption losses compared to solid-core fibers. Hollow-core PCFs are particularly beneficial for high-power applications and in environments where minimal interaction with the fiber material is desired.

Solid-core PCFs, on the other hand, have a solid glass core surrounded by air holes. These fibers rely on modified total internal reflection and photonic bandgap effects for light guidance. Solid-core PCFs offer flexibility in design and can be optimized for various applications, including nonlinear optics, dispersion compensation, and sensing. The interplay between the core and cladding structures in solid-core PCFs enables precise control over the fiber's optical properties [43].

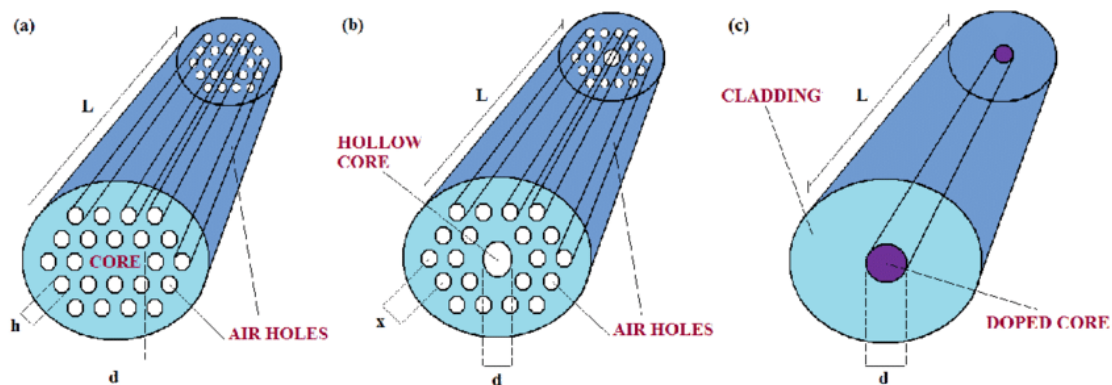


FIGURE 2.3: Different Types of Cores (a) Solid Core, (b) Hollow Core, (c) Doped Core [43]

2.3 Surface Plasmon Resonance

2.3.1 Brief Overview

Surface plasmon resonance (SPR) is an effect in which electrons present at the surface of a metal layer are excited by incident light photons with a specific angle of incidence and then travel along the metal surface.[44] The surface plasmon resonance is initiated when a photon of directed light incidents on a metal surface, called the plasmonic material. At a certain angle of incidence, part of the light interacts with the surface electrons, which are excited to move. These moving electrons are now called plasmons and propagate along the surface of the metal. Part of this energy of the light is then reflected off

the metal. The incidence angle is very sensitive to minor changes in the surface refractive index and the depth of the analyte and plasmonic material layer, respectively.[45] Therefore, an analyte is detected by monitoring the change in reflected light reaching a detector.

2.3.2 Basic Working Principle

The working principle of SPR involves the excitation of surface plasmons by incident light. When polarized light impinges on a thin metal film (typically gold or silver) at the interface with a dielectric medium, it can couple with the electron oscillations if the momentum of the photons matches that of the surface plasmons. This coupling condition is highly sensitive to the refractive index of the dielectric medium adjacent to the metal. Any changes in the refractive index near the surface alter the resonance condition, causing shifts in the reflected light intensity. By monitoring these changes, SPR can be used to detect and measure various biochemical analytes.

Implementing SPR involves several key components: a light source, a prism or grating coupler, a metal film, and a detector. The light source, usually a laser, provides polarized light that is directed onto the prism or grating coupler. The coupler ensures that the light hits the metal film at the correct angle to excite surface plasmons. The metal film, often gold due to its chemical stability and biocompatibility, supports the surface plasmons. The detector, positioned to capture the reflected light, records changes in light intensity corresponding to variations in the refractive index near the metal surface. Advanced SPR systems may also integrate microfluidics to facilitate the controlled delivery of analytes to the sensor surface.

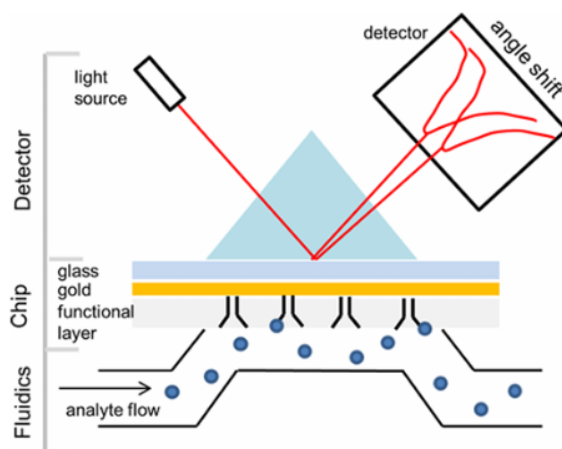


FIGURE 2.4: Surface Plasmon Resonance Based Shift in Transmittance[42]

2.3.3 Surface Plasmon Wave

The process excites the electrons at the metal surface when the frequency of the incident photons is equal to that of the surface electrons. The vibration of these electrons gives rise to an EM wave, referred to as a Surface Plasmon Wave (SPW) that propagates parallel to the surface. The angle of incidence of light on the metal surface to support the SPW highly depends on the refractive index (RI) at the surface. Therefore, small changes in the RI can lead to significant changes in the reflected wave, which is the core of the SPR phenomenon.[46]

2.3.4 Evanescent field

Total Internal Reflection occurs in optical sensors that restrict the light within the core and, therefore, pass it from one end to the other. For light reflecting at angles less than the critical angle, an equal amount of power is conducted to the cladding medium. The phenomenon is what is called the evanescent wave. Energy becomes very much attenuated in the cladding. Identification events that are surface-specific can be probed in real time in this field. The idea of wave penetration to cladding distance helps to make the evanescent wave more interactable with materials around the core, far from its boundary.[47]

2.4 Utility of SPR PCFs

Surface Plasmon Resonance (SPR) technology has garnered significant interest among researchers due to its numerous benefits:

1. **Label-Free Detection:** SPR technology detects analytes by utilizing differences in the refractive index, eliminating the need for labels. This allows for real-time inspection of biomolecular interactions among proteins, RNA/DNA, and small molecules.
2. **Recyclable Sensor Chips:** The performance and quality of data are heavily dependent on the sensor chips used in SPR technology. Remarkably, these sensor chips can be recycled, which enhances their utility and cost-effectiveness.
3. **Small Sample Sizes:** SPR technology requires only minimal sample volumes for its operations, making it cost-effective and enabling the use of less expensive materials.
4. **Handling Complex Samples:** SPR can be employed even with unrefined samples, making it suitable for analyzing complex matrices such as serum.

5. **Replicable Measurements:** SPR technology allows for repeated injections of samples at similar concentrations throughout a run, ensuring consistent results. This consistency across different days enhances the reliability of rate constants and the accuracy of results.
6. **Real-Time Monitoring:** SPR provides a cost-effective method for observing biomolecular interactions in real time. This capability is invaluable in the pharmaceutical and medical industries, as well as in genetics, kinetics, and nanoparticle applications.

While SPR is a highly effective sensing technology, it does have some limitations. The success rate of SPR sensors largely depends on the quality of the metal film and the precision of the coupling optics. Imperfections in the metal layer or misalignment of the optical components can reduce sensitivity and accuracy. Additionally, SPR is inherently sensitive to temperature fluctuations, which can affect the refractive index and lead to false readings. To mitigate this, temperature control and compensation mechanisms are often incorporated into SPR systems. Another drawback is the limited penetration depth of the evanescent field, which restricts the detection range to within a few hundred nanometers of the metal surface. Despite these challenges, ongoing advancements in material science and optical engineering continue to enhance the performance and reliability of SPR-based sensors.

2.5 Different SPR Based PCF Sensor Design

2.5.1 Introduction

Surface Plasmon Resonance (SPR) integrated with Photonic Crystal Fiber (PCF) technology has emerged as a highly effective method for developing advanced sensors. These sensors leverage the unique properties of both SPR and PCF to achieve superior sensitivity and specificity in detecting various biochemical analytes. This portion explores different types of SPR-based PCF sensors, highlighting their structural designs, operational principles, and performance characteristics.

2.5.2 Internal Sensing-based Sensor

Internal sensing-based SPR sensors feature a metal coating on the inner surface of the PCF's air holes. This design enables the interaction of the evanescent field with the metal layer, facilitating the excitation of surface plasmons[26]. The internal coating approach can improve sensitivity by maximizing the overlap between the guided mode and the

plasmonic mode. However, achieving uniform metal deposition inside the air holes can be challenging and may require sophisticated fabrication techniques.

2.5.3 External Sensing-based Sensor

External sensing-based SPR sensors apply the metal coating on the outer surface of the PCF. This approach simplifies the fabrication process and avoids the challenges associated with internal coating. The external coating facilitates the interaction of the evanescent field with the metal layer, enabling effective plasmon excitation[48]. Despite its simplicity, external sensing may exhibit lower sensitivity compared to internal designs due to reduced overlap between the guided mode and the plasmonic mode.

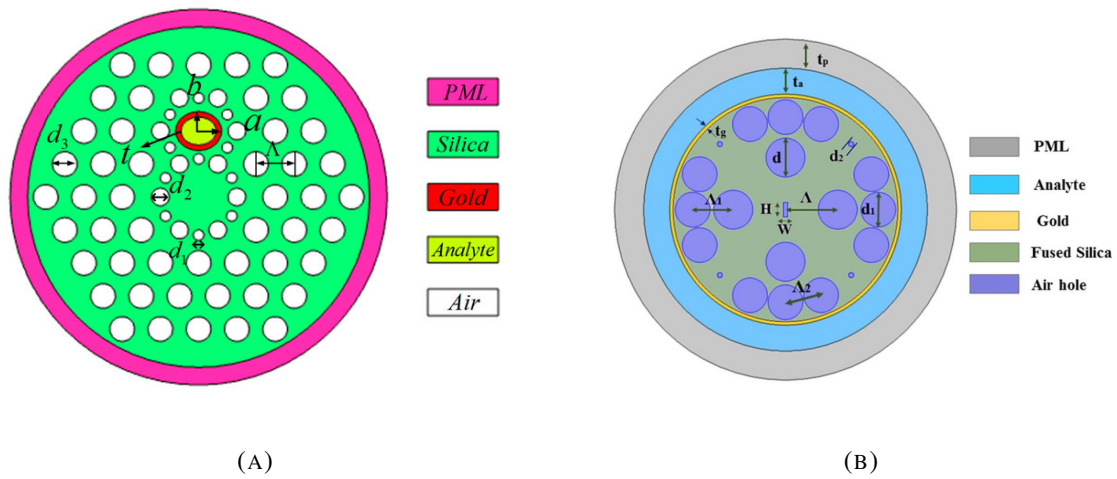


FIGURE 2.5: Different SPR sensors (a) Internal [26], (b) External [48]

2.5.4 Prism-based Sensor

Prism-based SPR sensors utilize a prism to couple light into the metal-coated PCF. The prism facilitates the excitation of surface plasmons by ensuring that the incident light strikes the metal surface at the optimal angle. This configuration allows for efficient coupling and enhanced sensitivity[49]. However, the use of prisms can complicate the design and increase the overall size of the sensor, making it less suitable for compact and portable applications.

2.5.5 D-shaped Sensor

D-shaped SPR sensors involve polishing one side of the PCF to create a flat surface, which is then coated with a thin metal layer. The D-shaped structure allows for the direct interaction of the guided light with the metal surface, enhancing the efficiency

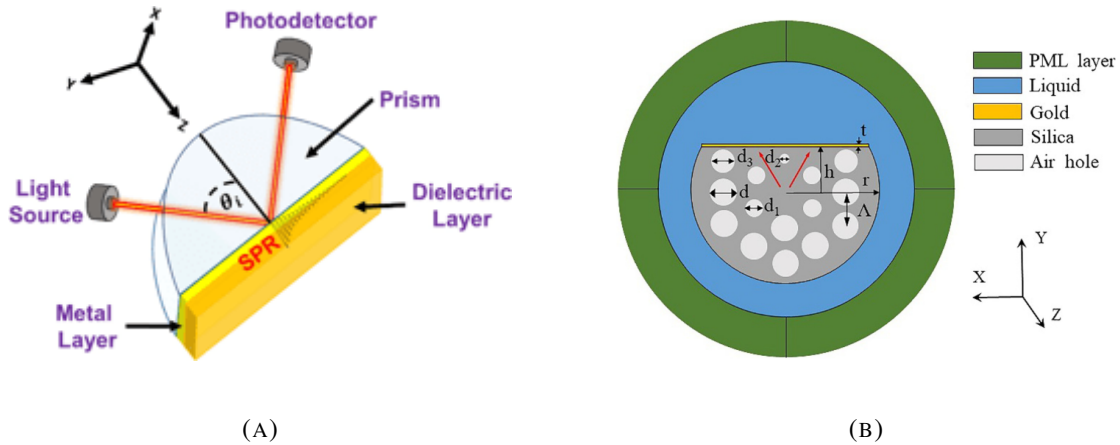


FIGURE 2.6: Different SPR sensors (a) Prism Based [49], (b) D-Shaped [50]

of plasmon excitation. This configuration offers high sensitivity and is relatively easier to fabricate compared to internal sensing designs[50]. Nevertheless, precise polishing is required to achieve the desired flatness, adding complexity to the manufacturing process.

2.5.6 Plasmonic Material Silver-based Sensor

Silver is commonly used as a plasmonic material in SPR-based sensors due to its high conductivity and strong plasmonic response. Silver-based SPR sensors can achieve high sensitivity and sharp resonance peaks, making them suitable for detecting small changes in the refractive index[51]. However, silver is prone to oxidation, which can degrade its performance over time. Protective coatings or alloying with other metals are often employed to mitigate this issue.

2.5.7 Bimetallic Silver-Graphene-based Sensor

Bimetallic sensors combining silver with graphene offer enhanced performance due to the complementary properties of the two materials. Graphene's excellent electrical conductivity and chemical stability, combined with silver's strong plasmonic response, result in sensors with high sensitivity and robustness[27]. The integration of graphene also helps protect silver from oxidation, extending the sensor's operational lifespan.

2.5.8 Bimetallic Silver-Gold-based Sensor

Combining silver with gold in a bimetallic SPR sensor leverages the advantages of both metals. Gold provides chemical stability and biocompatibility, while silver contributes

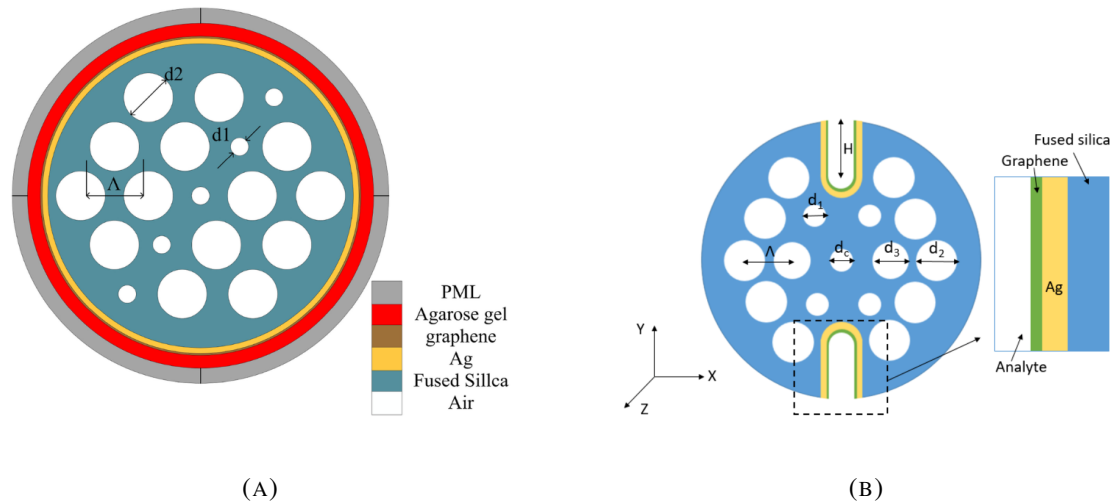


FIGURE 2.7: Different SPR sensors (a) Silver Based [51], (b) Silver Graphene Based [27]

to high plasmonic sensitivity. This combination results in sensors with improved durability and sensitivity. Bimetallic silver-gold sensors are particularly useful in biomedical applications where both performance and stability are critical.

2.5.9 Bimetallic Silver-TiN-based Sensor

Titanium Nitride (TiN) is another material that can be combined with silver to enhance SPR sensor performance. TiN offers excellent thermal stability and corrosion resistance, making it suitable for harsh environments. Bimetallic silver-TiN sensors can achieve high sensitivity while maintaining durability under challenging conditions. This combination is advantageous for industrial applications where sensor longevity is essential.

2.5.10 Plasmonic Material Gold-based Sensor

Gold is a widely used plasmonic material in SPR sensors due to its remarkable chemical stability and biocompatibility. Gold-based SPR sensors exhibit strong plasmonic resonance and high sensitivity[52]. Although gold's plasmonic response is slightly lower than silver, its resistance to oxidation makes it ideal for long-term applications. Gold sensors are extensively used in medical diagnostics and environmental monitoring.

2.5.11 Bimetallic Gold- TiO_2 -based Sensor

Bimetallic sensors that combine gold with Titanium Dioxide (TiO_2) benefit from the synergistic properties of both materials. TiO_2 enhances the stability and sensitivity of the sensor by improving the adhesion of the gold layer and providing a high refractive index contrast[53]. This combination results in sensors with superior performance

for detecting a wide range of analytes, making them suitable for various scientific and industrial applications.

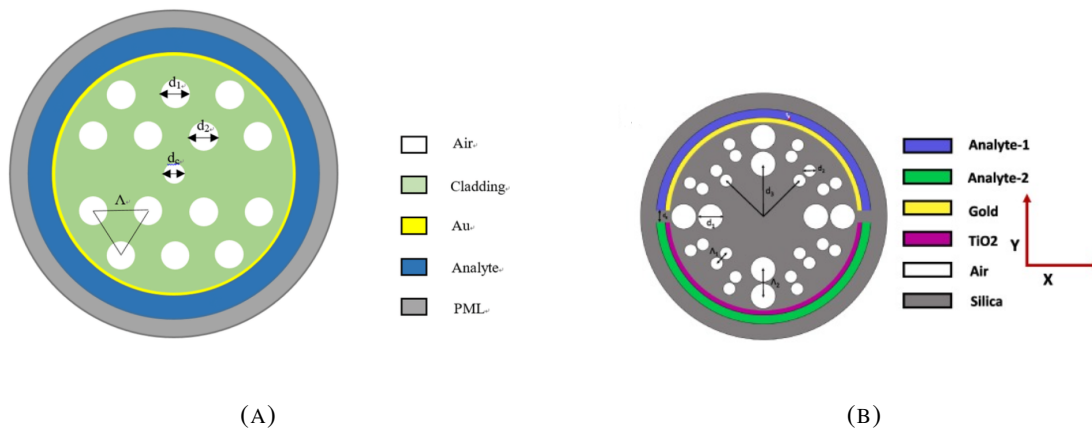


FIGURE 2.8: Different SPR sensors (a) Gold Based [52], (b) Gold TiO_2 Based [53]

2.5.12 ITO-based Sensor

Indium Tin Oxide (ITO) is used in SPR sensors due to its transparency and conductive properties. ITO-based SPR sensors can achieve high sensitivity and broad operational wavelength ranges[54]. The transparency of ITO allows for the integration of additional optical components, enhancing the sensor's versatility. ITO sensors are particularly useful in applications requiring multi-parameter sensing and complex optical setups.

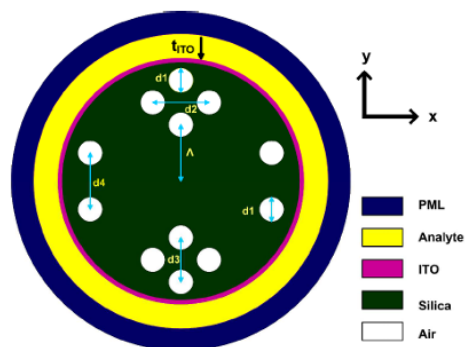


FIGURE 2.9: ITO Based SPR Sensor [54]

Chapter 3

Mathematical Modelling

3.1 Computational study of Performance Parameters

Different parameters have been employed for the formulation of our entire project. Several behavioral parameters of the photonic crystal fiber-based structures can verify their performances. In this section, we have attempted to formalize different aspects, including sensitivity (%), core power fraction (%), effective area (A_{eff}), effective refractive index, effective material loss (EML), numerical aperture, dispersion, confinement loss (CL), which are the basic features of a PCF based sensor. In contrast, wavelength sensitivity (WS), magnetic field sensitivity, amplitude sensitivity (AS), resolution, temperature sensitivity, and the figure of merit (FOM), etc., can evaluate the sensor performance based on SPR. Additionally, to investigate our suggested design for PCF-SPR based filters cross-talk (CT), Extinction ratio (ER), the output power can be taken into account apart from confinement loss. The equations that can be utilized to characterize the materials used for our project have been demonstrated in the later section of this chapter. It's worth noting that these materials' refractive index (RI) is our only point of focus. As a result, we've just presented the RI equations for these materials. We've included permittivity equations in some circumstances because the square root of permittivity equals the RI.

3.2 Conventional PCF sensors' characteristics

3.2.1 Confinement loss (CL)

One of the most crucial performance statistics for measuring PCF sensor performance can be termed as confinement loss because it is required to evaluate all other metrics. The CL denotes the energy diverted from core mode to SPP mode by modified total internal reflection (MTIR). Confinement losses are caused by the imperfect structural design of the PCF. A part of the light energy dispatched through the PCF sensor's core

reaches the metallic layer seeping from the core. The CL is the quantity of energy that is lost as a result of this leakage which can be qualified by[55] -

$$\alpha(dB/cm) = 8.686 \times \left(\frac{2\pi}{\lambda} \right) \times \text{Im}(n_{eff}) \times 10^4 \quad (3.1)$$

The $\text{Im}(n_{eff})$ is expressed as the effective mode index's imaginary part whereas, λ denotes the wavelength. The phase-matching condition occurs when the real component of the effective RI for the core and SPP mode become identical at resonance wavelength. The surge appears to be the confinement loss spectra that can be used to formulate the basis of PCF-SPR sensors and polarization filters.

3.2.2 Effective Material Loss (EML)

The effective material loss (EML) is one of the most important key performance parameters for a PCF. A minimum level of material absorption loss is required to develop the sensing abilities of a sensor for the waveguiding in the THz region. The formula $\alpha(v) = v^2 + 0.63v - 0.13$ (dB/cm) can explain the linear relationship between EML and frequency (v) [56].

3.2.3 Relative Sensitivity

One of the most essential aspects in determining the PCF's adaptability is its relative sensitivity. It defines how much light contacts with the specimen of an analyte. The given formulation can be used to evaluate it quantitatively[57].

$$r = \frac{n_r}{n_{eff}} \times P\% \quad (3.2)$$

Where the RI of the analyte and effective RI is n_r and n_{eff} , respectively. P stands for the power fraction, which is the ratio of % of the power of the air hole to overall power. The given expression can be used to compute it[41]:

$$P = \frac{\int_{\text{sample}} R_e(E_x H_y - E_y H_x) dx dy}{\int_{\text{total}} R_e(E_x H_y - E_y H_x) dx dy} \times 100 \quad (3.3)$$

Where E_x , E_y are the transverse electric fields, and H_x , H_y are the transverse magnetic fields for the fundamental guided mode.

3.2.4 Effective cross-sectional area (A_{eff})

The effective area is the best estimate of the area within the core that is constricted by light. Within this zone, electromagnetic waves propagate. The mathematical methodology can be used to measure effective area accurately[41]:

$$A_{eff} = \frac{[\int I(r)rdr]^2}{[I^2(r)dr]^2} \quad (3.4)$$

The transverse electric field's intensity distribution can be termed as $I(r) = |E(t)|^2$.

3.2.5 Effective refractive index (n_{eff})

The effective refractive index is the ratio of the speed of light in air to the speed of light in the media for the particular polarization to the direction of the axis of propagating light via the guiding structure. Any material's effective RI can be calculated using the formula below.[58] -

$$n_{effpm} = \frac{c}{v_{zpm}} = \frac{\beta_{pm}}{k_0} \quad (3.5)$$

Here, the propagation constant is defined as β_{pm} , And the quantity of waves in a void is $k_0 = \frac{\omega}{c} = \frac{2\pi v}{c} = \frac{2\pi}{\lambda_0}$ Whereas v is the frequency, and wavelength is expressed as λ_0 .

3.2.6 Numerical Aperture

The numerical aperture of fiber is an assessment of its light interaction strength. For a PCF sensor, a greater numerical aperture is preferable since it enhances the light constriction inside the core. The numerical aperture is determined by the following relationship where c, f is the velocity of light and frequency whereas A_{eff} is the effective area[41] -

$$NA = \frac{1}{\sqrt{1 + \frac{\pi A_{eff} f^2}{c^2}}} \quad (3.6)$$

3.2.7 Dispersion

As light travels along the route of a fiber, dispersion describes how light pulses spread out. Dispersion can be divided into two types. Material and waveguide dispersion are the two factors at play. For our project, waveguide dispersion is taken into consideration, which is measured by[59] -

$$\beta_2 = \frac{2}{c} \frac{dn_{eff}}{d\omega} + \frac{\omega}{c} \frac{d^2 n_{eff}}{d\omega^2} \quad (3.7)$$

Where angular frequency is ω , and the rest of the parameters have been already mentioned in the earlier section.

3.3 SPR-PCF based sensors' characteristics

3.3.1 Amplitude Sensitivity

The wavelength and amplitude interrogation techniques are two ways of determining the sensor potential. The variation in loss depth caused by changes in the RI of the analyte can be used to identify unidentified specimens. The amplitude interrogation (intensity-based measuring) approach is a method for detecting different analytes.

$$s_A = -\frac{1}{\alpha(\lambda, n_a)} \frac{\partial_a(\lambda, n_a)}{\partial n_a} (RIU^{-1}) \quad (3.8)$$

Here, $\alpha(\lambda, n_a)$ is the confinement loss for a certain sample RI whereas $\partial_a(\lambda, n_a)$ signifies disparity in analyte confinement loss between two adjacent refractive indices[60].

3.3.2 Wavelength Sensitivity

The wavelength interrogator (spectral-based assessment) technique, which considers the fluctuation in resonance wavelength, is another way to assess the sensor's performance. When compared to the approach mentioned in the earlier section, this method usually has a higher sensitive response. The cost-effectiveness of the phase-detection method (WI method) is one of its

perks. However, there is a consequence, which is the difficulty of assessing sensitivity In this approach[61]. The underlying formula is used to calculate a sensor's sensitivity[33]

$$s_\lambda = \Delta\lambda_{\text{Peak}} / \Delta n_a (nm/RIU) \quad (3.9)$$

The discrepancy between adjacent resonant wavelengths and two refractive indices is expressed as in this scenario λ_{Peak} and Δn_a respectively.

3.3.3 Full Width at Half Maximum

FWHM, or Full Width at Half Maximum, is a measure used in science to describe the width of a peak in a spectrum[62]. It represents the distance between two points on a graph of the spectrum where the intensity is half of its maximum value. This measurement is crucial in fields like spectroscopy, where it determines the resolution of instruments and the ability to distinguish between closely spaced spectral lines or peaks.

A narrower FWHM indicates higher resolution and greater precision in scientific measurements.

$$f(x) = \frac{1}{\sigma\sqrt{2\pi}} \exp \left[-\frac{(x - x_0)^2}{2\sigma^2} \right] \quad (3.10)$$

$$FWHM = 2\sqrt{2\ln 2} \sigma \approx 2.355 \sigma \quad (3.11)$$

3.3.4 Figure of Merit (FOM)

Aside from AS and WS, another measure referred to as the figure of merit is also utilized to estimate sensor efficiency. It's only the proportion between the WS (S_λ) and the FWHM[60]. The breadth of the confinement loss curve at half the peak loss is known as the FWHM. The sharpness of the loss peak is dictated by it. The sharper a sensor's loss peak, the superior its sensing efficiency.

$$FOM = \frac{S_\lambda}{FWHM} (RIU^{-1}) \quad (3.12)$$

3.3.5 Temperature Sensitivity

All of the preceding investigations are usually conducted at a constant temperature. However, in the real world, the weather, as well as the temperature, can change over time. To make the designs more interactive, we can use ethanol as a reagent to determine its temperature sensitivity. The equation can be used to predict temperature sensitivity[63]-

$$S_T = \frac{\Delta\lambda_{\text{Peak}}(T)}{\Delta T} (nm/^\circ C) \quad (3.13)$$

Where $\Delta\lambda_{\text{Peak}}(T)$ is the temperature deviation of the RW peak while ΔT is the difference in temperature.

3.3.6 Magnetic Field (MF) Sensitivity

A magnetic fluid with a refractive index that is affected by the varied MF and temperature should be used to do this investigation. The RI variation of the fluid owing to altering MF and temperature can be calculated using the Langevin function[64]-

$$n = [n_s - n_b] \left[\coth \left(\alpha \frac{H - H_{c,n}}{T} \right) - \frac{T}{\alpha(H - H_{c,n})} \right] + n_b \quad (3.14)$$

T denotes temperature (Kelvin), H is magnetic field strength (Oe), $H_{c,n}$ represents critical field strength, α expresses fitting parameters, n_s defines saturated RI, and n_b can be termed as magnetic fluid's RI for magnetic field strengths less than $H_{c,n}$. The RI of the analyte changes to 1.3808 from 1.3337 as we employed an MF span with a 125 Oe intermission from 0 Oe to 1000 Oe.

The MF sensitivity can be attained from the formulation[65] -

$$S_H = \frac{\Delta\lambda_{\text{Peak}}}{\Delta H} (nm/Oe) \quad (3.15)$$

Where ΔH denotes the variance in the magnetic field.

3.3.7 Resolution

Resolution is a characteristic that aids in determining the sensor's recognition accuracy. The resolution indicates the magnitude of the smallest variation in RI that may be determined. It can be manifested w.r.t amplitude ($R(A)$), wavelength ($R(w)$), temperature (R_T) [60] [63]-

$$R(A) = \frac{\Delta n_a}{s_A} (RIU) \quad (3.16)$$

$$R(w) = \frac{\Delta n_a}{\Delta\lambda_{\text{Peak}}} \times \Delta\lambda_{\text{min}} (RIU) \quad (3.17)$$

$$R_T = \frac{\Delta T \times \Delta\lambda_{\text{min}}}{\Delta\lambda_{\text{Peak}}} (^\circ C) \quad (3.18)$$

Here all the terms are mentioned in the preceding sections except $\Delta\lambda_{\text{min}}$ which defines the minimum wavelength resolution.

3.3.8 Novel dual peak shift sensitivity for structures having two consecutive resonance peaks

There can be sensor designs that may depict two distinct peaks for a particular refractive index (RI) of investigation due to the simultaneous usage of multiple plasmonic material layers (i.e. gold-AZO combination which will be discussed extensively in the forthcoming sections). A unique sensitivity factor named double peak shift sensitivity (s_{P-P}) is appointed, which is characterized by the subsequent formulations and extends the notion of two resonance wavelengths' (RW) peak to peak distance with analyte RI[66]-

$$S_{p-p} = \frac{(\lambda_{p2} - \lambda_{p1})_{n_b} - (\lambda_{p2} - \lambda_{p1})_{n_a}}{n_b - n_a} \times 10^3 (\text{nm}/\text{RIU}) \quad (3.19)$$

$$S_{p-p} = \frac{(\lambda_{p2,n_b} - \lambda_{p22,n_a}) - (\lambda_{p1,n_b} - \lambda_{p1,n_a})}{n_b - n_a} \times 10^3 (\text{nm}/\text{RIU}) \quad (3.20)$$

Primary RWs for consecutive RIs n_b and n_a are λ_{p1,n_b} and λ_{p1,n_a} . Whereas, λ_{p2,n_b} and λ_{p2,n_a} represent the secondary ones.

3.4 SPR-PCF based polarization filters' characteristics

3.4.1 Cross-talk (CT)

One of the most important goals in filter design is to emphasize the discrepancy in confinement losses between the two polarized modes. This phenomenon is best explained by cross-talk (CT), hence a greater CT is recommended. It can also be used to evaluate the signal quality used by polarization filters, which is an essential parameter for calculating the effects of unwanted modes. The following equation can be used to describe it[67]-

$$CT = 20 \lg \{ \exp [(\alpha_2 - \alpha_1) L] \} \quad (3.21)$$

Where L expresses the fiber length and the corresponding CL of x-y polarization modes are α_1 and α_2 .

3.4.2 Output Power (Pout)

When evaluating the filtering features of a polarization filter, one of the most crucial attributes to explore is output power. The following expression can be used to specify it where Pin is the input power, confinement loss is Lc [68] -

$$P_{out}(x, y) = P_{in}(x, y) \exp \left(-Lc(x, y) \times \left(\frac{\ln 10}{10} \right) \times L \right) \quad (3.22)$$

3.4.3 Extinction Ratio (ER)

The extinction ratio is crucial as it determines how well an optical fiber can maintain polarization. In decibels (dB), it compares the optical power on the desired axis to the optical power on the unwanted plane, the orthogonal polarizing condition. The ER is represented by the equation below [68] -

$$ER = 10 \log_{10} \left(\frac{P_{out}(y)}{P_{out}(x)} \right) \quad (3.23)$$

3.4.4 Confinement Loss Ratio (CLR)

The Confinement Loss Ratio (CLR) can be used to measure the filtering performance of a single polarization filter over a given spectral region. The following expression can be used to compute CLR -

$$CLR = \frac{Lc_x}{Lc_y} \quad (3.24)$$

3.5 Computational study of the materials used

3.5.1 Zeonex

Certain polymer materials, including topas, teflon, Zeonex, etc., are favored as bordering constituents in the PCF structures in terahertz applications to obtain improved effective area, high relative sensitivities, and increased core power fraction with lower confinement loss. However, in comparison to other materials, Zeonex should be employed as a background material because of its several significant features [69] -

- Fixed RI (1.529) for a broad span of wavelength
- Lesser absorption loss
- Improved transparency, absorption co-eff, dielectric loss tangents, and thermo-chemical stability.

3.5.2 Air

The PCF is filled with air to fill the voids. Air has a refractive index of almost 1 which remains real in all the cases, which means light travels through the environment at nearly the same speed as it does in a vacuum. We detect refraction with regard to the light path in the air because we are submerged in the atmospheric condition, and simple refraction experiments genuinely quantify Snell's Law with respect to air.

3.5.3 Fused Silica (SiO_2)

Typically, SPR-based sensors are made by laminating plasmonic metal on the surface of a PCF. The PCF can be built out of either glasses or polymers. Fused Silica, also known as silicon dioxide, is the material of choice for the SPR-PCF background. In most cases,

undoped silica is employed. Silica is preferred over other glasses and polymers because of its underlying beneficial characteristics[70] -

- Broader wavelength region possessing better optical transparency
- Lesser absorption and scattering losses
- Greater mechanical resilience
- Higher chemical stability
- Greater damage resistance

The RI of this surrounding component can be defined by the Sellmeier equation [63]

$$n^2(\lambda) = 1 + \frac{B_1\lambda^2}{\lambda^2 - C_1} - \frac{B_2\lambda^2}{\lambda^2 - C_2} - \frac{B_3\lambda^2}{\lambda^2 - C_3} \quad (3.25)$$

Here n represents RI which depends on the λ light wavelength. The corresponding values of the constants $B_1, B_2, B_3, C_1, C_2, C_3$ are 0.696, 0.408, 0.897, $0.0047\mu m^2$, $0.014\mu m^2$, and $97.934\mu m^2$.

Moreover, the adjusted Sellmeier equation for a fixed temperature (T) of 25°C is defined as[63] -

$$\begin{aligned} n^2(\lambda, T) = & (1.31552 + 6.90754 \times 10^{-6}T) \\ & + \frac{(0.788404 + 23.5835 \times 10^{-6}T) \lambda^2}{\lambda^2 - (0.0110199 + 0.584758 \times 10^{-6}T)} \\ & + \frac{(0.91316 + 0.548368 \times 10^{-6}T) \lambda^2}{\lambda^2 - 100} \end{aligned} \quad (3.26)$$

3.5.4 Gold

Because of their high conductivity, metals are good options for plasmonic purposes. Silver and gold are the most frequently utilized metals for plasmonic usage due to their low value of loss in the near-infrared and visible scale. Moreover, silver or gold has been employed as the plasmonic substance in practically all of the key research investigations on plasmonics [71]. Other than these two materials have also been employed in plasmonics, but their application is restricted due to their larger losses. Silver, on the other hand, degrades swiftly when it comes to manufacturing. The other advantages that gold provides due to which we have given preference to it [71][72] -

- Chemical stability
- High stability in air

- Better sensitivity
- No oxidization unlike silver

The Drude-Lorentz model can define the gold's dielectric constant (ε_g) [73] -

$$\varepsilon_g = \varepsilon_\infty - \frac{\omega_D^2}{\omega(\omega + j\gamma_D)} - \frac{\Delta\varepsilon\Omega_L^2}{(\omega^2 - \Omega_L^2) - J\tau_L\omega} \quad (3.27)$$

Where, the angular frequency is ω , damping frequency, and permittivity are defined by $\gamma_D = 31.84\pi$ THz, $\varepsilon_\infty = 5.9673$, respectively. Whereas $\omega_D = 4227.24\pi$ Hz expresses the plasmonic frequency, and $\Delta\varepsilon$ provides weighting factor. Spectral width $\frac{\Gamma_L}{\pi} = 209.72$ THz, and oscillator strength is denoted as $\frac{\Omega_L}{\pi} = 1300.14$ THz.

3.5.5 AZO

Another plasmonic material used as a substitute for gold is aluminum doped Zinc Oxide (2% weight of Al in ZnO), also known as AZO. Despite the oxidation impact on aluminum in the hydrous area, it holds potential. AZO has several benefits over gold as a plasmonic material[72] -

- Higher doping results in decreased losses due to enhanced crystallinity in heavily doped layers
- For wavelengths higher than around $1.8\mu\text{m}$, AZO exhibits metallic characteristics in the NIR
- The doping concentration can be changed to adjust the charge carrier density and hence the plasma frequency

The dielectric property of AZO can be expressed as -

$$\varepsilon_{AZO} = \varepsilon_b - \frac{\omega_p^2}{\omega(\omega + j\gamma_p)} + \frac{f_1\omega_1^2}{(\omega_1^2 - \omega^2 - j\omega\gamma_1)} \quad (3.28)$$

Where $\varepsilon_b = 3.5402$ is defined as the background permittivity and $\omega_p = 1.7473$ eV is the plasma frequency with $f_1 = 0.5095$, $\gamma_1 = 0.1017$ eV, $\gamma_p = 0.04486$ eV, $\omega_1 = 4.2942$ eV.

However, dual plasmonic materials exhibiting gold and AZO can be specified to be used in conjunction to identify analytes with a diverse range of indices of refraction starting from the ultraviolet range to the infrared region. At resonance circumstances, gold and AZO can be combined at three different orientations to form separate double peaks.

3.5.6 Titanium dioxide (TiO_2)

The use of a thin coating of titanium dioxide in between the plasmonic material and the fiber has gained popularity in recent years. The bimetallic layer will show some advantages[74] -

- Enhancement of surface plasmon response
- Accelerating the SPP and core mode coupling
- Alleviation of adhesion issue

The RI of TiO_2 can be defined as follows[33] -

$$n_t = \sqrt{5.913 + \frac{2.441 \times 10^7}{\lambda^2 - 0.803 \times 10^7}} \quad (3.29)$$

3.5.7 Ethanol

We're interested in ethanol because of its temperature sensitivity. Ethanol's refractive index is a real number that changes with temperature. Because of its temperature-sensitive characteristic, ethanol can be used to measure temperature. When the analyte of an SPR-based PCF sensor contains ethanol, the sensor can be used as a temperature sensor. As a result, we ought to determine ethanol's temperature-dependent RI, which may be written as[63]-

$$n_1 = n_0 + \frac{dn}{dT} (T_1 - T_0) \quad (3.30)$$

The ethanol's thermo-optical co-eff is $\frac{dn}{dT} = -3.117 \times 10^{-4} C^{-1}$. n_1 is the RI for temperature T_1 and for $T_0 = 20^\circ C$, the RI is $n_0 = 1.361$. When we steadily lowered the temperature from $70^\circ C$ to $70^\circ C$, the ethanol's RI varies from 1.3454 to 1.3891.

Chapter 4

Proffered Design for Highly Sensitive SPR-PCF Sensor

4.1 Introduction:

Analyte identification through surface plasmon resonance (SPR) has revolutionized optical sensing technology, finding applications in biomedical research, bio-imaging, pathological testing, and more. The interaction between the evanescent field and the sensor's plasmonic material generates oscillations in electrons at the material interface, leading to the formation of surface plasmon waves (SPW). SPR occurs when the electromagnetic (EM) wave and SPW frequencies align, creating a resonance peak. This peak shifts in response to slight changes in the analyte's refractive index (RI). Optimizing the sensor's performance involves fine-tuning structural characteristics and calibration.

This chapter introduces a highly sensitive SPR-based photonic crystal fiber (PCF) designed for detecting unknown solutes with varying RIs, boasting an exceptionally high wavelength sensitivity (WS). The sensor is also capable of analyzing RI changes in an analyte due to temperature and magnetic field variations, making it a versatile tool. To enhance the sensor's performance, a combination of gold (Au) and titanium dioxide (TiO_2) coatings is used, promoting stronger SPR excitation. Eight strategically placed medium air holes within the clustered cladding zone help reduce confinement loss (CL). Another small hole in the middle is intended to increase the sensitivity of the sensor[75]. The sensor's functionality is evaluated by adjusting the thickness of the bimetallic layer, the pitch, and the diameter of the air holes, ensuring alignment with fabrication capabilities.

4.2 Geometrical Structure of Model and Distribution of Field

The structure of a sensor significantly influences its performance. As discussed previously the guiding properties of the sensor are determined by its structural design, specifically the positioning of air holes within the core. **figure: 4.1** illustrates the 2D cross-sectional image of the proposed sensor fiber, which was designed using COMSOL Multiphysics v6.1. The cladding layer features a lattice made up of four clusters of large holes with diameter $d_1=0.9 \mu\text{m}$. In one pair of clusters, three round holes are arranged vertically, while in the other pair, five circular air gaps are positioned horizontally. In the core we have placed a tiny air hole of diameter $d_3=0.2 \mu\text{m}$ to help in guiding the light towards the core and surrounding it is another eight medium sized holes of diameter $d_2=0.5 \mu\text{m}$, equidistant from the center to further reinforce the guidance. The structure and positioning of these air holes significantly influence the fiber's guiding properties and sensing behavior. This cluster design aims to simplify the fabrication process.

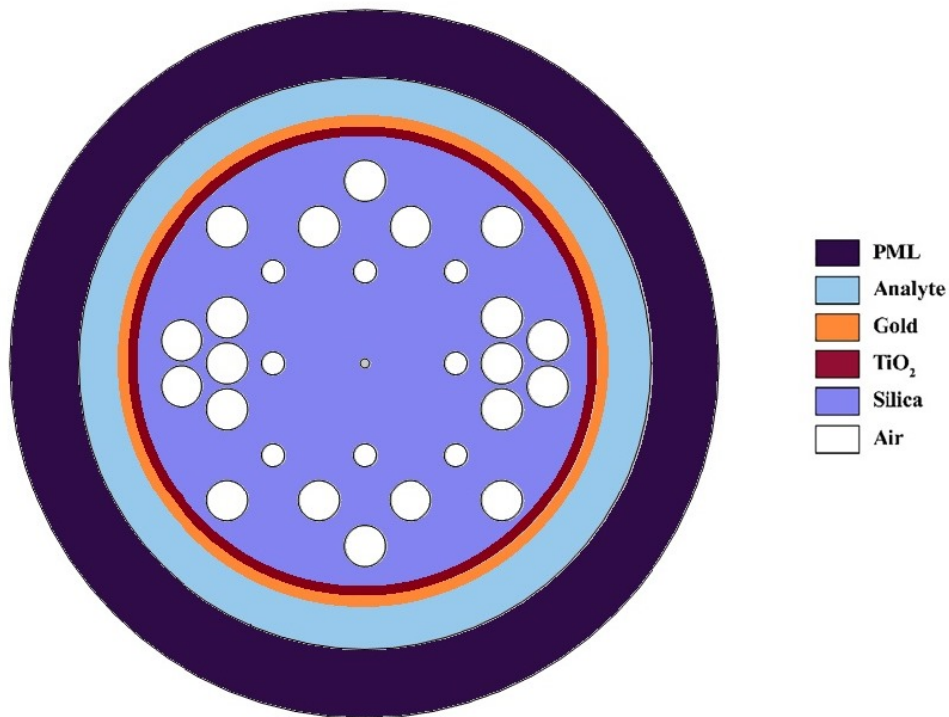


FIGURE 4.1: Proffered Sensor 2D cross-sectional view

The electromagnetic wave is directed and guided from the core to the plasmonic metal through four channels positioned 90 degrees apart. The distance between the centers of any consecutive air holes is known as the pitch. From our experience with other literature we have take a pitch of $p=1 \mu\text{m}$. To minimize light leakage from the core, holes with a diameter d_1 of $0.9 \mu\text{m}$ are inserted into the cladding between the

four clusters. Additionally, a perfectly matched layer (PML) with a thickness t_{PML} of $1.50 \mu\text{m}$ is applied to the outer surface to absorb the radiated evanescent field. This design employs an external sensing technique, which is particularly useful for detecting unknown mixtures with varying refractive indices (RI). The sensing layer has a constant thickness t_a of $1.20 \mu\text{m}$ [74]. A thin layer of gold (Au) is used to cover the cladding section, with the film thickness represented as $t_g=30 \text{ nm}$. In addition, a thin layer of TiO_2 with a thickness of $t_t=20 \text{ nm}$ is positioned between the fiber and the gold layer to improve their adhesion. Known for its non-toxicity and compatibility, this TiO_2 layer enhances the interaction between the filter layer and the surface plasmons.

The field distribution of the core mode and the SPP mode, as shown in **figure: 4.2**, results in resonance due to the coupling of the gold layer with the evanescent field, leading to the SPR phenomenon. The resonance wavelength and the peak amplitude of the loss spectrum are two key parameters that depend significantly on the sample being analyzed. The loss peak varies with changes in the RI, meaning each specimen has a distinct confinement loss (CL) peak at a specific resonant frequency.

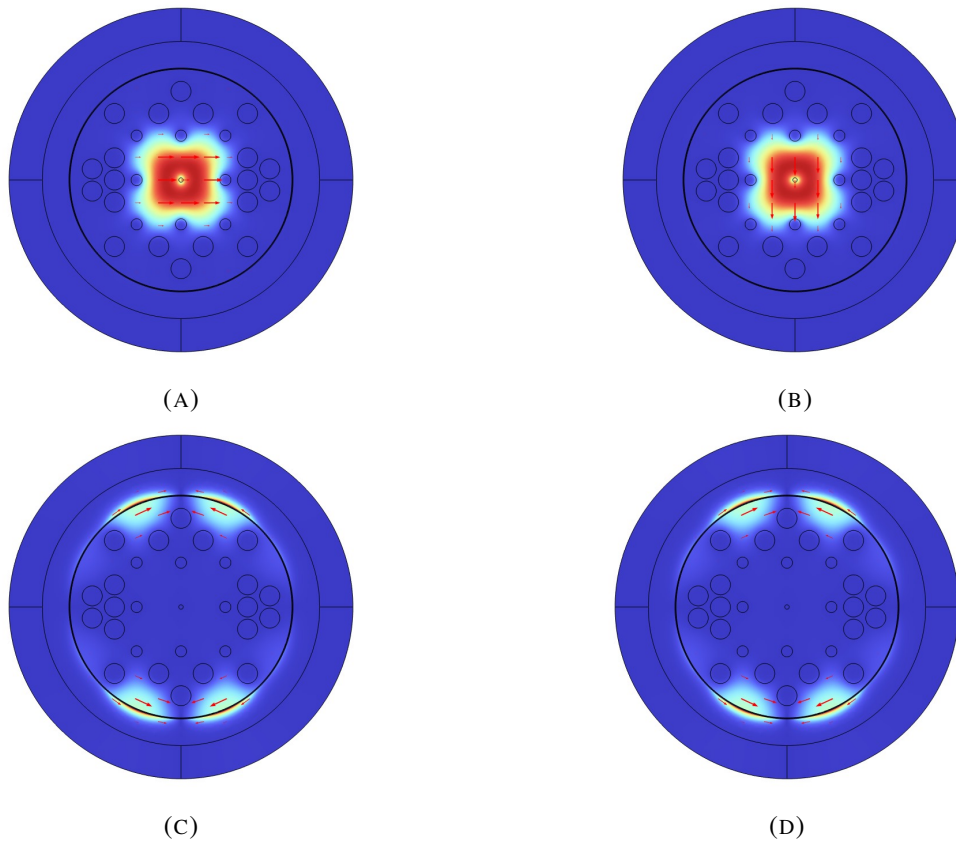


FIGURE 4.2: Field Distribution of (a) core mode (x-pol), (b) core mode (y-pol) and (c) SPP mode (x-pol), (d) SPP mode (y-pol)

Figure: 4.3 & **Figure: 4.4** depicts the dispersion relationship of the SPP and core modes at the pairing phase for an RI of 1.35, in both directional modes. It can be seen

that the real part of the effective mode index n_{eff} of the core mode and the SPP mode decreases with increasing wavelength of the incident light. The lines representing the real part of n_{eff} are associated with a specific wavelength called the envelope wavelength or resonance wavelength (RW). This point is called the equivalent phase state, where the energy transition from the core mode to the SPP mode occurs, resulting in a sharp peak in the CL curve. The RW and peak CL are very sensitive to the RI of the filter. Even small changes in the RI of the filter can shift RW to the left (blueshift) or to the right (redshift), decreasing or increasing CL. Therefore, accurate observation of RW and CL enables efficient analysis of unknown analytes.

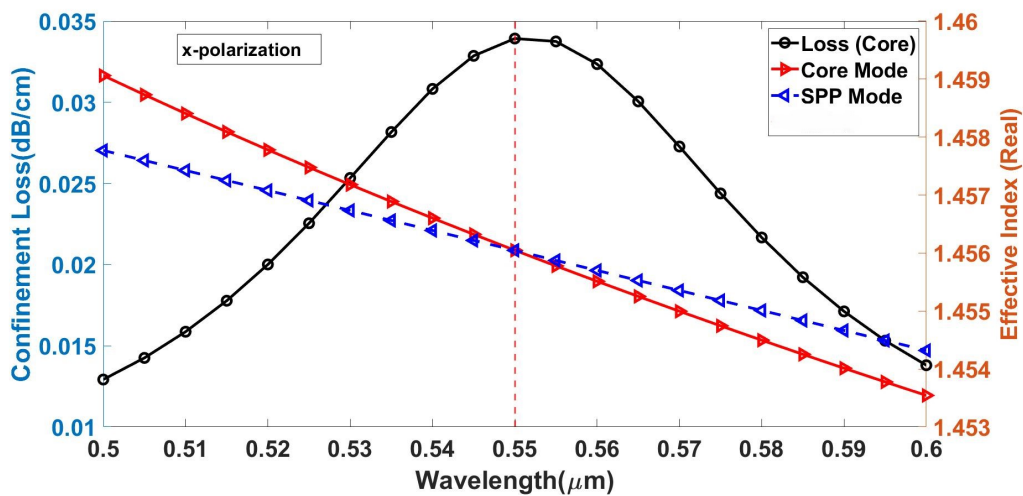


FIGURE 4.3: Dispersion property of the core and SPP mode and loss graph for RI 1.35 [x-pol]

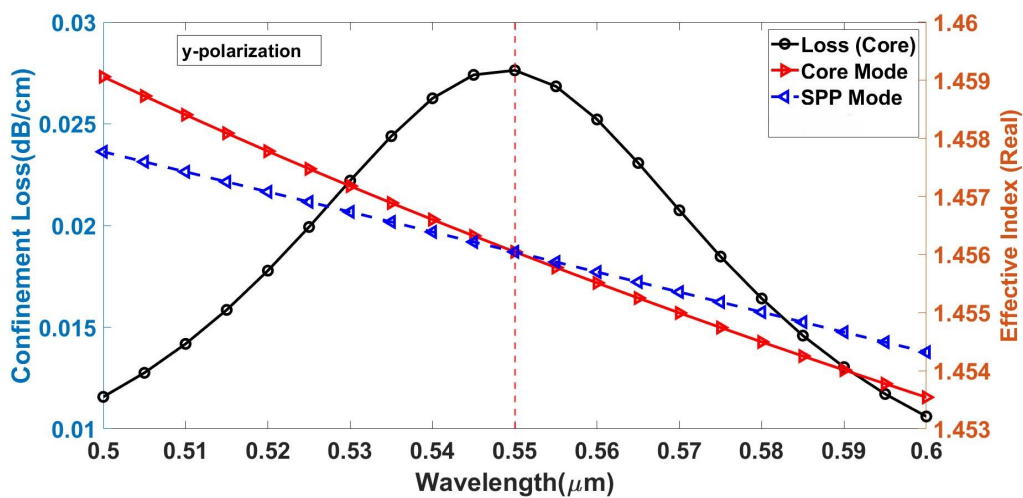


FIGURE 4.4: Dispersion property of the core and SPP mode and loss graph for RI 1.35 [y-pol]

From the figures, we can see that RW is $0.55 \mu\text{m}$ and CL is maximum for both x and y . However, x -polarized light (x -pol) has a higher CL (0.033929 dB/cm) than y -polarized light (y -pol), which has a CL of 0.027635 dB/cm . This indicates a stronger coupling of the x -bias mode. As a result, parameter optimization focuses on the x -pole mode to improve sensor performance.

4.3 Experimental Setup:

The experimental setup for this sensor begins with the initiation of incident light emitted by a supercontinuum light source with a spectrum range of 590 nm to 2500 nm , typically using the SuperK compact from NKTPhotonics™. This light is then directed through a polarizer, controlled by a polarizer controller, and transmitted via a single-mode fiber (SMF-28) into the sensor. After passing through the sensor, the light is sent to an Optical Spectrum Analyzer (AQ6370C, Yokokawa™) through another single-mode fiber. A pump (LSP01_1A) is used to circulate the sample through the sensor. The sensor is connected to a computer for data acquisition and analysis.

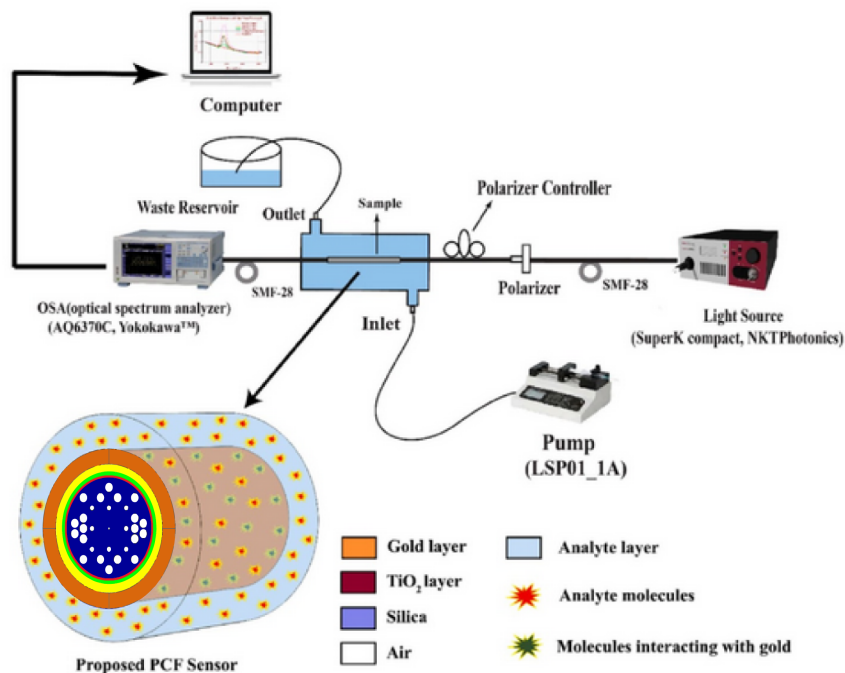


FIGURE 4.5: Experimental Setup

To ensure proper coupling between the sensor and the SMF-28, a technique called splicing is employed. This splicing process can be conducted using the Vytran FFS-2000 splicer, utilizing the filament fusion technique, with alignment facilitated manually through translational and rotational adjustments. Alternatively, another splicing method involves connecting the SMF and the PCF by inserting an etched SMF tip into the PCF,

achieving a reported coupling efficiency of 84.5%. Additionally, various high-efficiency SMF-PCF couplers are available, enabling coupling efficiencies ranging from 80% to 90%.

In the experimental setup, an analyte channel is strategically positioned to allow for the introduction and extraction of the liquid analyte. The analyte is injected into the channel using a programmable micro-injection pumper (LSP01-1A, LongerPump™). The outlet of the channel is connected to a waste reservoir for the storage of used analyte. The presence of various unknown analytes causes the resonance wavelength to shift either towards higher or lower wavelengths. These spectral shifts are detected through the optical spectrum analyzer. Finally, the wavelength peak shifts are analyzed via computer software, displaying the resulting SPR output spectra.

4.4 Design Optimization

A widely accepted method for evaluating sensor performance involves first optimizing the sensor's geometrical parameters and then assessing its response to variations in the analyte's refractive index (RI). In this study, we focus on optimizing parameters such as the thicknesses of the gold (Au) layer, denoted as t_g , and the titanium dioxide (TiO₂) layer, denoted as t_t . Additionally, we consider the diameters of both the four outer air holes and the eight air holes surrounding the central air hole. At the initial stage of optimization, the parameters are set as follows: $t_g = 20$ nm, $t_t = 10$ nm, $d_2 = 0.50$ μm, and $d_3 = 0.2$ μm.

4.4.1 Gold Layer Optimization:

Figure: 4.6 illustrates that increasing the gold thickness from 25 nm to 35 nm shifts the peak of the losses to the right and enhances the resonance wavelength values. For a refractive index (RI) of 1.35, the CL values for gold thicknesses of 25 nm, 30 nm, and 35 nm are 0.049653 dB/cm, 0.056898 dB/cm, and 0.04918 dB/cm, respectively. For RI 1.36, the corresponding CL values are 0.069522 dB/cm, 0.079267 dB/cm, and 0.076449 dB/cm. Additionally, gold thickness of 25 nm offers AS value 115.886 RIU⁻¹ and thickness of 35nm offers AS value 126.819 RIU⁻¹ for this design. The highest AS value of 138.05 RIU⁻¹ is achieved for a thickness of 30 nm, as depicted in **figure: 4.7**, making it the optimized value for further investigation.

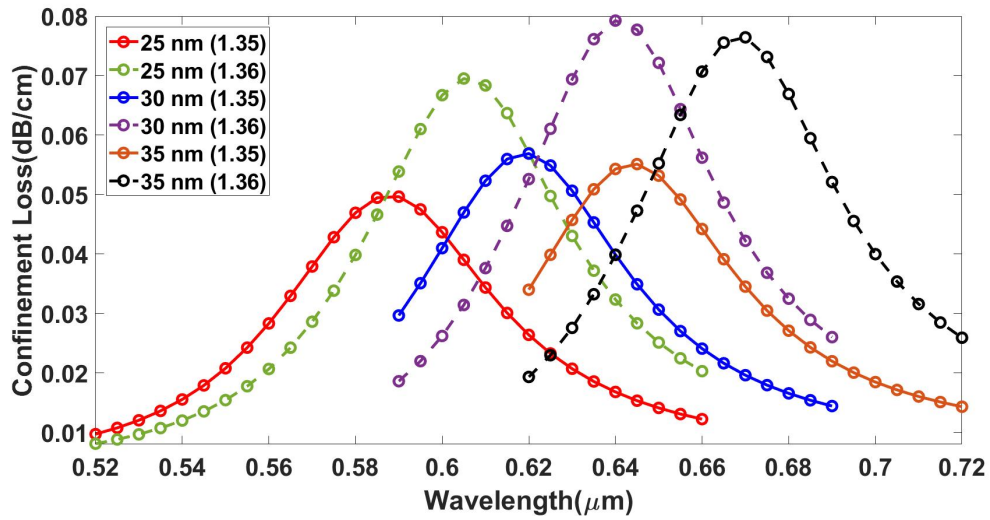


FIGURE 4.6: Confinement loss curves at analyte RI of 1.35 (solid lines) and 1.36 (dashed lines) for $t_g = 25$ nm, 30 nm, 35 nm

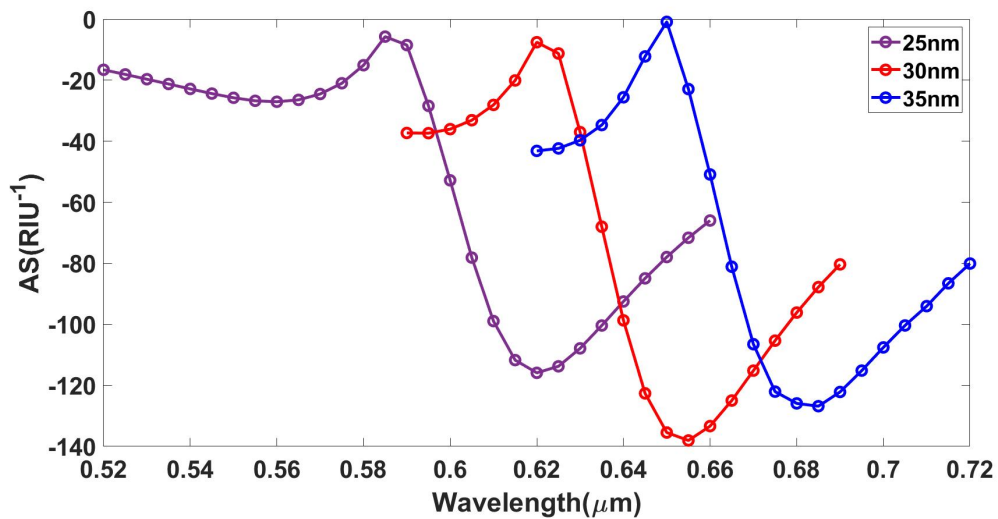


FIGURE 4.7: Amplitude Sensitivity curves for $t_g = 25$ nm, 30 nm, 35 nm at analyte RI of 1.35

4.4.2 TiO_2 Layer Optimization:

In **figure: 4.8**, for a refractive index (RI) value of 1.35, the TiO_2 thicknesses of 15 nm, 20 nm, and 25 nm yield consecutive CL peaks of 0.057997 dB/cm, 0.058555 dB/cm, and 0.059129 dB/cm, respectively. For a RI value of 1.36, the corresponding CL peaks are 0.080486 dB/cm, 0.081625 dB/cm, and 0.081572 dB/cm.

The highest AS value of 147.542 RIU^{-1} is achieved with a TiO_2 layer thickness of 20 nm, as depicted in **figure: 4.9**. Thickness of 15 nm and 25 nm offers AS values 143.115 RIU^{-1} and 144.319 RIU^{-1} respectively. Additionally, the loss at 20 nm is lower than the loss at 15 nm. Consequently, a TiO_2 thickness (t_t) of 20 nm is selected as the optimal thickness due to its high sensitivity.

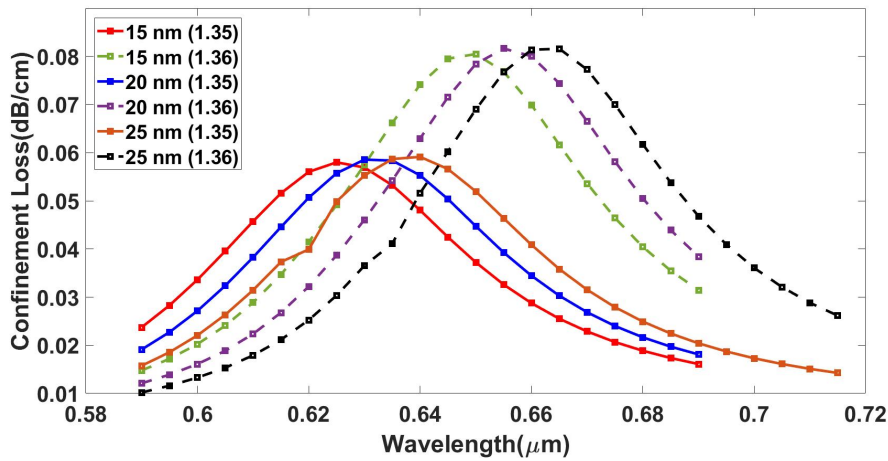


FIGURE 4.8: Confinement loss curves at analyte RI of 1.35 (solid lines) and 1.36 (dashed lines) for $t_t = 15 \text{ nm}$, 20 nm , 25 nm

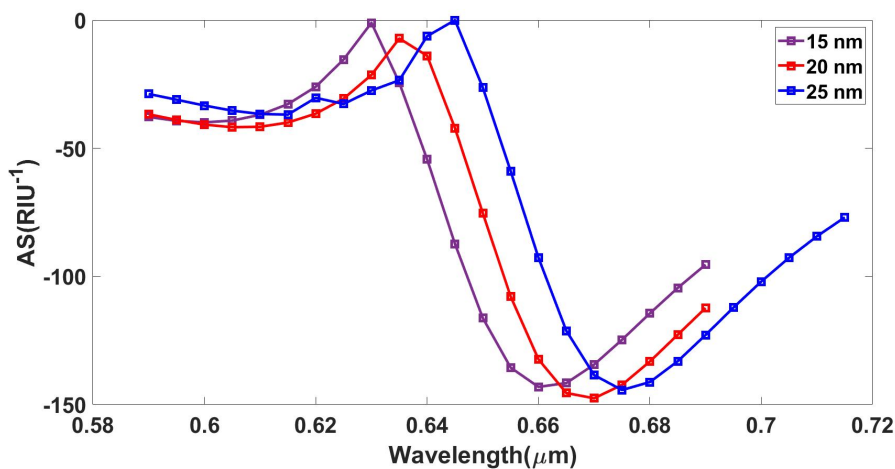


FIGURE 4.9: Amplitude Sensitivity curves for $t_t = 15 \text{ nm}$, 20 nm , 25 nm at analyte RI of 1.35

4.4.3 Air Hole Optimization:

The proposed design, as illustrated in Figure 4.1, incorporates three layers of air holes: outer, middle, and center. The diameters of these air holes are denoted as d_1 for the outer layer, d_2 for the middle layer, and d_3 for the center layer.

Air cavities are strategically positioned within the Photonic Crystal Fiber (PCF) to confine light within the core region. These air holes play a crucial role in guiding light toward the plasmonic layer through specific channels. Consequently, the diameters of these air holes directly influence the Confinement Loss (CL).

To optimize the design, we systematically varied the diameters of both the outer (d_1) and middle (d_2) air holes. It is noteworthy that the Resonant Wavelength (RW) remains stable and unaffected by changes in these parameters, indicating the robustness of the design. This stability is clearly demonstrated in **Figure 4.10** and **Figure 4.12**.

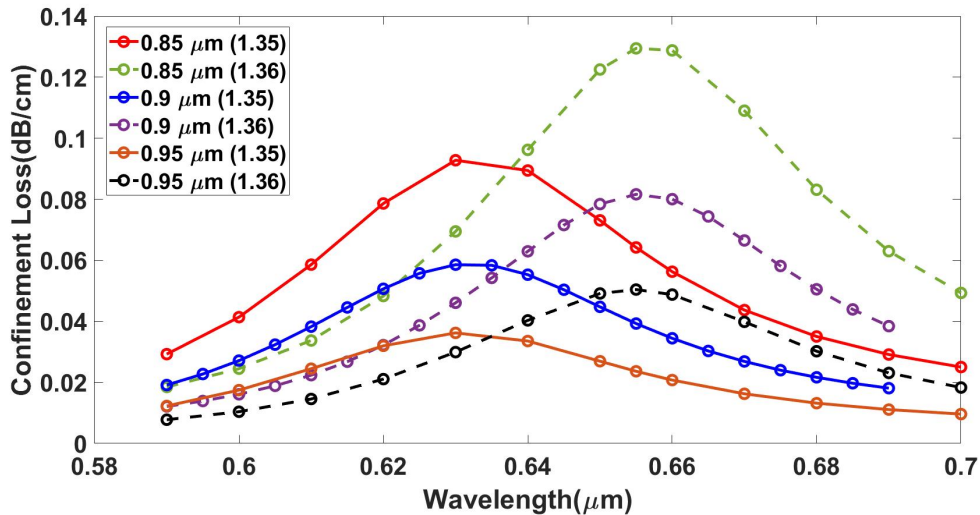


FIGURE 4.10: Confinement loss curves at analyte RI of 1.35 (solid lines) and 1.36 (dashed lines) for $d_1 = 0.85 \mu\text{m}$, $0.9 \mu\text{m}$, and $0.95 \mu\text{m}$.

In our optimization process, the outer air hole diameter d_1 was varied across three values: $0.85 \mu\text{m}$, $0.9 \mu\text{m}$, and $0.95 \mu\text{m}$, for analyte refractive index (RI) values of 1.35 and 1.36. Among these, the highest Analyte Sensitivity (AS) was achieved with $d_1 = 0.9 \mu\text{m}$, as demonstrated in **Figure 4.11**.

Similarly, the middle air hole diameter d_2 was varied at $0.4 \mu\text{m}$, $0.5 \mu\text{m}$, and $0.6 \mu\text{m}$ for the same analyte RI values. The optimization results indicate that the maximum AS was observed when d_2 was set to $0.5 \mu\text{m}$, as illustrated in **Figure 4.13**.

To optimize the design, d_1 was varied at $0.85 \mu\text{m}$, $0.9 \mu\text{m}$, and $0.95 \mu\text{m}$ for analyte RI values of 1.35 and 1.36. The highest AS was achieved with $d_1 = 0.9 \mu\text{m}$, as shown in **Figure 4.11**.

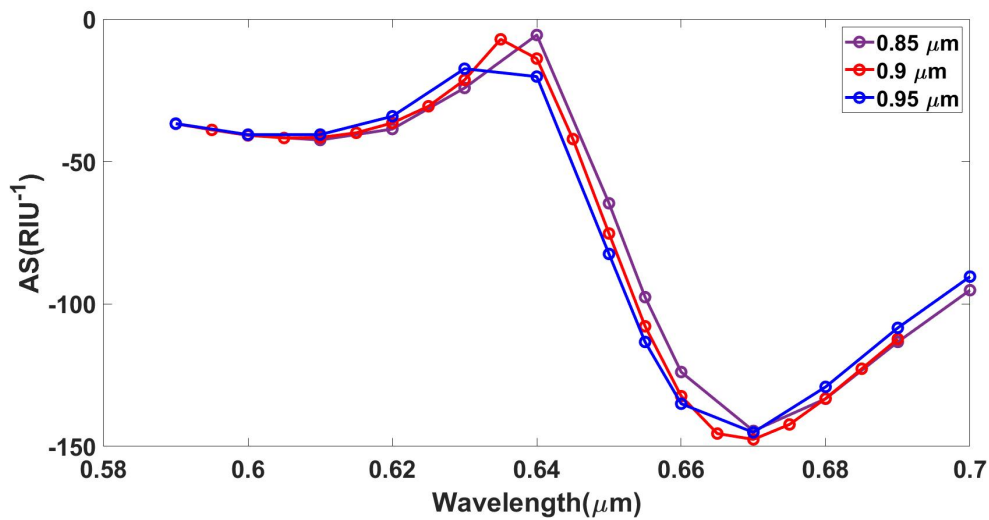


FIGURE 4.11: Amplitude Sensitivity curves for for $d_1 = 0.85 \mu\text{m}$, $0.9 \mu\text{m}$, and $0.95 \mu\text{m}$ at analyte RI of 1.35

Again for optimization, d_2 was varied at 0.4 , 0.5 , and $0.6 \mu\text{m}$ for analyte RI values of 1.35 and 1.36 . The maximum Analyte Sensitivity (AS) was observed with $d_2 = 0.5 \mu\text{m}$, as illustrated in **Figure 4.11**.

To prevent the overlapping of air cavities and reduce fabrication complexity, further expansion of these cavities is restricted.

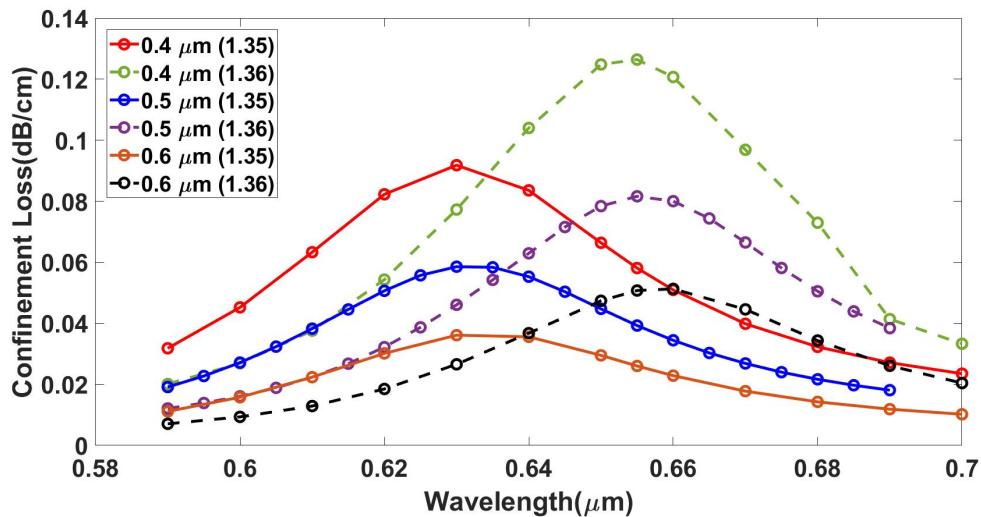


FIGURE 4.12: Confinement loss curves at analyte RI of 1.35 (solid lines) and 1.36 (dashed lines) for $d_2 = 0.4 \mu\text{m}$, $0.5 \mu\text{m}$, and $0.6 \mu\text{m}$.

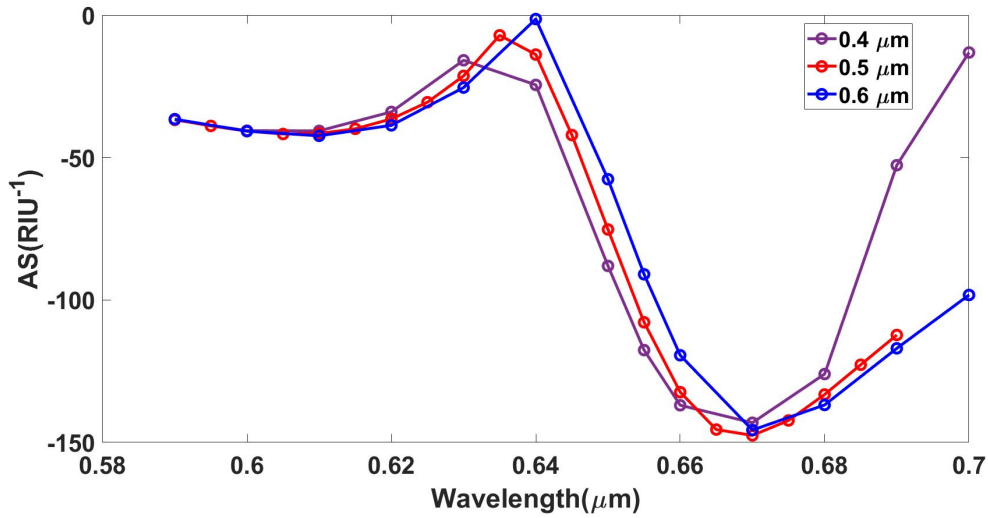


FIGURE 4.13: Amplitude Sensitivity curves for for $d_2 = 0.4 \mu\text{m}$, $0.5 \mu\text{m}$, and $0.6 \mu\text{m}$ at analyte RI of 1.35

4.4.4 Analysis of sensor performance at optimized parameters:

To evaluate the proposed sensor, the CL and AS of various analytes are studied across different RI values. The parameters t_t and t_g are kept at their optimal levels of 20nm and 30nm respectively to evaluate the RI.

The methodology for detecting incognito analytes using a sensor involves closely monitoring the CL and the shift in RW. A greater change in CL and RW indicates improved sensor performance. **Figure 4.14**, **Figure 4.15**, **Figure 4.17** & **Figure 4.18** illustrates the variations in CL and RW as the analyte's refractive index (RI) changes for both x- and y-polarization modes. As the analyte RI increases, the CL expands, and the RW shifts to the right; conversely, a decrease in analyte RI results in a contraction of CL and a leftward shift in RW.

The sensor performance analysis, conducted across a refractive index (RI) range of 1.35 to 1.42, reveals a progressive increase in wavelength shifts (RW) for both X and Y polarizations. Changes in the real part of their RIs lead to a shift in the phase matching position of the core-guided and SPP modes' wavelengths. A higher analyte RI results in less energy transfer from the core to the SPP mode, causing a rightward shift in the resonance wavelength (RW)[76].

As the RI increases, the intervals between consecutive wavelength shifts also increase. Starting with an interval of 25 nm for both X and Y polarizations from RI 1.35 to 1.36, the shifts progressively grow larger. Specifically, the interval increases to 30 nm from 1.36 to 1.37, and then to 40 nm from 1.37 to 1.38. A slightly larger shift is observed from 1.38 to 1.39, with the X polarization shifting by 50 nm and the Y polarization by 40 nm. This trend continues, with the interval expanding to 80 nm and 75 nm

for X and Y polarizations, respectively, from 1.39 to 1.40. A significant jump occurs between 1.40 and 1.41, with the X polarization shifting by 165 nm and the Y polarization by 130 nm. The most dramatic increase is seen from RI 1.41 to 1.42, where the intervals surge to 1340 nm for X polarization and 1250 nm for Y polarization. The highest wavelength sensitivity (WS) of 134000 nm/RIU for x-polarization and 125000 nm/RIU for y-polarization is obtained due to the this RW shift. This pattern of increasing shifts indicates a strong response of the sensor to higher refractive indices.

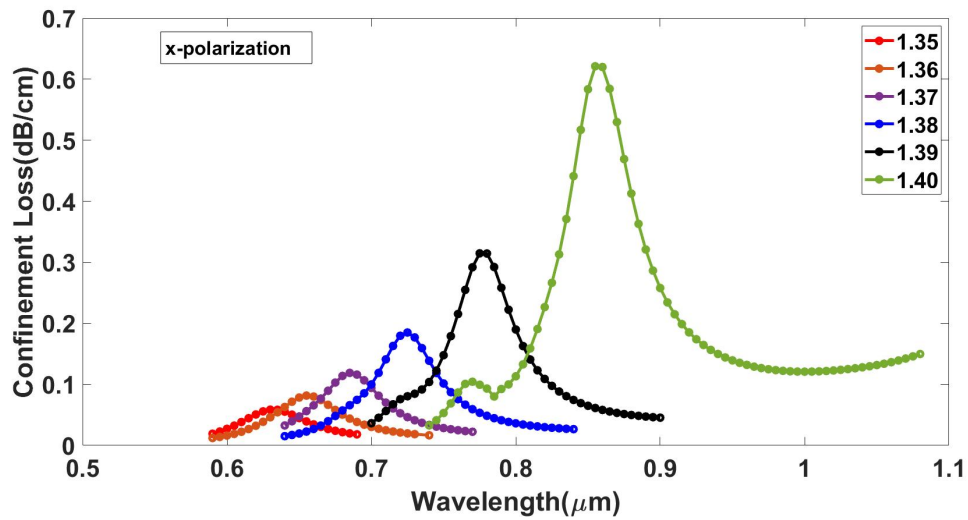


FIGURE 4.14: Confinement Loss curves for x-pol (RI 1.35-1.40)

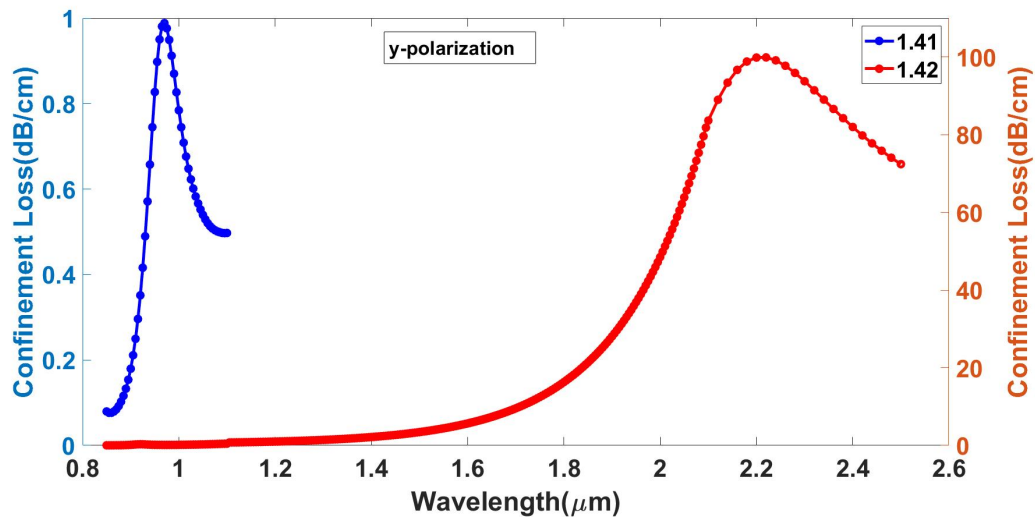


FIGURE 4.15: Confinement Loss curves for x-pol (RI 1.41-1.42)

The modification of the analyte's RI significantly affects the CL, leading to substantial changes in amplitude sensitivity (AS). **Figure 4.16** & **Figure 4.19**, illustrate the relationship between AS and variations in RI for both x- and y-polarization modes. It is

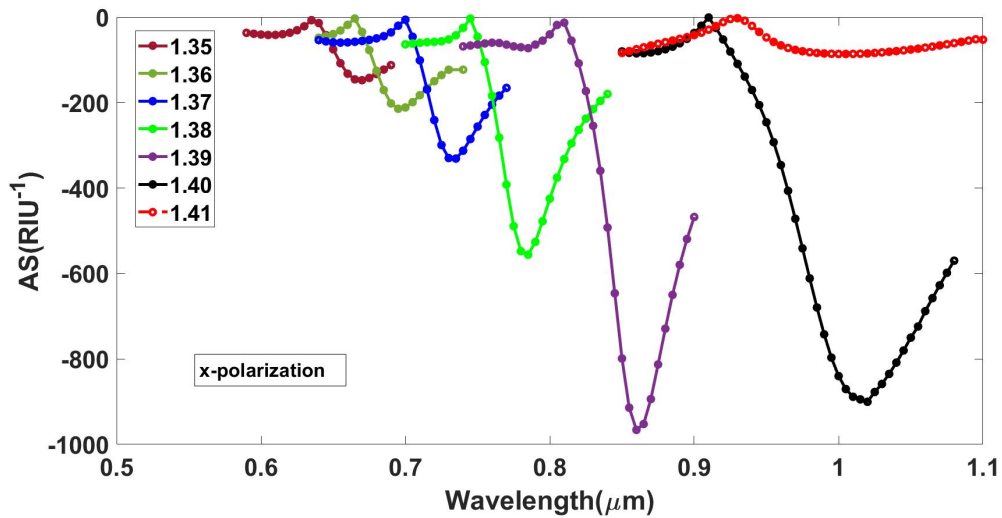


FIGURE 4.16: Amplitude Sensitivity Curves for X-pol

evident that as the RI increases, AS also enhances. However, a sharp decline in AS is observed at an analyte RI of 1.41. Despite this reduction, the maximum AS achieved is 965.976 RIU^{-1} for x-polarization at RI 1.39 and 1167.53 RIU^{-1} for y-polarization at RI 1.41. Furthermore, the sensor's maximum resolution, in terms of AS, is observed to be 4.0×10^{-4} for x-polarization and 5.0×10^{-4} for y-polarization.

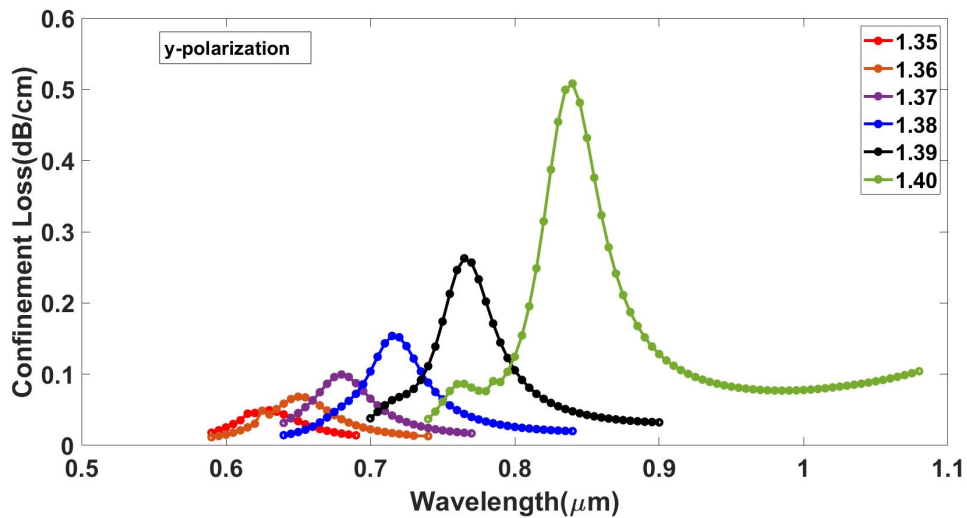


FIGURE 4.17: Confinement Loss curves for y-pol (RI 1.35-1.40)

In addition to the enhanced AS and WS, our proposed sensor demonstrated good performance in terms of the figure of merit (FOM). The sensor exhibited strong FOM values, with the highest values recorded at 832.422 for x-polarization and 1246.99 for y-polarization, both at an analyte RI of 1.41. The FWHM and FOM values for each RI are detailed in Table 4.1.

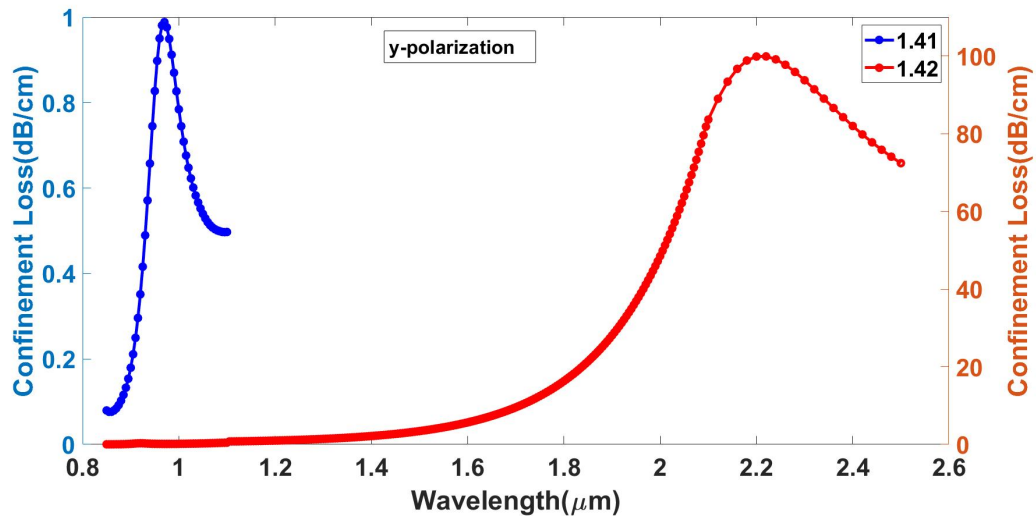


FIGURE 4.18: Confinement Loss curves for y-pol (RI 1.31-1.42)

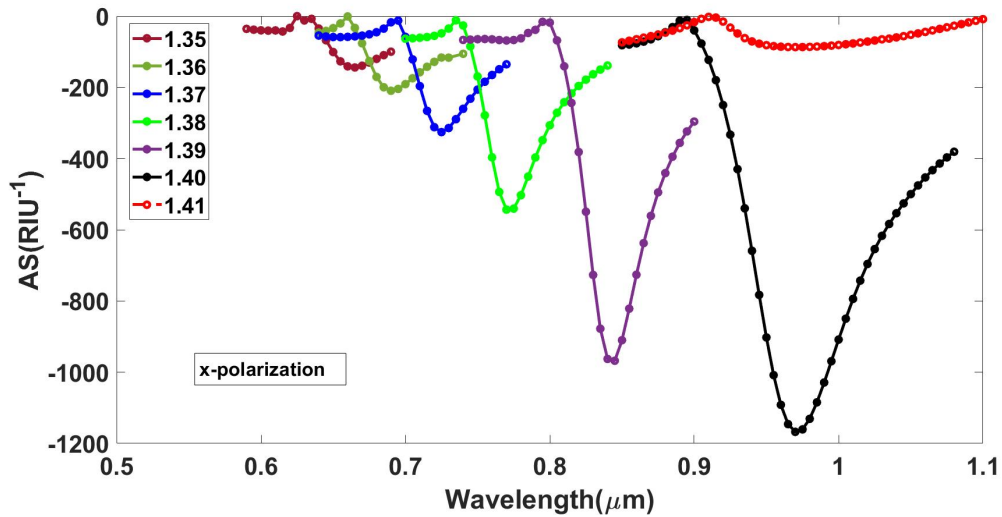


FIGURE 4.19: Amplitude Sensitivity Curves for Y-pol

In **Figure 4.20**, the relationship between the resonance wavelength (RW) and the analyte refractive index (RI) is illustrated, along with the polynomial fitting curves of the 3rd and 4th order. The coefficient of determination (R^2) for the 3rd order fit is 0.9430, whereas the 4th order fit yields a higher R^2 value of 0.9538, indicating that the 4th order polynomial provides a more accurate fit.

The fitting curve is represented by the equation $y = A + Bx + Cx^2 + Dx^3 + Ex^4$, where x denotes the analyte RI and y represents the RW. The coefficients A , B , C , D , and E are calculated as 379178.9688, -1137161.719, 1277617.5, -637365.9375, and 119130.0586, respectively. Additionally, **Figure 4.22** displays the corresponding sensor lengths for various RI values. As sensor length is inversely related to the CL, it decreases with increasing RI. The figure suggests that sensors with lengths ranging from

millimeters to centimeters are suitable for practical sensing applications.

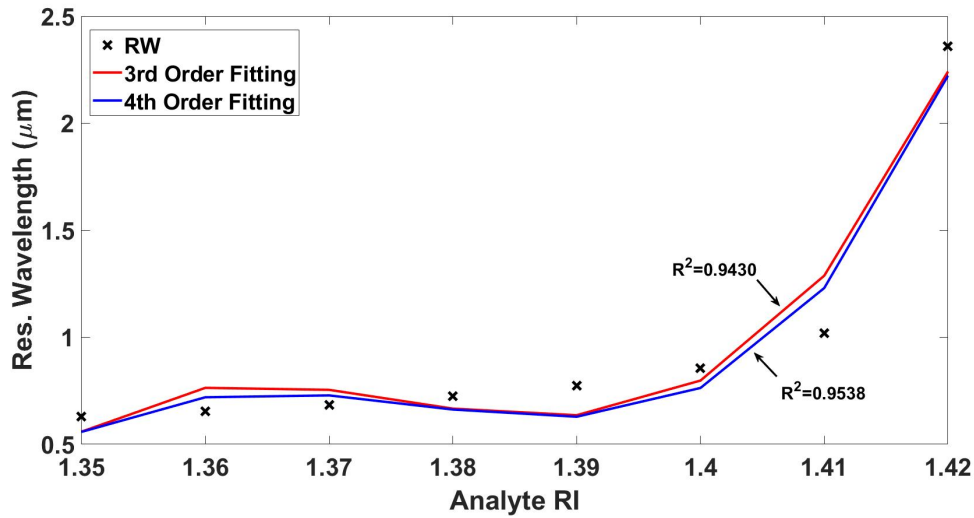


FIGURE 4.20: Polynomial fitting curve for the relationship between RI and RW in the x-polarized mode.

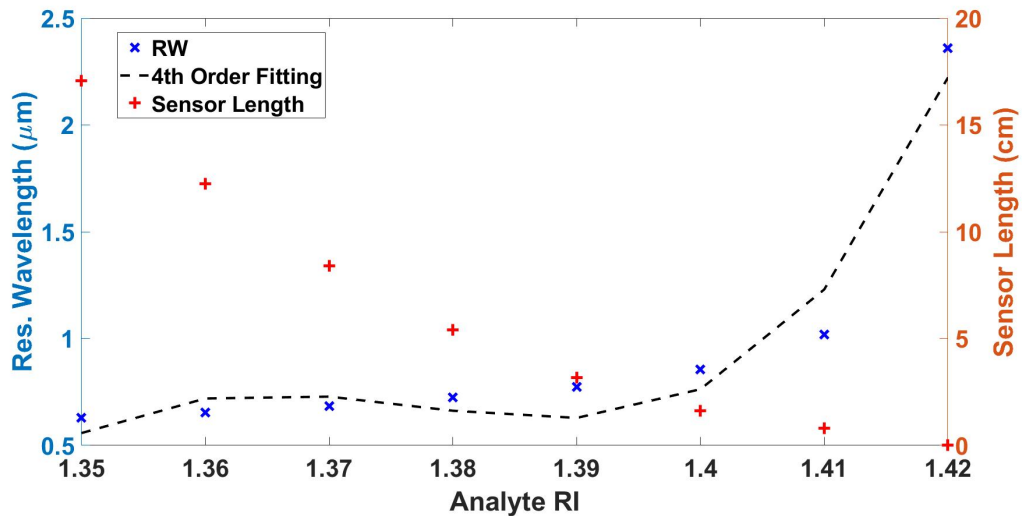


FIGURE 4.21: Plotting of RW and sensor length with varying analyte RI

In addition to other performance metrics, the birefringence of our sensor was analyzed. Birefringence is a key parameter, as sensors with high birefringence can exhibit markedly different sensitivities depending on the polarization mode of the incoming light [60]. Furthermore, birefringent sensors are particularly effective at preserving the polarization state of the input signal [60], which eliminates polarization mode dispersion (PMD) and contributes to greater operational stability of the optical system [77]. Given these advantages for sensing applications, achieving high birefringence is highly desirable. Our sensor demonstrated a maximum birefringence of $19.80034414 \times 10^{-4}$

at an analyte RI of 1.42. This notable birefringence was achieved through the strategic arrangement of circular air holes in the sensor design, without adding to the complexity of fabrication. **Figure 4.21** presents the birefringence observed at an analyte RI of 1.42.

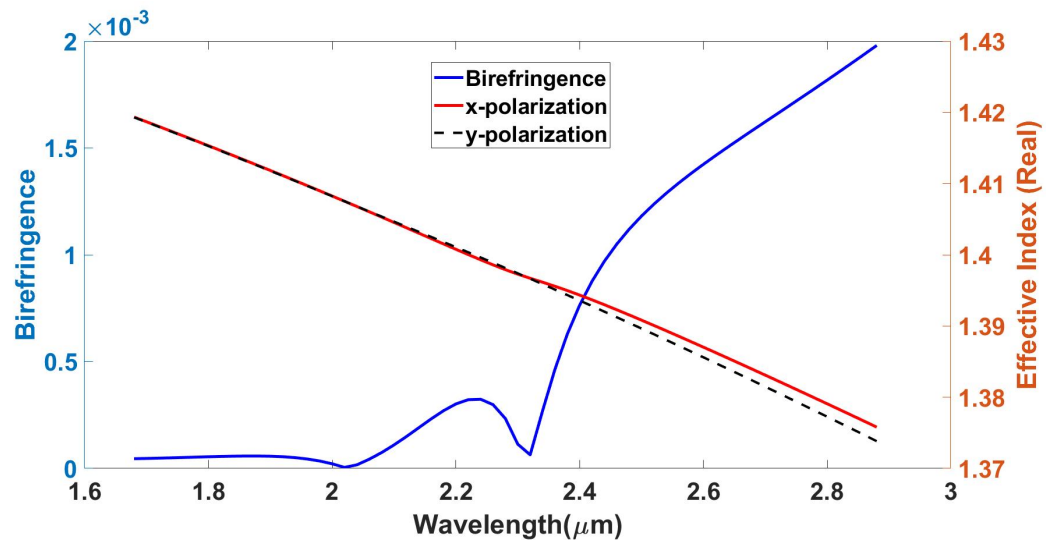


FIGURE 4.22: Plotting birefringence and the real part of the effective refractive index as a function of wavelength

4.5 Final Results & Comparative Analysis:

We conducted the sensor performance evaluation within the RI range of 1.35–1.42. This range is essential because many critical biological agents and biochemical solutions fall within these refractive indices. Our sensor can identify several prominent analytes, including acetone (1.36), silicone oil (1.403), ethanol (1.36), glucose solutions in water (10% solution = 1.3477, 20% solution = 1.3635), ethylene tetrafluoroethylene (1.403), white blood cells (1.36), human liver (1.369), blood plasma (1.35), human urine concentration (1.3415–1.3464), red blood cells (1.40), hemoglobin (1.38), cervical cancer cells (HeLa), skin cancer cells (Basal), blood cancer cells (Jurkat), adrenal gland cancer cells (PC12), and breast cancer cells (MDA-MB-231 and MCF-7) (1.36–1.40), among others.

Detailed values for different performance parameters of the sensor across various RIs are provided in **Table 4.1** below:

RI	CL (dB/cm)		RW (nm)		WS (nm/RIU)		Resolution (WS) ($\times 10^{-4}$)		AS (RIU ⁻¹)		FWHM		FOM		Biref. ($\times 10^{-4}$)
	X	Y	X	Y	X	Y	X	Y	X	Y	X	Y	X	Y	
1.35	0.059	0.049	630	630	2500	2000	4.00	5.00	147.54	144.07	62.98	62.24	39.69	32.13	0.01
1.36	0.082	0.068	655	650	3000	3000	3.33	3.33	214.42	209.52	61.17	61.54	49.04	48.75	0.02
1.37	0.119	0.100	685	680	4000	3500	2.50	2.86	330.99	325.62	58.81	56.81	68.01	61.61	0.02
1.38	0.185	0.154	725	715	5000	5000	2.00	2.00	555.90	543.30	58.83	55.73	84.99	89.73	0.03
1.39	0.315	0.263	775	765	8000	7500	1.25	1.33	965.98	967.84	56.87	52.14	140.68	143.84	0.04
1.40	0.621	0.508	855	840	16500	13000	0.61	0.77	900.21	1167.53	62.45	53.17	264.22	244.52	0.08
1.41	1.228	0.988	1020	970	134000	125000	0.07	0.08	86.15	86.95	160.98	100.24	832.42	1246.99	10.34
1.42	388.294	99.897	2360	2220	-	-	-	-	-	-	-	-	-	-	19.80

TABLE 4.1: Sensor performance for analyte RI 1.35–1.42

Table 4.2 provides a comparison between our proposed sensor and existing sensors, focusing on amplitude sensitivity (AS), wavelength sensitivity (WS), resolution, birefringence, and figure of merit (FOM):

Ref.	Amplitude Sensitivity (RIU ⁻¹) Max.	Wavelength Sensitivity (nm/RIU) Max.	Resolution (RIU)	FOM	Biref.	Sensing range
[32]	6829	28000	3.57×10^{-6}	2800	-	1.33–1.42
[60]	1411	25000	4.00×10^{-6}	502	1.60×10^{-3}	1.33–1.38
[74]	1170	34000	2.94×10^{-6}	310	-	1.32–1.41
[78]	2050	111000	9.01×10^{-7}	-	-	1.33–1.43
[79]	1415	62000	1.61×10^{-6}	1140	1.20×10^{-3}	1.33–1.43
[63]	5060	41500	2.11×10^{-6}	1068.7	1.568×10^{-3}	1.32–1.43
This Work x-pol	965.98	134000	0.04×10^{-6}	832.422	1.98×10^{-3}	1.35–1.42
This Work y-pol	1167.53	125000	0.05×10^{-6}	1246.99	-	1.35–1.42

TABLE 4.2: Comparative Analysis of Sensor Performance

Chapter 5

Sensor Fabrication

5.1 Fabrication Process for the Proposed SPR-PCF Sensor

The fabrication of Surface Plasmon Resonance (SPR) based Photonic Crystal Fiber (PCF) sensors incorporating Gold (Au) and Titanium Dioxide (TiO_2) layers involves several critical steps, each designed to ensure the optimal performance and sensitivity of the sensor.

5.2 Design and Preform Preparation

5.2.1 Structural Design:

- **Hexagonal Lattice Structure:** The sensor is based on a hexagonal lattice PCF structure with circular air holes. This configuration is chosen for its favorable guiding properties and ease of fabrication[80].
- **Air Hole Arrangement:** The core consists of three pentagonal clusters of air holes, each cluster containing five air holes. Different diameters are used for the holes: d_1 for smaller holes and d_2 for larger ones[81].

5.2.2 Preform Fabrication:

- **Stack-and-Draw Method:** The preform is fabricated using the stack-and-draw technique. This method involves arranging thick-walled capillaries and solid rods in a hexagonal pattern. The capillaries are initially produced at 100 times their final size and then drawn down to the required dimensions[82].
- **Cleaning and Sealing:** Capillaries are cleaned using acetone and isopropanol (IPA) to remove any impurities. One end of each capillary is sealed to ensure no interstitial holes remain[20].

5.3 Drawing and Structuring

5.3.1 Drawing Process:

- **Preform Heating:** The preform is heated to a softening temperature (typically between 1500°C and 1700°C) to allow it to be drawn into a cane. This process may be repeated several times to achieve the desired dimensions[83].
- **Capillary Formation:** The drawn preform is further processed to form thin-walled and thick-walled capillaries. The dimensions are controlled by adjusting the feeding rate and drawing speed[84].

5.3.2 Assembly:

- **Stacking Capillaries:** The capillaries are stacked into a jacket tube using hexagonal jigs to form the desired lattice structure. This assembly is crucial for defining the core and cladding regions of the PCF[85].
- **Jacket Tube Transfer:** The capillary stack is transferred into a longer jacket tube for final drawing. A glass handle is attached to the preform using a high-temperature H₂-O₂ fuel burner for handling during the drawing process[86].

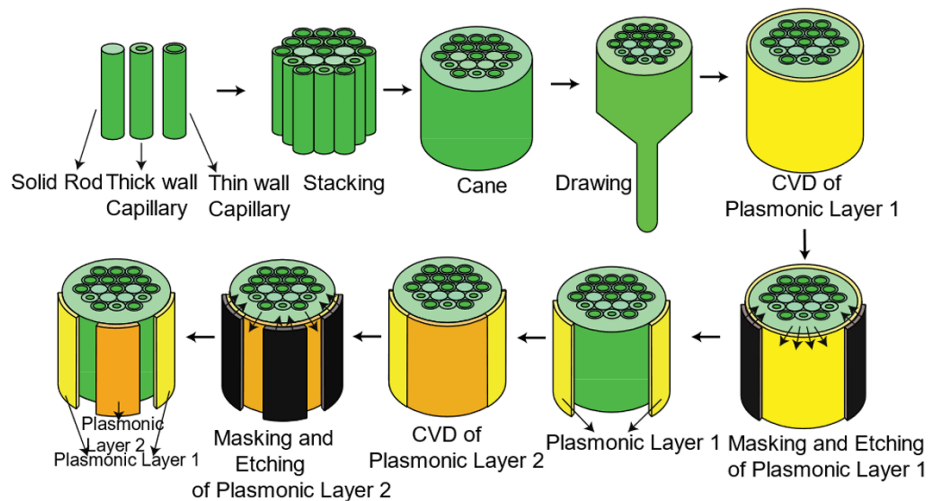


FIGURE 5.1: Stacking, Drawing and Masking

5.4 Coating with Gold and TiO_2

5.4.1 Chemical Vapor Deposition (CVD):

- **TiO_2 Layer Deposition:** A thin layer of TiO_2 is deposited on the fiber surface using the CVD technique. The thickness of the TiO_2 layer is optimized to enhance the adhesion of the gold layer and improve the sensor's performance[87].
- **Gold Layer Deposition:** Following the TiO_2 layer, a thin gold layer is deposited using the same CVD technique. The gold layer thickness is critical for ensuring the sensor's sensitivity and performance[80].

5.4.2 Photolithography:

- **Patterning:** The gold layer is patterned using a two-step photolithography process. Initially, the entire fiber surface is coated with gold, and specific regions are masked off. The exposed areas are then etched away to create the desired pattern. This process is repeated for the TiO_2 layer[20].

5.5 Final Assembly and Testing

5.5.1 Sensor Assembly:

- **Splicing with Single-Mode Fiber (SMF):** The sensor is coupled with a single-mode fiber (SMF-28) using a splicing technique. This ensures efficient light transmission and minimal loss. Techniques such as filament fusion splicing are used to achieve high coupling efficiency[83].
- **Anodization:** The outer surface of the sensor is anodized to improve durability and performance in various environmental conditions[82].

5.5.2 Performance Testing:

- **Sensitivity and Resolution Measurement:** The sensor's performance is evaluated by measuring its wavelength and amplitude sensitivity. The optimal geometric parameters (air hole diameter, pitch, gold and TiO_2 layer thicknesses) are fine-tuned to maximize the sensor's sensitivity and resolution[85].
- **Refractive Index Detection:** The sensor's ability to detect changes in the refractive index (RI) is tested using a controlled setup with a supercontinuum light source and an optical spectrum analyzer[86].

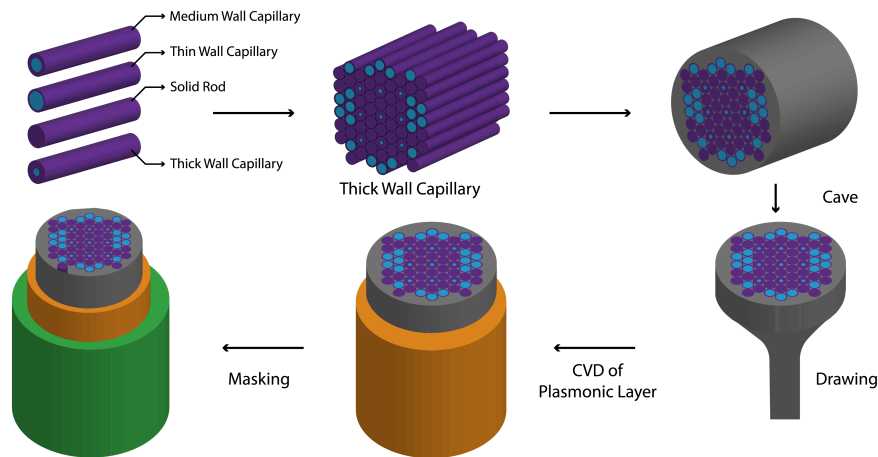


FIGURE 5.2: Fabrication of the proffered sensor

Overall, the fabrication process for SPR-PCF sensors with Gold and TiO_2 layers involves meticulous planning and execution of various steps, including preform preparation, drawing and structuring, coating, and final assembly. The use of advanced techniques such as CVD and photolithography ensures the high performance and sensitivity of the sensor, making it suitable for various applications in biochemical sensing and environmental monitoring.

5.5.3 Fabrication Tolerance:

The fabrication techniques commonly used in sensor manufacturing often fall short of achieving precise dimensions, typically resulting in deviations of $\pm 1\%$ or $\pm 2\%$ from the intended structural specifications. This variability necessitates a thorough analysis of fabrication tolerance (FT) [32]. To address this, we conducted an FT analysis for our sensor by adjusting d_1 , d_2 , and t_g by $\pm 5\%$ from their optimal values, thereby accounting for a broad spectrum of potential fabrication errors.

Figure 5.3, illustrate that a $\pm 5\%$ variation in d_1 and d_2 does not significantly affect the resonance wavelength (RW), indicating that the wavelength sensitivity (WS) of our proposed sensor remains stable even after these adjustments. The CL experiences minor modifications due to these variations. However, this change is consistent across all refractive indices (RI), resulting in minimal impact on amplitude sensitivity (AS). Specifically, we observed changes of 1.24% and 1.49% in AS due to $\pm 5\%$ variations in d_1 , and changes of 0.705% and 0.62% in AS due to $\pm 5\%$ variations in d_2 , respectively.

Further analysis depicted in **Figure 5.4**, demonstrates that a $\pm 5\%$ variation in the gold layer thickness leads to a shift in the RW. A 5% reduction in thickness results in

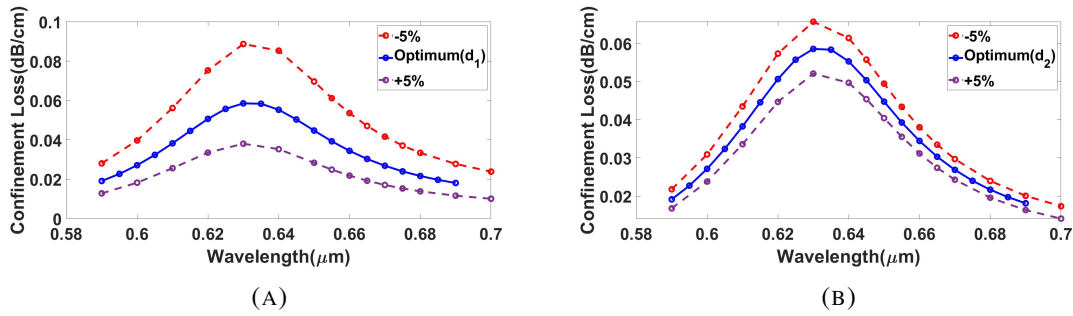


FIGURE 5.3: CL spectrum at analyte RI 1.35 with a variation of $\pm 5\%$ in (a) parameter d_1 and (b) parameter d_2

the RW decreasing from the optimized value of $0.63 \mu\text{m}$ to $0.625 \mu\text{m}$. Conversely, a 5% increase in thickness shifts the RW to $0.64 \mu\text{m}$. Thus, the RW undergoes a maximum change of 1.59%, implying that the variation in wavelength sensitivity is also minimal. The peak change in CL reaches 1.42%, but this alteration is insufficient to significantly impact amplitude sensitivity, with the maximum observed variation being 1.787%.

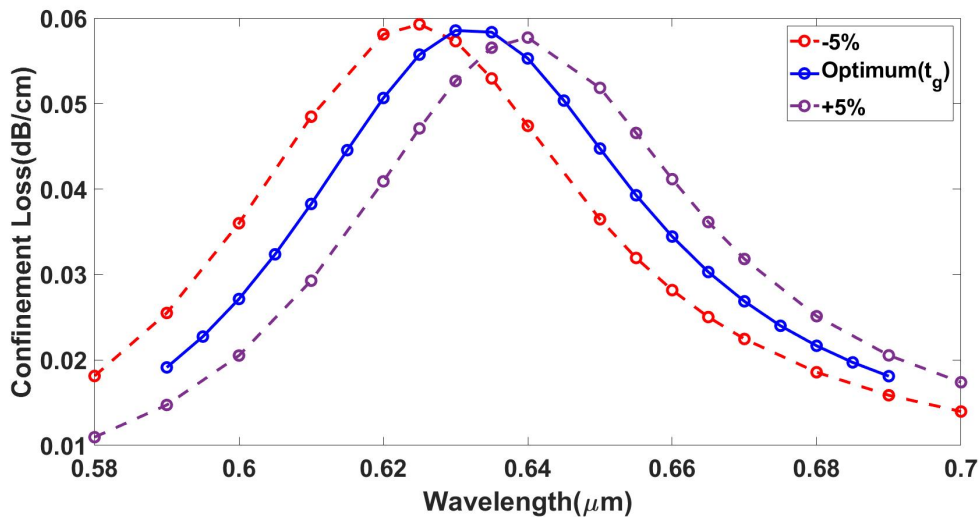


FIGURE 5.4: CL spectrum at analyte RI 1.35 with a variation of $\pm 5\%$ in parameter t_g

In conclusion, the performance of our sensor is expected to deviate by no more than 2% from the specified values due to fabrication errors. The observed changes in CL, RW, WS, and AS during the FT analysis are presented in **Table 5.1**, **Table 5.2** & **Table 5.3**.

Variation of d_1			
Change in dimension	CL (dB/cm)	RW (nm)	% decrease in AS
-5%	0.065681469	630	1.24%
0%	0.05855523	630	0%
+5%	0.05209216	630	1.49%

TABLE 5.1: Fabrication tolerance analysis by variation of d_1

Variation of d_2			
Change in dimension	CL (dB/cm)	RW (nm)	% decrease in AS
-5%	0.059275974	630	0.70%
0%	0.05855523	630	0%
+5%	0.057725401	630	0.62%

TABLE 5.2: Fabrication tolerance analysis by variation of d_2

Variation of t_g			
Change in dimension	CL (dB/cm)	RW (nm)	% decrease in AS
-5%	0.088692194	625	1.79%
0%	0.05855523	630	0%
+5%	0.038034432	640	0.25%

TABLE 5.3: Fabrication tolerance analysis by variation of t_g

Chapter 6

Conclusion And Future Work

6.1 Conclusion

Over the years, a wide array of innovative designs for traditional photonic crystal fibers (PCFs) and surface plasmon resonance photonic crystal fibers (SPR-PCFs) has been developed, each offering distinct structural advancements, varying levels of sensitivity, and different strategies for minimizing confinement losses. Building on an extensive analysis of these previous developments, we present a new design of SPR-based photonic crystal fiber biosensor. This sensor, characterized by its exceptional performance, has been meticulously designed and optimized using COMSOL Multiphysics 6.1.

This research has culminated in the successful design and optimization of a high-performance SPR-based PCF biosensor. By incorporating air holes of varying diameters and optimizing plasmonic materials, such as gold and TiO_2 layers, the sensor achieves outstanding sensitivity and resolution across a refractive index range of 1.35-1.42. Through careful fine-tuning of all fiber parameters, we achieved a maximum amplitude sensitivity of 965.976 RIU^{-1} and a wavelength sensitivity of $134,000 \text{ nm/RIU}$ for the x-polarization, with a maximum sensor resolution of $4 \times 10^{-4} \text{ RIU}$. For the y-polarization, we attained a maximum amplitude sensitivity of 1167.53 RIU^{-1} and a wavelength sensitivity of $125,000 \text{ nm/RIU}$, with a maximum sensor resolution of $5 \times 10^{-4} \text{ RIU}$. Additionally, the sensor achieved a maximum figure of merit of 832.422 for the x-polarization and 1246.986 for the y-polarization. The maximum birefringence observed was 1.980×10^{-3} . The overall analyte sensing range spans refractive indices from 1.35 to 1.42, with the sensor demonstrating a fabrication tolerance limit of $\pm 5\%$.

The innovative design approach in this study effectively addresses challenges such as high confinement loss and fabrication complexity, resulting in a sensor that not only meets but, in some cases, exceeds the performance benchmarks of existing SPR-PCF sensors. The broad analyte sensing range and robust fabrication tolerance further enhance the practical applicability of this sensor, positioning it as a strong candidate for real-world deployment.

In conclusion, the SPR-PCF biosensor developed in this research represents a significant advancement in optical sensing technology, achieving a maximum amplitude sensitivity (AS) of 1167.53 RIU^{-1} and a wavelength sensitivity (WS) of $134,000 \text{ nm/RIU}$, with a maximum sensor resolution of $5 \times 10^{-4} \text{ RIU}$. The combination of high sensitivity and a fabrication-friendly design highlights the potential of this sensor to drive progress in medical diagnostics as well as a wide range of scientific and industrial applications.

6.2 Future Work and Scopes of Improvement

While this research has made significant strides in the design and optimization of a high-performance Surface Plasmon Resonance (SPR) based Photonic Crystal Fiber (PCF) biosensor, there are several areas where future work can further enhance the capabilities and applications of this technology.

- **Material Innovations:** Future research could explore the use of alternative plasmonic materials beyond gold and TiO_2 . Materials like silver, platinum, or novel nanocomposites might offer improved plasmonic properties or greater stability under different environmental conditions. Additionally, investigating hybrid materials or multilayer structures could further enhance the sensor's sensitivity and operational lifespan.
- **Temperature and Strain Analysis:** Future research could focus on evaluating the sensor's performance under varying temperatures and strain conditions. Understanding how temperature fluctuations and mechanical strain affect the sensor's accuracy is crucial, as real-world applications may not always maintain constant conditions. This analysis will determine the sensor's reliability across different environments, ensuring consistent performance despite temperature variations and the strain induced by analyte flow.
- **Air Hole Shape Variations:** Beyond circular air holes, future research could investigate the use of different air hole shapes, such as elliptical and rectangular, to further explore the performance of PCF-based sensors or filters.
- **Broadening the Sensing Range:** The current sensor design is optimized for a specific range of refractive indices. Future work could focus on broadening this sensing range to detect a wider variety of analytes, particularly those with refractive indices outside the current range. This could involve modifications to the PCF structure, such as adjusting the air hole geometry or exploring different core materials.

- **Integration with Data Analytics:** The integration of SPR-PCF sensors with advanced data analytics, such as machine learning algorithms, could significantly enhance their functionality. By analyzing large datasets generated by the sensors, it would be possible to improve the accuracy of analyte detection and potentially identify new patterns or trends in the data, leading to more insightful diagnostics and monitoring solutions.
- **Multi-channel Sensor Development:** Future work could also explore the development of Multi-channel sensors that can simultaneously detect multiple analytes or environmental parameters. By leveraging the versatility of PCF structures and SPR technology, it may be possible to create sensors capable of performing complex diagnostics or monitoring tasks in a single, integrated device.

In summary, while the current research lays a strong foundation for SPR-PCF sensor technology, there are numerous opportunities for further improvement and exploration. Continued research in these areas will not only enhance the performance and applicability of these sensors but also contribute to the advancement of optical sensing technologies in general. By addressing the challenges and exploring the new avenues outlined above, future work can lead to the development of even more innovative and impactful sensing solutions.

Chapter 7

Demonstration of Outcome Based Education

The work presented in this thesis stands as a testament to the principles and objectives of Outcome-Based Education (OBE) by addressing complex engineering challenges and showcasing proficiency across various spheres of OBE. At its core, the work is a journey of problem analysis, starting with the identification and formulation of intricate issues surrounding the photonic crystal fiber design. Through extensive research and an in-depth exploration of existing literature, the thesis delves into the environmental effects associated with SPR based PCF technology, recognizing the urgent need for more sustainable alternatives. The significance of this work extends far beyond the confinements of academic discourse, with potential consequences spanning across diverse contexts. From environmental sustainability to technological innovation, the implications of embracing SPR based PCF span a number of societal, economic, and environmental dimensions.

7.1 Introduction

The challenge of biomolecule detection in medical science necessitates advanced sensing technologies. This paper focuses on the development of an SPR-PCF sensor, leveraging theoretical photonics frameworks and engineering principles for rapid and accurate detection. Optimized through simulation and practical testing, this sensor holds promise for enhanced health diagnostics, safety measures, and environmental sustainability in biosensing applications.

7.2 Course Outcomes (COs) Addressed

The Course Outcomes [88] that we addressed in our thesis are discussed in the **table: 7.1**

COs	CO Statement	POs	Put Tick(✓) EEE 4800
CO1	Identify a contemporary real-life problem related to electrical and electronic engineering by reviewing and analyzing existing research works.	PO2	✓
CO2	Determine functional requirements of the problem considering feasibility and efficiency through analysis and synthesis of information.	PO4	✓
CO3	Select a suitable solution and determine its method considering professional ethics, codes and standards.	PO8	✓
CO4	Adopt modern engineering resources and tools for the solution of the problem.	PO5	✓
CO5	Prepare management plan and budgetary implications for the solution of the problem.	PO11	✓
CO6	Analyze the impact of the proposed solution on health, safety, culture and society.	PO6	✓
CO7	Analyze the impact of the proposed solution on environment and sustainability.	PO7	✓
CO8	Develop a viable solution considering health, safety, cultural, societal and environmental aspects.	PO3	✓
CO9	Work effectively as an individual and as a team member for the accomplishment of the solution.	PO9	✓
CO10	Prepare various technical reports, design documentation, and deliver effective presentations for demonstration of the solution.	PO10	✓
CO11	Recognize the need for continuing education and participation in professional societies and meetings.	PO12	✓

TABLE 7.1: COs Addressed

The **Table: 7.2** below provides an explanation or justification for how the COs and their corresponding POs have been addressed in this work:

COs	POs	Explanation/Justification
CO1	PO2	<p>Problem Identification: The project begins by identifying the pressing need for advanced biosensors in medical applications. Specifically, it focuses on the detection of biomolecules, which is a critical aspect in medical diagnostics. This identification is achieved through a comprehensive review and analysis of existing research works. By scrutinizing the current state of biosensor technology, especially those employing Surface Plasmon Resonance in Photonic Crystal Fiber (SPR-PCF), the project establishes a foundation for addressing contemporary challenges. This foundation is crucial for developing sensors that can offer rapid, accurate, and reliable detection of biomolecules, which is essential for early disease diagnosis and treatment. The identification process not only highlights the gaps in current technologies but also underscores the potential improvements and innovations that SPR-PCF biosensors can bring to the field.</p>
CO2	PO4	<p>Functional Requirements Analysis: To design effective SPR-PCF biosensors, it is imperative to understand their functional requirements. This involves conducting detailed analyses and synthesizing information from various sources. The project determines these requirements by optimizing design parameters such as sensitivity, selectivity, and stability. Sensitivity refers to the sensor's ability to detect minute concentrations of biomolecules, while selectivity ensures the sensor can distinguish between different biomolecules. Stability is crucial for the sensor's performance over time. By ensuring these parameters are finely tuned, the project enhances the feasibility and efficiency of SPR-PCF biosensors in real-world applications. This comprehensive analysis is not just theoretical but also practical, ensuring that the biosensors can operate effectively under varying conditions and provide reliable results in diverse medical settings.</p>

Continued on next page

COs	POs	Explanation/Justification
CO3	PO8	<p>Ethical and Professional Standards: In the realm of biosensor development, adhering to ethical and professional standards is of utmost importance. The project emphasizes this by carefully considering ethical implications and professional responsibilities during the design and development phases. This involves ensuring that the sensors do not cause harm to patients, maintaining patient confidentiality, and adhering to regulatory standards. Additionally, the project considers the broader ethical context, such as the equitable access to advanced medical technologies. By integrating these considerations, the project ensures that the SPR-PCF biosensors not only meet technical standards but also contribute positively to societal well-being. The adherence to professional ethics codes and standards throughout the project underlines the commitment to developing technologies that are both innovative and responsible.</p>
CO4	PO5	<p>Modern Engineering Tools Utilization: The project leverages state-of-the-art engineering tools, such as COMSOL Multiphysics, for the simulation and optimization of SPR-PCF biosensors. COMSOL Multiphysics is a powerful tool that allows for detailed modeling and simulation of physical phenomena, which is crucial for optimizing the sensor design. By using such advanced tools, the project can accurately predict the performance of the sensors, identify potential issues, and refine the design before moving to the fabrication stage. This utilization of modern engineering resources not only enhances the precision and reliability of the sensor performance but also significantly reduces the time and cost associated with experimental trials. The ability to simulate and optimize in a virtual environment ensures that the final product is well-tested and ready for practical applications, thereby bridging the gap between theoretical research and real-world implementation.</p>

Continued on next page

COs	POs	Explanation/Justification
C05	PO11	<p>Project Management and Budgeting: Effective project management and budgeting are critical for the successful execution of any engineering project. The project prepares a comprehensive management plan that outlines the various phases of the project, from design and simulation to fabrication and testing. This plan includes detailed budgetary implications, ensuring that all resources are allocated efficiently. Cost-effective simulation strategies are employed to minimize expenses while maximizing output. The budget plan also accounts for potential contingencies, ensuring that the project can proceed smoothly even in the face of unforeseen challenges. By meticulously planning and managing the project, the team ensures that all aspects of the SPR-PCF biosensor development are well-coordinated, leading to timely and successful completion. This systematic approach to management and budgeting underscores the project's commitment to delivering high-quality results within the constraints of available resources.</p>
C06	PO6	<p>Health, Safety, and Societal Impact Analysis: The project conducts a thorough analysis of the health, safety, cultural, and societal impacts of SPR-PCF biosensors. By enhancing rapid and accurate detection capabilities, the biosensors significantly contribute to medical diagnostics and public health safety. Early and precise detection of diseases can lead to timely and effective treatments, ultimately saving lives and improving patient outcomes. The project also considers cultural factors, ensuring that the biosensors are acceptable and beneficial across different societal contexts. By addressing these diverse impacts, the project aims to create a technology that is not only effective but also socially responsible. This holistic approach ensures that the benefits of SPR-PCF biosensors extend beyond the technical realm, contributing positively to the broader society.</p>

Continued on next page

COs	POs	Explanation/Justification
CO7	PO7	<p>Environmental and Sustainability Considerations: In developing SPR-PCF biosensors, the project evaluates their environmental impact and sustainability. Emphasis is placed on designing sensors that are compact and reusable, thereby minimizing their environmental footprint. The choice of materials and the design process are guided by principles of sustainability, ensuring that the sensors can be produced and used without causing significant harm to the environment. This consideration is critical in today's context, where there is a growing emphasis on green technologies and sustainable practices. By focusing on environmental and sustainability aspects, the project aims to create biosensors that not only advance medical technology but also contribute to the global effort of environmental conservation. This dual focus on technological innovation and environmental responsibility highlights the project's comprehensive approach to biosensor development.</p>
CO8	PO3	<p>Viable Solution Development: Developing a viable SPR-PCF biosensor involves considering a multitude of factors, including health, safety, cultural, societal, and environmental aspects. The project integrates these considerations into the design and optimization process, ensuring that the final product meets all necessary requirements. This involves iterative testing and refinement to balance performance with practicality. The goal is to create a biosensor that is not only technically superior but also viable for widespread adoption in real-world applications. By addressing these multifaceted requirements, the project ensures that the SPR-PCF biosensor is a robust and versatile tool capable of meeting the diverse needs of modern medical diagnostics. This comprehensive development process underscores the project's commitment to creating solutions that are both innovative and practical.</p>

Continued on next page

COs	POs	Explanation/Justification
CO9	PO9	<p>Effective Team Collaboration: The project emphasizes the importance of teamwork and collaboration. Tasks are segmented into various phases such as design optimization and application exploration, with each team member contributing their expertise to achieve the project's objectives. This collaborative approach ensures that all aspects of the project are thoroughly addressed, leveraging the diverse skills and perspectives of the team members. Effective communication and coordination among team members are crucial for the successful completion of the project. By working cohesively, the team can tackle complex challenges more efficiently and innovate more effectively. This focus on teamwork not only enhances the quality of the project outcomes but also fosters a collaborative spirit that is essential for success in any engineering endeavor.</p>
CO10	PO10	<p>Technical Communication: Effective communication is vital for the success of any engineering project. The project entails the preparation of comprehensive technical reports, design documentation, and presentations. These documents and presentations are essential for conveying the design concepts, methodologies, and outcomes to various stakeholders, including the engineering community, funding bodies, and regulatory agencies. Clear and detailed communication ensures that all stakeholders are well-informed and can provide valuable feedback and support. Additionally, effective communication facilitates knowledge sharing and collaboration, contributing to the broader academic and professional community. By prioritizing technical communication, the project ensures that its findings and innovations are disseminated effectively, maximizing their impact and fostering further research and development in the field.</p>

Continued on next page

COs	POs	Explanation/Justification
CO11	PO12	<p>Continuing Education and Professional Development: The project recognizes the importance of continuous learning and professional development. By incorporating insights from related works and presenting outcomes in academic journals and conferences, the project contributes to the ongoing advancement of knowledge in the field of SPR-PCF biosensors. Engaging with professional societies and attending conferences provide opportunities for networking, knowledge exchange, and staying updated with the latest developments in the field. This commitment to continuing education ensures that the project team remains at the forefront of research and innovation, continually improving their skills and knowledge. By fostering a culture of continuous learning and professional engagement, the project not only advances the field of biosensors but also contributes to the professional growth of its team members.</p>

TABLE 7.2: Justification of the COs and their corresponding POs

7.3 Aspects of Program Outcomes Addressed

The **Table: 7.3** shows the Program Outcomes addressed in this work:

	Statement	Different Aspects	Put Tick (✓)
PO3	Design/development of solutions: Design solutions for complex electrical and electronic engineering problems and design systems, components or processes that meet specified needs with appropriate consideration for public health and safety, cultural, societal, and environmental considerations.	Public Health	✓
		Safety	✓
		Cultural	
		Societal	✓
PO4	Investigation: Conduct investigations of complex electrical and electronic engineering problems using research-based knowledge and research methods including design of experiments, analysis and interpretation of data, and synthesis of information to provide valid conclusions.	Design of experiment	✓
		Analysis and interpretation of data	✓
		Synthesis of information	✓
PO6	The engineer and society: Apply reasoning informed by contextual knowledge to assess societal, health, safety, legal, and cultural issues and the consequent responsibilities relevant to professional engineering practice and solutions to complex electrical and electronic engineering problems.	Societal	✓
		Health	✓
		Safety	✓

Continued on next page

	Statement	Different Aspects	Put Tick (✓)
		Legal	✓
		Cultural	
PO7	Environment and sustainability: Understand and evaluate the sustainability and impact of professional engineering work in the solution of complex electrical and electronic engineering problems in societal and environmental contexts.	Societal	✓
		Environmental	✓
PO8	Ethics: Apply ethical principles embedded with religious values, professional ethics and responsibilities, and norms of electrical and electronic engineering practice.	Religious Values	
		Professional ethics and responsibilities	✓
		Norms	
PO9	Individual work and teamwork: Function effectively as an individual, and as a member or leader in diverse teams and in multi-disciplinary settings.	Diverse Teams	✓
		Multi-disciplinary settings	✓
PO10	Communication: Communicate effectively on complex engineering activities with the engineering community and with society at large, such as being able to comprehend and write effective reports and design documentation, make effective presentations, and give and receive clear instructions.	Comprehend and write effective reports	✓
		Design Documentation	✓

Continued on next page

	Statement	Different Aspects	Put Tick (✓)
		Make effective presentations	✓
		Give and receive clear instructions	✓
PO11	Project management and finance: Demonstrate knowledge and understanding of engineering management principles and economic decision-making and apply these to one's own work, as a member and leader in a team, to manage projects and in multidisciplinary environments.	Engineering management principles	✓
		Economic decision-making	✓
		Manage projects	✓
		Multi-disciplinary environment	

TABLE 7.3: Program Outcomes Addressed

7.4 Knowledge Profiles (K3-K8) Addressed

The **Table: 7.4** shows the Knowledge Profiles [88] (K3 – K8) addressed the Thesis:

K	Knowledge Profile (Attributes)	Put Tick(✓)
K3	A systematic, theory-based formulation of engineering fundamentals required in the engineering discipline	✓
K4	Engineering specialist knowledge that provides theoretical frameworks and bodies of knowledge for the accepted practice areas in the engineering discipline; much is at the forefront of the discipline	✓
K5	Knowledge that supports engineering design in a practice area	✓
K6	Knowledge of engineering practice (technology) in the practice areas in the engineering discipline	✓
K7	Comprehension of the role of engineering in society and identified issues in engineering practice in the discipline: ethics and the engineer's professional responsibility to public safety; the impacts of engineering activity; economic, social, cultural, environmental and sustainability	✓
K8	Engagement with selected knowledge in the research literature of the discipline	✓

TABLE 7.4: Knowledge Profiles

The **Table: 7.5** below provides an explanation or justification for how the Knowledge Profiles have been addressed in this work:

K	Explanation/Justification
K3	<p>Understanding Theoretical Principles: The project necessitates a deep understanding of the theoretical principles underlying Surface Plasmon Resonance (SPR) and Photonic Crystal Fiber (PCF) technologies for effective biomolecule detection. This involves comprehending the interactions between light and plasmonic materials, as well as the propagation of light through photonic crystal fibers. Such theoretical knowledge is crucial for designing SPR-PCF sensors that can achieve rapid and accurate biomolecule sensing, which is essential for medical diagnostics. The design process leverages these photonics frameworks to create sensors that are both sensitive and specific to the target biomolecules, enabling early and accurate detection of diseases. This foundational knowledge ensures that the project builds on a solid scientific basis, facilitating the development of advanced biosensing technologies.</p>
K4	<p>Optimizing Detection Capabilities: To ensure efficient and rapid detection of biomolecules, the project focuses on optimizing SPR-PCF sensors based on their refractive index values. This involves detailed analysis and fine-tuning of the sensor's parameters to enhance its sensitivity and selectivity. The optimization process includes adjusting the geometrical and material properties of the PCF to maximize the interaction between the light and the target biomolecules. By doing so, the project aims to achieve high-performance biosensors capable of identifying specific biomolecules with great accuracy. This optimization is critical for medical issue identification, where timely and precise detection can significantly impact patient outcomes. Through this process, the project advances the state of SPR-PCF sensor technology, making it more effective and reliable for practical applications.</p>
Continued on next page	

K	Explanation/Justification
K5	<p>Utilizing Refractive Index Values: A key aspect of SPR-PCF sensor functionality is the ability to detect biomolecules based on their unique refractive index values. The project utilizes these values to observe the behavior of Surface Plasmon Resonances (SPRs) and Surface Plasmon Polaritons (SPPs) through transmitted light. This involves monitoring changes in the light's intensity and wavelength as it interacts with different biomolecules. By accurately detecting these changes, the sensors can identify specific biomolecules with high precision. This capability is essential for applications in medical diagnostics, where distinguishing between different biomolecules is crucial for accurate disease detection and monitoring. The project's focus on this aspect ensures that the SPR-PCF sensors developed are not only effective but also versatile, capable of detecting a wide range of biomolecules in various environments.</p>
K6	<p>Simulation and Optimization: The project employs COMSOL Multiphysics for the simulation and optimization of SPR-PCF sensors. This advanced simulation tool allows for detailed modeling of the sensors' performance under different conditions. Through these simulations, the project can predict how changes in the sensor's design will affect its performance, enabling iterative optimization. This process involves testing various configurations and materials to find the optimal design that offers the best sensitivity and specificity. The practical outcomes of these simulations are then validated through fabrication and testing, ensuring that the sensors perform as expected in real-world applications. This use of modern simulation tools streamlines the development process, reducing the need for costly and time-consuming experimental trials. It also ensures that the final sensor designs are based on rigorous scientific analysis, enhancing their reliability and effectiveness.</p>
Continued on next page	

K	Explanation/Justification
K7	<p>Ethical Compliance and Professional Standards: Ensuring ethical compliance is a fundamental aspect of the project. This involves adhering to professional standards and codes in the design and usage of SPR-PCF sensors for health diagnostics and environmental contamination detection. The project considers the potential impacts of the sensors on patients and the environment, ensuring that they are safe and sustainable. This includes using non-toxic materials, minimizing waste during production, and ensuring that the sensors can be safely disposed of or recycled. By promoting safety and sustainability, the project aligns with broader societal goals of environmental conservation and public health. Ethical considerations also extend to data privacy and patient confidentiality, ensuring that the use of these sensors in medical diagnostics does not compromise the security and privacy of sensitive information.</p>
K8	<p>Leveraging Existing Research: The project leverages insights from existing research in photonics, biosensors, and SPR-PCF technologies to inform the design, optimization, and fabrication of the sensors. This involves a thorough review of the latest advancements in these fields, identifying best practices and innovative approaches that can be applied to the project. By building on the existing body of knowledge, the project can avoid common pitfalls and incorporate proven techniques into its development process. Additionally, the project contributes to the academic community by presenting its findings in research journals and conferences. These presentations showcase the satisfactory results and advancements made in SPR-PCF sensor technology, fostering knowledge exchange and encouraging further research and development. This engagement with the academic community ensures that the project remains at the cutting edge of biosensor technology, continually improving and innovating based on the latest research.</p>

TABLE 7.5: Justification of Knowledge Profiles

7.5 Use of Engineering Problems

In the development of Surface Plasmon Resonance-based Photonic Crystal Fiber (SPR-PCF) biosensors and their subsequent performance simulation, the application of Complex Engineering Problems is evident in various aspects. Primarily, the project involves the design and optimization of SPR-PCF biosensors for biomolecule detection, a process that presents numerous intricate engineering challenges. The complexity arises from the need to achieve high sensitivity and specificity while ensuring the biosensor is practical for real-world medical applications. This requires a profound understanding of photonic principles, material properties, and biological interactions, necessitating sophisticated problem-solving methodologies.

The simulation of the SPR-PCF biosensor's performance involves a comprehensive examination of various parameters and their intricate interactions, including resonance wavelength shifts, sensitivity to refractive index changes, and signal-to-noise ratios. These represent multifaceted engineering challenges that require advanced mathematical modeling, meticulous computational analysis, and rigorous empirical validation processes. The simulation tools, such as COMSOL Multiphysics, are employed to model the interactions between light and the sensor's materials, optimizing the design to enhance performance metrics.

The broader context of biosensing for medical diagnostics introduces an additional layer of complexity to the project. With the growing demand for rapid, accurate, and non-invasive diagnostic tools, the development of advanced biosensors becomes crucial. The project addresses this need by focusing on SPR-PCF technology, which has the potential to revolutionize the field of biosensing. Achieving the desired performance and reliability in these sensors involves addressing challenges related to miniaturization, material compatibility, and signal enhancement, all while ensuring that the sensors are cost-effective and easy to use in clinical settings.

In grappling with these multifaceted engineering challenges, the project aims to propose innovative solutions, such as the integration of optimized photonic crystal fibers and plasmonic materials, to propel the domain of biosensing towards more efficient and reliable diagnostic tools. By addressing the technical, practical, and societal aspects of SPR-PCF biosensor development, the project contributes to advancing the field of medical diagnostics, offering new avenues for early disease detection and monitoring, ultimately enhancing patient care and public health outcomes.

7.6 Socio-Cultural, Environmental, And Ethical Impact

7.6.1 Cultural Diversity and Sensitivity

- **Ensuring Inclusivity:** The SPR-PCF biosensor project is designed to be inclusive, free from biases, and considerate of a wide range of socio-cultural backgrounds. This involves engaging with diverse communities to ensure that the technology meets the needs of various cultural contexts.
- **Accessibility Standards:** Adhering to accessibility standards to accommodate users of different abilities, languages, and cultural contexts within the SPR-PCF biosensor framework. This includes designing interfaces and user experiences that are intuitive and accessible to all.

7.6.2 Environmental Sustainability

- **Resource Optimization:** Streamlining resource usage to reduce waste and energy consumption throughout the SPR-PCF biosensor development process. This involves using eco-friendly materials and optimizing manufacturing processes to minimize environmental impact.
- **Sustainable Practices:** Embedding sustainable practices at every stage of the project's lifecycle, considering the environmental impact of materials and processes involved in developing and deploying SPR-PCF biosensors. This ensures that the project contributes positively to environmental conservation efforts.

7.6.3 Ethical Standards

- **Transparency and Trust:** Maintaining transparency about project goals, methodologies, and potential impacts to build trust among stakeholders. Clear communication and ethical disclosure of project developments are essential for fostering a trustworthy environment.
- **Fair Access:** Ensuring fair access to the benefits of the SPR-PCF biosensor project, especially considering the needs of marginalized communities. This involves designing cost-effective solutions that are accessible to underrepresented populations.

7.6.4 Community Engagement

- **Stakeholder Involvement:** Engaging various stakeholders, including local communities, healthcare providers, and regulatory bodies, to gather insights and address concerns specific to the SPR-PCF biosensor project. This collaborative approach ensures that the technology is aligned with community needs and expectations.
- **Cultural Heritage Respect:** Acknowledging and respecting local cultural heritage while developing and implementing SPR-PCF biosensors. This includes being sensitive to cultural norms and practices in the regions where the technology will be deployed.

7.6.5 Impact Evaluation

- **Social Impact Assessment:** Conducting thorough assessments of social impacts to understand and mitigate any negative effects on communities and societal structures resulting from the deployment of SPR-PCF biosensors. This involves evaluating potential disruptions and benefits to ensure a balanced approach.
- **Environmental Impact Evaluation:** Evaluating the environmental effects of the SPR-PCF biosensor project and proactively identifying and mitigating potential harm. This includes monitoring the lifecycle impact of the sensors and ensuring eco-friendly disposal practices.

7.6.6 Compliance and Ethical Framework

- **Legal Adherence:** Adhering strictly to local and international laws governing socio-cultural, environmental, and ethical aspects within the SPR-PCF biosensor project. This ensures that the project complies with all relevant regulations and standards.
- **Ethical Alignment:** Aligning the project with established ethical frameworks and industry-specific guidelines to ensure ethical conduct throughout the SPR-PCF biosensor development efforts. This includes adhering to principles of fairness, transparency, and responsibility.

7.6.7 Continuous Monitoring and Enhancement

- **Feedback Mechanisms:** Establishing feedback mechanisms from stakeholders to identify and resolve unforeseen socio-cultural, environmental, or ethical issues

in the SPR-PCF biosensor project. This allows for continuous improvement and adaptation based on real-world feedback.

- **Adaptive Strategies:** Developing adaptable strategies tailored to the project's requirements to proactively respond to evolving socio-cultural dynamics, environmental concerns, and ethical considerations throughout its lifecycle. This ensures that the project remains relevant and responsible over time.

7.7 Attributes of Ranges of Complex Engineering Problem Solving (P1 – P7) Addressed

The **Table: 7.7** shows the attributes of Complex Engineering Problem Solving (P1-P7) [88] addressed for this thesis:

P Attribute	Range of Complex Engineering Problem Solving (Complex Engineering Problems have characteristic P1 and some or all of P2 to P7)	Put Tick (✓)
Depth of Knowledge required	P1: Cannot be resolved without in-depth engineering knowledge at the level of one or more of K3, K4, K5, K6 or K8 which allows a fundamentals-based, first principles analytical approach	✓
Range of Conflicting requirements	P2: Involve wide-ranging or conflicting technical, engineering, and other issues	✓
Depth of analysis required	P3: Have no obvious solution and require abstract thinking, originality in analysis to formulate suitable models	✓
Familiarity of issues	P4: Involve infrequently encountered issues	✓
Extent of applicable codes	P5: Are outside problems encompassed by standards and codes of practice for professional engineering	✓
Extent of stakeholder involvement and conflicting requirements	P6: Involve diverse groups of stakeholders with widely varying needs	✓
Interdependence	P7: Are high level problems including many component parts or sub problems	✓

TABLE 7.6: P1-P7 addressed

The **Table: 7.7** below provides an explanation or justification for how P attributes have been addressed in this work:

P	Explanation/Justification
P1	<p>Depth of Knowledge Required: The project necessitates a profound understanding of SPR and PCF principles, requiring in-depth engineering knowledge at the level of theoretical photonics frameworks. This foundational knowledge (K3, K4) is crucial for developing effective biosensors that can achieve the desired sensitivity and specificity. The principles of SPR involve the resonance of electrons at the surface of a metal under specific conditions, while PCF involves the manipulation of light within a microstructured fiber. A thorough understanding of these concepts allows for the precise design and optimization of the sensor, ensuring it can reliably detect biomolecules at low concentrations. The depth of knowledge also extends to the ability to predict and analyze the interactions between light and matter at the nanoscale, which is essential for fine-tuning the sensor's performance.</p>
P2	<p>Range of Conflicting Requirements: The design process involves balancing various conflicting requirements such as sensitivity, specificity, and ethical considerations. Sensitivity refers to the sensor's ability to detect low concentrations of biomolecules, while specificity ensures that the sensor can distinguish between different types of biomolecules. These technical requirements often conflict with ethical considerations, such as ensuring patient safety and data privacy. Additionally, the sensor must be designed to meet regulatory standards and societal expectations, which can further complicate the design process. The project addresses these conflicting requirements (K5, K7) by employing a multidisciplinary approach that integrates technical expertise with ethical and societal considerations. This ensures that the biosensor meets diverse and often conflicting needs, resulting in a solution that is both technically sound and socially responsible.</p>
Continued on next page	

Addressed

P	Explanation/Justification
P3	<p>Depth of Analysis Required: The project requires innovative approaches and abstract thinking for optimizing sensor parameters. This involves complex problem-solving techniques and originality in analysis to formulate effective models (K4, K6). For instance, the project uses advanced simulation tools like COMSOL Multiphysics to model the interactions between light and plasmonic materials, allowing for the optimization of sensor design. These simulations involve iterative testing and refinement of various parameters, such as the thickness of the metal layer, the geometry of the photonic crystal fiber, and the refractive index of the biomolecules. By employing these innovative approaches, the project can identify the optimal design that maximizes the sensor's performance. The depth of analysis also includes the ability to interpret complex data and draw meaningful conclusions, which is essential for validating the sensor's functionality and reliability.</p>
P4	<p>Familiarity of Issues: Addressing the unique and infrequently encountered challenges in biosensor development demonstrates familiarity with novel engineering problems. These challenges include optimizing plasmonic materials, such as gold or silver, to enhance their resonance properties and integrating these materials with photonic crystal fibers to create a functional sensor. The project tackles these issues by leveraging advanced materials science techniques and cutting-edge fabrication methods (K5). This involves experimenting with different materials and fabrication processes to find the optimal combination that enhances the sensor's performance. The project also explores new ways to integrate the sensors with existing medical diagnostic tools, ensuring they can be easily adopted in real-world applications.</p>
Continued on next page	

P	Explanation/Justification
P5	<p>Extent of Applicable Codes: The project extends beyond standard codes and practices, incorporating new engineering principles and societal considerations that are not fully covered by existing standards. This emphasizes the importance of innovation and adaptation (K7). For example, the project may need to develop new protocols for sensor calibration, data interpretation, and patient data handling that are not yet standardized. Additionally, the project considers the environmental impact of sensor production and disposal, promoting sustainable practices that go beyond traditional engineering codes. By addressing these broader issues, the project not only ensures the biosensor meets current technical standards but also anticipates future regulatory and societal trends. This proactive approach ensures the biosensor remains relevant and compliant with evolving standards, making it a robust and future-proof solution.</p>
P6	<p>Stakeholder Involvement: The project involves engaging with diverse stakeholders, including medical professionals, engineers, and regulatory bodies, to address their varying needs and expectations. Medical professionals provide insights into the practical requirements and constraints of using the biosensor in clinical settings, while engineers contribute technical expertise in design and fabrication. Regulatory bodies ensure that the sensor meets safety and efficacy standards. By engaging these stakeholders (K7), the project ensures that the biosensor's societal and health impact is maximized. This collaborative approach also facilitates the adoption of the biosensor in real-world applications, as it aligns the development process with the needs and expectations of all relevant parties. The project may also involve patients and patient advocacy groups to ensure the sensor meets the end-users' needs and addresses any concerns they may have. This comprehensive stakeholder involvement ensures the biosensor is well-rounded, addressing all aspects of its intended use.</p>
Continued on next page	

P	Explanation/Justification
P7	<p>Interdisciplinary Integration: The project integrates knowledge from multiple disciplines, including photonics, materials science, and biomedical engineering, to develop a comprehensive solution that addresses various components of the problem. This interdisciplinary approach (K3, K4, K6) is essential for developing a biosensor that can perform reliably in diverse environments and applications. For instance, photonics provides the theoretical basis for understanding light-matter interactions, while materials science contributes to the development and optimization of the plasmonic materials used in the sensor. Biomedical engineering ensures the sensor meets the practical requirements of medical diagnostics, including biocompatibility and usability. By integrating these diverse fields, the project can develop a biosensor that not only meets technical specifications but also addresses practical and clinical needs. This holistic approach ensures the biosensor is robust, versatile, and ready for real-world applications.</p>

TABLE 7.7: Justification of the Attributes of Ranges of Complex Engineering Problem Solving (P1 – P7)

7.8 Attributes of Ranges of Complex Engineering Activities (A1-A5) Addressed

The **Table: 7.8** shows the attributes of range of Complex Engineering Activities [88] (A1-A5) addressed in this thesis:

A Attribute	Range of Complex Engineering Attributes (Complex activities mean (engineering) activities or projects that have some or all of the following characteristics)	Put Tick (✓)
Range of resources	A1: Involve the use of diverse resources (and for this purpose resources include people, money, equipment, materials, information, and technologies)	✓
Level of interaction	A2: Require resolution of significant problems arising from interactions between wide-ranging or conflicting technical, engineering, or other issues	✓
Innovation	A3: Involve creative use of engineering principles and research-based knowledge in novel ways	✓
Consequences for society and the environment	A4: Have significant consequences in a range of contexts, characterized by difficulty of prediction and mitigation	✓
Familiarity	A5: Can extend beyond previous experiences by applying principles-based approaches	✓

TABLE 7.8: A1-A5 addressed

The **Table: 7.9** below provides an explanation or justification for how A attributes have been addressed in this work:

A	Explanation/Justification
A1	<p>Range of Resources: The project utilizes a diverse array of resources, including advanced simulation tools like COMSOL Multiphysics, research funding, and biomolecular samples. COMSOL Multiphysics enables detailed modeling and simulation of SPR-PCF biosensors, allowing for precise optimization of design parameters. Research funding provides the financial support necessary to conduct extensive simulations, fabrications, and testing phases. Access to biomolecular samples is crucial for validating the biosensor's effectiveness in detecting specific biomolecules. Comprehensive resource management ensures that all these diverse elements are effectively coordinated, maximizing the efficiency and impact of the project. This approach not only streamlines the development process but also ensures that the project remains within budget and on schedule, contributing to its overall success.</p>
A2	<p>Level of Interaction: The project addresses significant challenges arising from the interactions between photonics, biomolecular science, engineering design, and ethical considerations. Each of these disciplines brings its own set of complexities and requirements. For instance, photonics involves the manipulation of light at the nanoscale, biomolecular science focuses on the detection and interaction of biomolecules, and engineering design ensures that these interactions are effectively translated into a functional sensor. Ethical considerations include patient safety, data privacy, and environmental sustainability. By addressing these interactions comprehensively, the project ensures the seamless integration and functionality of the biosensor. This holistic approach facilitates the development of a biosensor that is not only technically advanced but also ethically sound and practically viable, meeting the needs of all stakeholders.</p>
Continued on next page	

A	Explanation/Justification
A3	<p>Innovation: The project implements creative engineering solutions by combining theoretical photonics frameworks with practical design and optimization techniques. This innovative approach leads to the development of novel and effective SPR-PCF biosensors for medical diagnostics. Theoretical frameworks provide the foundational knowledge needed to understand and manipulate light-matter interactions, while practical techniques involve the actual design, fabrication, and testing of the biosensors. By merging these elements, the project fosters innovation, resulting in biosensors that are highly sensitive, specific, and reliable. This creative problem-solving process involves continuous iteration and refinement, ensuring that the final product is optimized for performance and usability. The innovative solutions developed through this project have the potential to significantly advance the field of biosensing, providing new tools for medical diagnostics and other applications.</p>
A4	<p>Consequences for Society and Environment: The project considers the significant societal and environmental impacts of SPR-PCF biosensors. Improved health diagnostics enable earlier and more accurate detection of diseases, leading to better patient outcomes and overall public health. Enhanced safety measures ensure that the biosensors are safe to use and do not pose any risks to patients or healthcare providers. The project also emphasizes sustainability benefits, designing compact and reusable biosensors to minimize environmental footprint. This involves selecting eco-friendly materials, optimizing manufacturing processes to reduce waste, and ensuring that the sensors can be easily recycled or disposed of safely. By addressing these societal and environmental impacts, the project contributes to the broader goals of public health, safety, and sustainability, demonstrating a commitment to creating technology that benefits both people and the planet.</p>
Continued on next page	

A	Explanation/Justification
A5	<p>Familiarity: The project extends beyond conventional sensor development approaches by applying principles-based engineering methodologies. This involves leveraging insights from existing research, utilizing advanced simulation and optimization techniques, and adopting a systematic approach to design, fabricate, and test the SPR-PCF biosensors. Principles-based methodologies ensure that the design process is grounded in solid scientific principles, allowing for more predictable and reliable outcomes. By building on the latest research and continuously refining the design through simulation and testing, the project ensures that the biosensors are optimized for performance and reliability. This familiarity with advanced engineering methodologies and the ability to adapt and innovate based on new information and techniques is critical for the successful development of high-performance biosensors. The project's approach ensures that the final product is not only effective but also robust and adaptable to various real-world applications.</p>

TABLE 7.9: Justification of the Attributes of Ranges of Complex Engineering Activities (A1–A5)

Bibliography

- [1] Q. Wang, J.-Y. Jing, B.-T. Wang, and S. Li, “Recent progress and applications of optical microfiber and nanofiber devices,” en, *Instrum. Sci. Technol.*, vol. 47, no. 2, pp. 117–139, Mar. 2019.
- [2] M. Sibley, *Optical Communications: Components and Systems*. 2020.
- [3] J. Laegsgaard, K. P. Hansen, M. D. Nielsen, *et al.*, “Photonic crystal fibers,” in *Proceedings of the 2003 SBMO/IEEE MTT-S International Microwave and Optoelectronics Conference - IMOC 2003. (Cat. No.03TH8678)*, Foz do Iguacu, Brazil: IEEE, 2004.
- [4] T. P. Hansen, J. Broeng, S. E. B. Libori, *et al.*, “Highly birefringent index-guiding photonic crystal fibers,” *IEEE Photonics Technol. Lett.*, vol. 13, no. 6, pp. 588–590, Jun. 2001.
- [5] T. Sylvestre, E. Genier, A. N. Ghosh, *et al.*, “Recent progress in fiber-based supercontinuum sources,” in *Fiber Lasers and Glass Photonics: Materials through Applications III*, S. Taccheo, M. Ferrari, and A. B. Seddon, Eds., Strasbourg, France: SPIE, May 2022.
- [6] R. K. Sinha and S. K. Varshney, “Dispersion properties of photonic crystal fibers,” en, vol. 37, no. 2, pp. 129–132, Apr. 2003.
- [7] X. Yang, C. Gong, Y. Liu, Y. Rao, M. Smietana, and Y. Gong, “Recent progress in fiber optofluidic lasing and sensing,” en, *Photonic Sens.*, vol. 11, no. 2, pp. 262–278, Jun. 2021.
- [8] H. C. L. Tsui and N. Healy, “Recent progress of semiconductor optoelectronic fibers,” en, *Front. Optoelectron.*, vol. 14, no. 4, pp. 383–398, Dec. 2021.
- [9] A. Bhargav and N. Kumar Rai, “SPR-based biosensors in the diagnostics and therapeutics,” in *Recent Advances in Biosensor Technology*, BENTHAM SCIENCE PUBLISHERS, Apr. 2023, pp. 78–96.
- [10] N. Islam, M. Faizul Huq Arif, M. Abu Yousuf, and S. Asaduzzaman, “Highly sensitive open channel based PCF-SPR sensor for analyte refractive index sensing,” en, *Results Phys.*, vol. 46, no. 106266, p. 106 266, Mar. 2023.

- [11] B. Mulyanti, H. S. Nugroho, C. Wulandari, *et al.*, “SPR-based sensor for the early detection or monitoring of kidney problems,” *en, Int. J. Biomater.*, vol. 2022, p. 9 135 172, Jun. 2022.
- [12] C. M. Miyazaki, F. M. Shimizu, and M. Ferreira, “Surface plasmon resonance (SPR) for sensors and biosensors,” in *Nanocharacterization Techniques*, Elsevier, 2017, pp. 183–200.
- [13] C. Zhang and F. Ito, “Recent progress of fiber diagnostic technologies for optical fiber networks: Distributed fiber sensing and fiber characterization,” in *Metro and Data Center Optical Networks and Short-Reach Links V*, M. Glick, A. K. Srivastava, Y. Akasaka, S. Mikroulis, B. B. Dingel, and R. Llorente, Eds., San Francisco, United States: SPIE, Mar. 2022.
- [14] L. Li, W. Li, X. Zong, Y. Zheng, L. Cui, and Y. Liu, “Label-free detection of ultra-low weight molecules based on fiber optic sensors with low loss dielectric nanostructures,” *J. Lightwave Technol.*, vol. 41, no. 13, pp. 4405–4410, Jul. 2023.
- [15] M. A. Islam, M. R. Islam, S. Siraz, M. Rahman, M. S. Anzum, and F. Noor, “Wheel structured zeonex-based photonic crystal fiber sensor in THz regime for sensing milk,” *en, Appl. Phys. A Mater. Sci. Process.*, vol. 127, no. 5, p. 311, Apr. 2021.
- [16] M. R. Islam, M. M. I. Khan, R. Al Rafid, *et al.*, “Trigonal cluster-based ultra-sensitive surface plasmon resonance sensor for multipurpose sensing,” *en, Sens. BioSensing Res.*, vol. 35, no. 100477, p. 100 477, Feb. 2022.
- [17] X. Li, L. Zhang, T. Geng, and Y. Qiao, “Highly sensitive bending sensor based on c-shaped-core long-period fiber gratings,” *IEEE Sens. J.*, vol. 22, no. 24, pp. 23 968–23 974, Dec. 2022.
- [18] D. Yang, Y. Li, B. Xu, Z. Wei, T. Cheng, and X. Wang, “Modified d-type surface plasmon resonance (SPR)-based photonic crystal fiber (PCF) for application as a polarization filter and refractive index sensor,” *en, Instrum. Sci. Technol.*, pp. 1–21, Aug. 2022.
- [19] M. Benhaddad and F. Kerrou, “Modeling of low non-linearity and low confinement loss photonic crystal fiber by introducing asymmetric defect structures,” *en, Phosphorus Sulfur Silicon Relat. Elem.*, vol. 195, no. 11, pp. 957–959, Nov. 2020.
- [20] M. R. Islam, M. M. I. Khan, S. Siraz, *et al.*, “Design and analysis of a QC-SPR-PCF sensor for multipurpose sensing with supremely high FOM,” *en, Appl. Nanosci.*, vol. 12, no. 1, pp. 29–45, Jan. 2022.

- [21] M. S. Wahl, Ø. Wilhelmsen, and D. R. Hjelle, "Addressing challenges in fabricating reflection-based fiber optic interferometers," en, *Sensors (Basel)*, vol. 19, no. 18, p. 4030, Sep. 2019.
- [22] A. H. El-Saeed, A. E. Khalil, M. F. O. Hameed, M. Y. Azab, and S. S. A. Obayya, "Highly sensitive SPR PCF biosensors based on Ag/TiN and Ag/ZrN configurations," en, *Opt. Quantum Electron.*, vol. 51, no. 2, Feb. 2019.
- [23] M. J. B. M. Leon and M. A. Kabir, "Design of a liquid sensing photonic crystal fiber with high sensitivity, birefringence & low confinement loss," en, *Sens. BioSensing Res.*, vol. 28, no. 100335, p. 100 335, Jun. 2020.
- [24] S. Singh, B. Chaudhary, A. Upadhyay, D. Sharma, N. Ayyanar, and S. A. Taya, "A review on various sensing prospects of SPR based photonic crystal fibers," en, *Photonics Nanostruct.*, vol. 54, no. 101119, p. 101 119, May 2023.
- [25] M. Elsherif, A. E. Salih, M. G. Muñoz, *et al.*, "Optical fiber sensors: Working principle, applications, and limitations," en, *Adv. Photonics Res.*, p. 2 100 371, Jul. 2022.
- [26] F. Wang, Y. Wei, and Y. Han, "High sensitivity and wide range refractive index sensor based on surface plasmon resonance photonic crystal fiber," en, *Sensors (Basel)*, vol. 23, no. 14, Jul. 2023.
- [27] T. Li, L. Zhu, X. Yang, X. Lou, and L. Yu, "A refractive index sensor based on h-shaped photonic crystal fibers coated with ag-graphene layers," en, *Sensors (Basel)*, vol. 20, no. 3, p. 741, Jan. 2020.
- [28] M. B. Hossain, T. Mahendiran, L. F. Abdulrazak, I. M. Mehedi, M. A. Hossain, and M. M. Rana, "Numerical analysis of gold coating based quasi d-shape dual core pcf spr sensor," *Optical and Quantum Electronics*, vol. 52, pp. 1–13, 2020.
- [29] Z. Guo, Z. Fan, X. Kong, and Z. Meng, "Photonic crystal fiber based wide-range of refractive index sensor with phase matching between core mode and metal defect mode," *Optics Communications*, vol. 461, p. 125 233, 2020, ISSN: 0030-4018. DOI: <https://doi.org/10.1016/j.optcom.2020.125233>. [Online]. Available: <https://www.sciencedirect.com/science/article/pii/S003040182030002X>.
- [30] S. Jain, K. Choudhary, and S. Kumar, "Photonic crystal fiber-based spr sensor for broad range of refractive index sensing applications," *Optical Fiber Technology*, vol. 73, p. 103 030, 2022, ISSN: 1068-5200. DOI: <https://doi.org/10.1016/j.yofte.2022.103030>. [Online]. Available: <https://www.sciencedirect.com/science/article/pii/S1068520022002139>.

- [31] A. A. S. Falah, W. R. Wong, G. A. Mahdiraji, and F. R. Mahamd Adikan, "Single-mode d-shaped photonic crystal fiber surface plasmon resonance sensor with open microchannel," en, *Opt. Fiber Technol.*, vol. 74, no. 103105, p. 103 105, Dec. 2022.
- [32] M. A. Mahfuz, M. A. Hossain, E. Haque, N. H. Hai, Y. Namihira, and F. Ahmed, "Dual-core photonic crystal fiber-based plasmonic RI sensor in the visible to near-IR operating band," *IEEE Sens. J.*, vol. 20, no. 14, pp. 7692–7700, Jul. 2020.
- [33] M. R. Islam, M. A. Jamil, M. S.-U. Zaman, *et al.*, "Design and analysis of birefringent SPR based PCF biosensor with ultra-high sensitivity and low loss," en, *Optik (Stuttg.)*, vol. 221, no. 165311, p. 165 311, Nov. 2020.
- [34] A. K. Shakya, A. Ramola, S. Singh, and V. Van, "Design of an ultra-sensitive bimetallic anisotropic PCF SPR biosensor for liquid analytes sensing," en, *Opt. Express*, vol. 30, no. 6, pp. 9233–9255, Mar. 2022.
- [35] M. Rakibul Islam, A. N. M. Iftekher, M. S. Anzum, M. Rahman, and S. Siraz, "Lspr based double peak double plasmonic layered bent core pcf-spr sensor for ultra-broadband dual peak sensing," *IEEE Sensors Journal*, vol. 22, no. 6, pp. 5628–5635, 2022. DOI: [10.1109/JSEN.2022.3149715](https://doi.org/10.1109/JSEN.2022.3149715).
- [36] M. R. Islam, K. R. Hasan, M. M. I. Khan, *et al.*, "Design of a dual cluster and dual array-based pcf-spr biosensor with ultra-high ws and fom," *Plasmonics*, vol. 17, no. 3, pp. 1171–1182, 2022.
- [37] P. Damborský, J. Švitel, and J. Katrlík, "Optical biosensors," *Essays in Biochemistry*, vol. 60, no. 1, pp. 91–100, Jun. 2016. DOI: [10.1042/EBC20150010](https://doi.org/10.1042/EBC20150010). [Online]. Available: <https://doi.org/10.1042/EBC20150010>.
- [38] H. F. Fakhrudeen, A. Zahid, R. Jaafar, and A. Abdulkareem, "An overview of photonic crystal fiber (pcf)," vol. 9, pp. 17 250–17 256, Apr. 2019.
- [39] W. C. W. Chan and S. Nie, "Quantum dot bioconjugates for ultrasensitive nonisotopic detection," en, *Science*, vol. 281, no. 5385, pp. 2016–2018, Sep. 1998.
- [40] B. Liu, Y. Lu, X. Yang, and J. Yao, "Tunable surface plasmon resonance sensor based on photonic crystal fiber filled with gold nanoshells," *Plasmonics*, vol. 13, no. 3, pp. 763–770, Jun. 2018.
- [41] M. R. Islam, M. A. Hossain, K. M. A. Talha, and R. K. Munia, "A novel hollow core photonic sensor for liquid analyte detection in the terahertz spectrum: Design and analysis," en, *Opt. Quantum Electron.*, vol. 52, no. 9, Sep. 2020.

- [42] N. De Acha, A. B. Socorro-Leránoz, C. Elosúa, and I. R. Matías, “Trends in the design of intensity-based optical fiber biosensors (2010–2020),” *Biosensors*, vol. 11, no. 6, p. 197, Jun. 2021. DOI: [10.3390/bios11060197](https://doi.org/10.3390/bios11060197). [Online]. Available: <https://doi.org/10.3390/bios11060197>.
- [43] B. Troia, A. Paolicelli, and M. De Vittorio, *Photonic Crystals for Optical Sensing: A Review*. InTech eBooks, 2013. DOI: [10.5772/53897](https://doi.org/10.5772/53897). [Online]. Available: <https://doi.org/10.5772/53897>.
- [44] F. Markey, “Principles of surface plasmon resonance,” in *Real-Time Analysis of Biomolecular Interactions*, Tokyo: Springer Japan, 2000, pp. 13–22.
- [45] H. Raether, *Surface plasmons on smooth and rough surfaces and on gratings* (Springer tracts in modern physics), en. Berlin, Germany: Springer, Mar. 1988.
- [46] K.-W. Koch, “Surface plasmon resonance,” in *Encyclopedic Reference of Genomics and Proteomics in Molecular Medicine*, Springer Berlin Heidelberg, 2006, pp. 1832–1835.
- [47] M. C. Fenta, D. K. Potter, and J. Szanyi, “Fibre optic methods of prospecting: A comprehensive and modern branch of geophysics,” en, *Surv. Geophys.*, Mar. 2021.
- [48] M. S. Islam, J. Sultana, A. Dinovitser, B. W.-H. Ng, and D. Abbott, “A gold coated plasmonic sensor for biomedical and biochemical analyte detection,” in *2018 43rd International Conference on Infrared, Millimeter, and Terahertz Waves (IRMMW-THz)*, Nagoya: IEEE, Sep. 2018.
- [49] D. Monzón Hernández, J. S. Velázquez-González, D. Luna-Moreno, M. Torres-Cisneros, and I. Hernández-Romano, “Prism-based surface plasmon resonance for dual-parameter sensing,” *IEEE Sensors Journal*, vol. 18, no. 10, pp. 4030–4037, 2018. DOI: [10.1109/JSEN.2018.2818064](https://doi.org/10.1109/JSEN.2018.2818064).
- [50] S. Wang, Y. Lu, W. Ma, N. Liu, and S. Fan, “D-shaped surface plasmon photonic crystal fiber temperature sensor,” en, *Plasmonics*, vol. 17, no. 5, pp. 1911–1919, Oct. 2022.
- [51] H. Liang, Y. Feng, H. Liu, W. Han, and T. Shen, “High-performance PCF-SPR sensor coated with ag and graphene for humidity sensing,” en, *Plasmonics*, vol. 17, no. 4, pp. 1765–1773, Aug. 2022.
- [52] M. Zhu, L. Yang, J. Lv, *et al.*, “Highly sensitive dual-core photonic crystal fiber based on a surface plasmon resonance sensor with gold film,” en, *Plasmonics*, vol. 17, no. 2, pp. 543–550, Apr. 2022.

- [53] S. Chowdhury, L. Faisal Abdulrazak, S. Akhtar Mitu, *et al.*, “A highly sensitive multi-channel SPR-PCF based biosensor with deep learning prediction approach,” *en, Alex. Eng. J.*, vol. 77, pp. 189–203, Aug. 2023.
- [54] K. M. Mustafizur Rahman, M. Shah Alam, R. Ahmed, and M. Asiful Islam, “Irregular hexagonal core based surface plasmon resonance sensor in near-infrared region,” *en, Results Phys.*, vol. 23, no. 103983, p. 103 983, Apr. 2021.
- [55] M. R. Islam, A. N. M. Iftekher, K. R. Hasan, *et al.*, “Design and numerical analysis of a gold-coated photonic crystal fiber based refractive index sensor,” *en, Opt. Quantum Electron.*, vol. 53, no. 2, Feb. 2021.
- [56] S. Islam, M. R. Islam, M. Faisal, *et al.*, “Extremely low-loss, dispersion flattened porous-core photonic crystal fiber for terahertz regime,” *en, Opt. Eng.*, vol. 55, no. 7, p. 076 117, Jul. 2016.
- [57] M. R. Hasan, S. Akter, T. Khatun, A. A. Rifat, and M. S. Anower, “Dual-hole unit-based kagome lattice microstructure fiber for low-loss and highly birefringent terahertz guidance,” *en, Opt. Eng.*, vol. 56, no. 4, p. 043 108, Apr. 2017.
- [58] K. Ahmed, F. Ahmed, S. Roy, *et al.*, “Refractive index-based blood components sensing in terahertz spectrum,” *IEEE Sens. J.*, vol. 19, no. 9, pp. 3368–3375, May 2019.
- [59] I. K. Yakasai, P. E. Abas, S. Ali, and F. Begum, “Modelling and simulation of a porous core photonic crystal fibre for terahertz wave propagation,” *en, Opt. Quantum Electron.*, vol. 51, no. 4, Apr. 2019.
- [60] M. S. Islam, C. M. B. Cordeiro, J. Sultana, *et al.*, “A hi-bi ultra-sensitive surface plasmon resonance fiber sensor,” *IEEE Access*, vol. 7, pp. 79 085–79 094, 2019.
- [61] S. Chakma, M. A. Khalek, B. K. Paul, K. Ahmed, M. R. Hasan, and A. N. Bahar, “Gold-coated photonic crystal fiber biosensor based on surface plasmon resonance: Design and analysis,” *en, Sens. BioSensing Res.*, vol. 18, pp. 7–12, Apr. 2018.
- [62] M. S. Aruna Gandhi, K. Senthilnathan, P. R. Babu, and Q. Li, “Visible to near infrared highly sensitive microbiosensor based on surface plasmon polariton with external sensing approach,” *en, Results Phys.*, vol. 15, no. 102590, p. 102 590, Dec. 2019.
- [63] M. Rakibul Islam, M. M. I. Khan, F. Mehjabin, J. Alam Chowdhury, and M. Islam, “Design of a fabrication friendly & highly sensitive surface plasmon resonance-based photonic crystal fiber biosensor,” *en, Results Phys.*, vol. 19, no. 103501, p. 103 501, Dec. 2020.

- [64] H. Wang, X. Yan, S. Li, and X. Zhang, “Tunable surface plasmon resonance polarization beam splitter based on dual-core photonic crystal fiber with magnetic fluid,” en, *Opt. Quantum Electron.*, vol. 49, no. 11, Nov. 2017.
- [65] H. Huang, Z. Zhang, Y. Yu, *et al.*, “A highly magnetic field sensitive photonic crystal fiber based on surface plasmon resonance,” en, *Sensors (Basel)*, vol. 20, no. 18, p. 5193, Sep. 2020.
- [66] M. Rakibul Islam, A. N. M. Iftekher, M. S. Anzum, M. Rahman, and S. Siraz, “LSPR based double peak double plasmonic layered bent core PCF-SPR sensor for ultra-broadband dual peak sensing,” *IEEE Sens. J.*, vol. 22, no. 6, pp. 5628–5635, Mar. 2022.
- [67] C. Liu, L. Wang, L. Yang, *et al.*, “The single-polarization filter composed of gold-coated photonic crystal fiber,” en, *Phys. Lett. A*, vol. 383, no. 25, pp. 3200–3206, Sep. 2019.
- [68] Q. Liu, S. Li, H. Li, *et al.*, “Broadband single-polarization photonic crystal fiber based on surface plasmon resonance for polarization filter,” en, *Plasmonics*, vol. 10, no. 4, pp. 931–939, Aug. 2015.
- [69] M. S. Islam, C. M. B. Cordeiro, M. J. Nine, *et al.*, “Experimental study on glass and polymers: Determining the optimal material for potential use in terahertz technology,” *IEEE Access*, vol. 8, pp. 97 204–97 214, 2020.
- [70] R. Paschotta, “Silica fibers,” in *RP Photonics Encyclopedia*, RP Photonics AG, 2004.
- [71] P. R. West, S. Ishii, G. V. Naik, N. K. Emani, V. M. Shalaev, and A. Boltasseva, “Searching for better plasmonic materials,” en, *Laser Photon. Rev.*, vol. 4, no. 6, pp. 795–808, Nov. 2010.
- [72] G. V. Naik, V. M. Shalaev, and A. Boltasseva, “Alternative plasmonic materials: Beyond gold and silver,” en, *Adv. Mater.*, vol. 25, no. 24, pp. 3264–3294, Jun. 2013.
- [73] H. Abdullah, K. Ahmed, and S. A. Mitu, “Ultrahigh sensitivity refractive index biosensor based on gold coated nano-film photonic crystal fiber,” en, *Results Phys.*, vol. 17, no. 103151, p. 103 151, Jun. 2020.
- [74] M. S. Islam, M. R. Islam, J. Sultana, A. Dinovitser, B. W.-H. Ng, and D. Abbott, “Exposed-core localized surface plasmon resonance biosensor,” en, *J. Opt. Soc. Am. B*, vol. 36, no. 8, p. 2306, Aug. 2019.
- [75] H. N. Rafi, M. R. Kaysir, and M. Jahirul Islam, “Air-hole attributed performance of photonic crystal fiber-based SPR sensors,” en, *Sens. BioSensing Res.*, vol. 29, no. 100364, p. 100 364, Aug. 2020.

- [76] A. A. Rifat, G. A. Mahdiraji, D. M. Chow, Y. G. Shee, R. Ahmed, and F. R. M. Adikan, "Photonic crystal fiber-based surface plasmon resonance sensor with selective analyte channels and graphene-silver deposited core," en, *Sensors (Basel)*, vol. 15, no. 5, pp. 11 499–11 510, May 2015.
- [77] M. S. Islam, J. Sultana, K. Ahmed, *et al.*, "A novel approach for spectroscopic chemical identification using photonic crystal fiber in the terahertz regime," *IEEE Sensors Journal*, vol. 18, pp. 575–582, 2018. DOI: [10.1109/JSEN.2017.2775642](https://doi.org/10.1109/JSEN.2017.2775642). [Online]. Available: <https://doi.org/10.1109/JSEN.2017.2775642>.
- [78] M. S. Islam, J. Sultana, R. Ahmmmed Aoni, *et al.*, "Localized surface plasmon resonance biosensor: An improved technique for SERS response intensification," en, *Opt. Lett.*, vol. 44, no. 5, pp. 1134–1137, Mar. 2019.
- [79] M. S. Islam, J. Sultana, A. A. Rifat, *et al.*, "Dual-polarized highly sensitive plasmonic sensor in the visible to near-IR spectrum," en, *Opt. Express*, vol. 26, no. 23, p. 30 347, Nov. 2018.
- [80] S. Jain, K. Choudhary, A. Kumar, C. Marques, and S. Kumar, "(invited paper) PCF-based plasmonic sensor for the detection of cervical and skin cancer cell," en, *Results in Optics*, vol. 14, no. 100589, p. 100 589, Feb. 2024.
- [81] M. H. K. Anik, S. M. R. Islam, H. Talukder, *et al.*, "A highly sensitive quadruple d-shaped open channel photonic crystal fiber plasmonic sensor: A comparative study on materials effect," en, *Results Phys.*, vol. 23, no. 104050, p. 104 050, Apr. 2021.
- [82] M. Abdelghaffar, Y. Gamal, R. A. El-Khoribi, *et al.*, "Highly sensitive v-shaped SPR PCF biosensor for cancer detection," en, *Opt. Quantum Electron.*, vol. 55, no. 5, May 2023.
- [83] S. Yao, Y. Yu, S. Qin, D. Wang, P. Yan, and Z. Zhang, "Research on optimization of magnetic field sensing characteristics of PCF sensor based on SPR," en, *Opt. Express*, vol. 30, no. 10, pp. 16 405–16 418, May 2022.
- [84] A. M. T. Hoque, K. F. Al-Tabatabaie, M. E. Ali, A. M. Butt, S. S. I. Mitu, and K. K. Qureshi, "U-grooved selectively coated and highly sensitive PCF-SPR sensor for broad range analyte RI detection," *IEEE Access*, vol. 11, pp. 74 486–74 499, 2023.
- [85] M. R. Islam, M. M. I. Khan, F. Mehjabin, *et al.*, "Design of a dual spider-shaped surface plasmon resonance-based refractometric sensor with high amplitude sensitivity," en, *IET Optoelectron.*, Nov. 2022.

-
- [86] J. Lv, M. Zhu, L. Yang, *et al.*, “Surface plasmon resonance sensor based on the dual core d-shape photonic crystal fiber for refractive index detection in liquids,” *Opt. Eng.*, vol. 61, no. 08, Aug. 2022.
- [87] Q. Zhang, W. Li, Q. Ren, J. Zheng, Q. Xie, and X. Wang, “A d-type dual side-polished, highly sensitive, plasma refractive index sensor based on photonic crystal fiber,” *Front. Phys.*, vol. 10, Sep. 2022.
- [88] BAETE Admin. “BAETE.” [Accessed 16 Aug. 2024]. (2022), [Online]. Available: <https://www.baetebangladesh.org/Archived-Manuals%20-Guidelines.html>.